Formes curvilinéaires avancées pour la modélisation centrée objet des écoulements souterrains par la méthode des éléments analytiques

Philippe Le Grand

Ecole Nationale Supérieure des Mines
SAINT-ETIENNE

UNIVERSITE JEAN MONNET
Saint-Etienne

THESE

présentée par

Philippe LE GRAND

pour obtenir le grade de

Docteur

de l'Ecole Nationale Supérieure des Mines de Saint-Etienne

et de l'Université Jean Monnet

Spécialité Science de la terre et de l'environnement

Formes curvilinéaires avancées pour la modélisation centrée objet des écoulements souterrains par la méthode des éléments analytiques

Advanced curvilinear shapes for object centered modeling of groundwater flow with the analytic element method

Soutenue le 4 Avril 2003 devant le jury composé de :

Dr. R.J. Barnes	président
Pr. M. Razack	rapporteur
Pr. O.D.L. Strack	rapporteur
Dr. M. Batton-Hubert	examinateur
Dr. D. Graillot	examinateur

Année 2003

N° d'ordre : 310ID

Ecole Nationale Supérieure des Mines
SAINT-ETIENNE

UNIVERSITE JEAN MONNET
Saint-Etienne

THESE

présentée par

Philippe LE GRAND

pour obtenir le grade de

Docteur

de l'Ecole Nationale Supérieure des Mines de Saint-Etienne

et de l'Université Jean Monnet

Spécialité Science de la terre et de l'environnement

Formes curvilinéaires avancées pour la modélisation centrée objet des écoulements souterrains par la méthode des éléments analytiques

Advanced curvilinear shapes for object centered modeling of groundwater flow with the analytic element method

Soutenue le 4 Avril 2003 devant le jury composé de :

Dr. R.J. Barnes	président
Pr. M. Razack	rapporteur
Pr. O.D.L. Strack	rapporteur
Dr. M. Batton-Hubert	examinateur
Dr. D. Graillot	examinateur

Année 2003

N° d'ordre : 310ID

Acknowledgements

The present work would not have been possible without the support and encouragement of many people, so many that they cannot all be included here. Those whom I omit know who they are, and the extent of my gratitude.

I wish to thank Professor Moumtaz Razack, from the Université de Poitiers, for kindly accepting the role of reviewer of this work.

Professor Otto Strack, from the University of Minnesota, must accept my most profound thanks, as a reviewer of this dissertation, and as the most constant source of support, encouragements, comments and challenges throughout my post graduate studies. I am gratefully in his debt.

Dr. Randal Barnes, associate professor at the University of Minnesota, earned my gratitude in many ways. His direction while advising me on my Master's degree, his patience with a strong headed student, his challenging my ideas, and his comments on the work included here or elsewhere have all been crucial in teaching me to do research. For all that, for his hosting me as an exchange student and researcher, and for his acceptance to participate in the jury for this thesis, I am thankful.

Professor Philippe Davoine, now retired from the Ecole des Mines, introduced me to water issues in general, and groundwater by consequence, as well as the art of teaching, which he has mastered. His wit, his intelligence, and his witness to the quality that an individual can reach as a researcher have all led me down the academic path. My sincere thanks accompany him.

Dr. David Steward, Kansas State University, deserves to have his work acknowledged here. Without his excellent counsel, his encouragements and other support, the present dissertation would not have come to an end on time.

My co-advisor, Dr. Mireille Batton-Hubert, researcher at SITE, has the capacity to push my reflections further, to force me to put my thoughts into words, and to make me explore areas of science from which I might have shyed away otherwise. How I wish I had recorded some of our discussions! I am grateful for her presence and support.

my advisor in this process, Dr. Didier Graillot, research director and head of the center SITE, deserves my deepest thanks. Besides securing the financial means without which I could not have continued a life in research. His creativity, and his willingness to deal with the administrative complications of a student whose heart was overseas are all commendable; his open-mindedness, his experience and his capacity to perceive the larger picture were instrumental in giving me the freedom, and the bounds, that I needed.

Remerciements

Le présent travail n'aurait pas été possible sans le soutien et les encouragements d'un grand nombre de personnes, trop grand pour qu'ils soient tous inclus ici. Ceux que j'omets savent qui ils sont, et l'étendue de ma gratitude.

Je souhaite remercier le professeur Moumtaz Razack, de l' Université de Poitiers, pour avoir accepté le rôle de rapporteur sur mon travail.

Professeur Otto Strack, de l' University of Minnesota, doit accepter mes plus profonds remerciements, comme rapporteur sur ce mémoire, et comme la source la plus constante de soutien, d'encouragements, de commentaires et de mises à l'épreuve tout au long de mes études de troisième cycle. Avec gratitude, je lui suis redevable de beaucoup.

Dr. Randal Barnes, professeur associé à University of Minnesota, a gagné ma gratitude de nombreuses façons. Son instruction alors qu'il me dirigeait durant mon Master of Science, sa patience avec un étudiant têtu, sa mise à l'épreuve de mes idées, ses commentaires, sur les travaux inclus ici ou ailleurs, ont tous été cruciaux pour m'apprendre à faire de la recherche. Pour tout cela, pour son accueil quand j'étais étudiant, puis chercheur, en échange, et pour son acceptation à prendre part au jury de cette thèse, je le remercie.

Professeur Philippe Davoine, aujourd'hui retraité de l' Ecole de Mines, m'a ouvert l'esprit aux problèmes de l'eau en général, et aux eaux souterraines par conséquent, ainsi qu'à l'art de l'enseignement, dont il était maître. Son esprit, son intelligence, et son témoignage de la qualité que peut atteindre un individu en tant que chercheur m'ont tous conduit vers une carrière académique. Mes sincères remerciements l'accompagnent.

Dr. David Steward, de Kansas State University, mérite de voir ses efforts reconnus ici. Sans son excellent conseil, ses encouragements et autres soutiens, le présent mémoire n'aurait jamais vu le jour.

Ma co-directrice, Dr. Mireille Batton-Hubert, maître de conférence à SITE a eu la capacité à pousser mes reflexions plus loin, a me forcer à exprimer mes pensées, et à me faire explorer des secteurs scientifiques que j'aurais autrement évités avec timidité. Comme je regrette de n'avoir pas enregistré certaines de nos conversations ! Je suis reconnaissant de sa présence et de son soutien.

Mon directeur de thèse, Dr. Didier Graillot, directeur de recherche et directeur du centre SITE, mérite mes profond remerciements. En plus de la fourniture des moyens financiers sans lesquels je n'aurais pas pu poursuivre ma vie de chercheur, sa créativité et sa volonté de gérer les complications administratives liées à un étudiant dont le coeur était à l'étranger sont toutes louables. Son ouverture d'esprit, son expérience et sa capacité à percevoir la vue d'ensemble ont contribué à me donner la liberté, ainsi que les limites, qui m'étaient nécessaires.

Summary

Using GIS for the design of groundwater models motivates the search for numerical methods that do not require the discretization of the flow domain: GIS are natively vectorized.

Numerical methods that relie on the discretization of the boundaries rather than the domain offer the advantage of retaining the native description of information in vector form as provided by the GIS, thus reducing the loss inherent to raterization and subsequent vectorization. The Analytic Element Method is especially promising. However, it lacks the capacity to handle a specific type of object, NURBS curves.

The functions necessary to allow the inclusion of these curves in the AEM are derived, and examples are provided. Their versatility is presented, also showing that existing smooth curves can be represented as NURBS, thus allowing backward compatibility, should they be replaced.

A method is offered to allow for faster model response when using these curvilinear elements, based on the Direct Boundary Integral Method. Standard line elements are also improved to allow greater precision and control in the speed-improving scheme.

Keywords: GIS, analytic elements, curvilinear elements, NURBS, Direct Boundary Integrals

Résumé

L'utilisation des SIG pour la conception de modèles d'écoulements souterrains motive la recherche de méthodes numériques qui ne requièrent pas la discrétisation du domaine de l'écoulement : les SIG sont par nature vectorisés.

Les méthodes numériques qui se fient à la discrétisation des frontières plutôt que du domaine offrent l'avantage de garder le description originale de l'information sous forme vecteur, telle que fournie par le SIG, réduisant ainsi les pertes inhérentes à la rastérisation et la vectorisation ultérieure. La méthode des éléments analytiques est particulièrement prometteuse. Cependant, il lui manque la capacité à gérer un type spécifique d'objets, les courbes NURBS.

Les fonctions nécessaires à l'inclusion de ces courbes dans le cadres de l'AEM sont dérivées, et des exemples sont fournis. Leur souplesse est présentée, et on montre que les formes courbes existantes dans l'AEM peuvent être représentées par des NURBS, permettant ainsi la compatibilité, si elles devaient être supplantées.

Une méthode est proposée pour améliorer le temps de réponse des modèles lorsque les éléments curvilinéaires sont utilisés, basée sur la méthode des intégrales frontières directes. Les éléments linéaires classiques sont également améliorés pour permettre meilleurs précision et contrôle dans la technique d'accélération.

Mots clef : SIG, éléments analytiques, éléments curvilinéaires, NURBS, Intégrales Frontières Directes

Contents

List of Figures

Chapter 1

Introduction

In this dissertation, a new class of elements used in the modeling of groundwater flow is proposed for inclusion within the Analytic Element Method. These new elements allow the definition of boundary conditions along complex shapes known as Non-Uniform Rational B-Spline curves. NURBS curves are popular tools in many fields of engineering, as they allow the artist, the designer, the freedom he requires to project his vision onto the digital world of the computer, while giving the engineer the structured framework he needs to implement that vision.

Another contribution to the field of groundwater modeling, needed in fact to render the Non-Uniform Rational Bézier Spline curves usable as boundaries for analytic element models, is the use of polygons as closed boundaries over which the direct boundary integral method is applied. This enables the creation of a new type of far-field, used here for the NURBS elements only, but that could be expanded to any collection of elements, still within the framework of the AEM.

Much is written on NURBS curves, and it remains a vivid field of study in computer graphics. Most of what is to be found refers to their geometry, specific algorithms to deal with seldom encountered cases, or to their application in fitting datasets, sometimes for the purpose of extrapolation. The present dissertation does not add knowledge on these curves per-se, except in the way that they can be related to potential theory. Instead much use is made of these shapes, and key concepts are described when needed. Although the literature is fairly extensive on the subject, dating back to the 1960's and the works of Bézier and de Casteljau, for Renault and Peugeot, respectively, reference is usually made to *the* reference text in the

matter at the present time; *The NURBS book*, by Piegl and Tiller, contains all the elements necessary for the derivations herein.

The direct boundary integral method is described in Liggett and Liu's *The boundary integral method for porous media flow*, and many more describe it extensively, but no other reference than Strack's *Groundwater mechanics* seem to detail it in its complex variable form, regardless of the field of application.

1.1 On the approach

Research in engineering fields differs greatly from its counterparts in liberal arts or pure sciences. It shares much in common with them in terms of methodology, as far as bibliography, subject definition or dissertation are concerned. However, the characteristic of the engineer, his capacity to produce new material out of the combination of knowledge acquired in diverse and previously unrelated sciences, set this type of research apart.

The focus on GIS, used by many in hydrogeology as a CAD tool for the conception of groundwater models, is found primarily in the discussion of chapter 2. Its relative importance in the present dissertation is less than originally expected, since larger contributions to the field of modeling were found in other sections of the work. The argument to be found there remains central however, that an object centered modeling technique is inherently better than any other, be it simply for aesthetic reasons.

The investigation of GIS revealed that the choices made there for the representation of information had repercussions on the requirements placed to numerical modeling techniques meant to interact with this design tool. In particular, the use of NURBS curves in some cases prompted an investigation of these shapes for the AEM.

Much remains to be studied in connection with the accomplishments detailed here, in particular with respect to the choices made for the representation and storage of spatially continuously varying information. Some possible expansions are described in the conclusion; it is hoped that some will find here material to investigate.

1.2 On notation and symbols

In dissertations that involve the analytic element method, the notation often becomes elaborate, because many things need to be numbered, ordered and sorted. However, computer code is often trivial, mainly because of the notion of scope: the first endpoint of a segment S_j is may be noted e.g.$\overset{1}{z}_j$ in the literature, but in the computer code, a variable $z1$ will be defined within the context of segment Sj to contain $\overset{1}{z}_j$ and will only make sense there. Thus, when the computer handles segment Sj, it needs not worry about the first endpoints of other segments, which are simply not defined within its context: $z1$ is explicit enough to be satisfactory.

Considering that computers are essentially stupid, however fast they may be, the decision for the present dissertation was made to keep the notation as simple as possible by applying the same concept of scope, since the human reader will not be challenged by something that even his digital companion can grasp. This allows the reuse of symbols, greatly valuable considering the limited number of symbols available in the Greek and Roman alphabets.

Another note of attention is brought to the symbols used to represent variables commonly used in the description of groundwater flow. Although this dissertation is submitted to a French institution, the standard chosen is the one used in the field of the AEM. The discharge potential is Φ, the piezometric head ϕ, the porosity is ν and the flow is characterized by specific discharge -sometimes integrated-, rather than velocity. These choices influence the look of Darcy's Law, which is expressed in a fashion that may be unusual to the French. It is offered in the chosen form for the sake of integration of the present work into the AEM.

1.3 On the use of English

The choice of language for this thesis was not easy. The need for a text published in France on the analytic element method, virtually ignored there, seemed to call for French to be used, as this would have maximized the size of the audience of the present text. However, the level of comfort of the author with English rather than French in technical writing, the fact that most -if not all- research revolving around the AEM is published in English, and the accepted fact that French researchers are comfortable when reading English led to choosing English in the

end. For clarity, and to facilitate the comprehension of the thesis, the following are provided in French: This introduction, the conclusion, and the synopsis at the beginning of each chapter.

Chapitre 1

Introduction - version française

Dans ce mémoire, une nouvelle classe d'éléments utilisés dans la modélisation des écoulements souterrains est proposée pour ajout à la méthode des éléments analytiques. Ces nouveaux éléments permettent la définition de conditions limites le long de formes complexes connues sous le nom de courbes NURBS. Les NURBS sont des outils populaires dans de nombreux domaines du génie, car ils permettent à l'artiste, le créateur, la liberté qu'il requière pour projeter sa vision sur le monde digital de l'ordinateur, tout en donnant à l'ingénieur le cadre structuré dont il a besoin pour implémenter cette vision.

Une autre contribution au champ de la modélisation des eaux souterraines, nécessaire en fait pour rendre opérationnelle l'usage des NURBS comme frontières pour la méthode des éléments analytiques, se trouve dans l'utilisation de polygones en tant que frontières fermées suivant lesquelles la méthode des intégrales frontières directes est appliquée. Cela permet la création d'un nouveau type de *champ lointain* [1], utilisé ici pour les NURBS seulement, mais qui pourrait être étendu à tout groupe d'éléments, toujours dans le cadre de l'AEM.

Beaucoup a été publié sur les courbes NURBS, et ce domaine reste un champ d'études actif dans le graphisme informatique. La plupart concerne leur géometrie, des algorithmes spécifiques pour gérer des cas rarement rencontrés, ou à leur application à l'approximation de jeux de données spécifiques, parfois à des fins d'extrapolation. Le présent mémoire n'ajoute pas de connaissance sur ces courbes en tant que telles, si ce n'est dans la façon dont on peut les relier à la théorie des potentiels. On utilise plutôt ces formes autant que possible, si bien

[1] Far-Field en Anglais

que certains concepts clef sont décrits quand cela est nécessaire. Bien que la littérature soit relativement étendue sur le sujet, allant jusqu'aux années 60 et aux travaux de Bézier et de Casteljau, pour Renault et Peugeot respectivement, référence est faite à *la* référence en la matière à l'heure actuelle; *The NURBS book*, de Piegl et Tiller, contient tous les éléments nécessaires aux dérivations ci-contenues.

La méthode des intégrales frontières directes est décrite dans *The boundary integral method for porous media flow* de Liggett et Liu, et d'autres la décrivent en détail, mais aucune autre référence que *Groundwater mechanics* de Strack ne semble la détailler sous sa forme en variable complexe, sans discriminer le domaine d'application.

1.1 De l'approche

La recherche dans les Sciences du génie diffère grandement de ses équivalents en sciences humaines et sciences pures. Elle partage beaucoup en matière de méthodologie, c'est á dire pour autant que la bibliographie, la définition du sujet ou l'écriture du mémoire soient concernés. Cependant, le propre de l' ingénieur est sa capacité à produire de la nouvelle matière à partir de la combinaison de connaissances acquises dans des sciences diverses et sans rapport au préalable; cela place ce type de recherche dans une catégorie à part.

Le point sur les SIG, utilisés par un grand nombre en hydrogéologie comme outil de CAO pour le conception de modèles d'écoulements souterrains, se trouve essentiellement dans le discours du chapitre 2. Son importance relative est plus faible qu'originalement supposée, compte tenu des plus importantes contributions à l'état de l'art dans les sections suivantes du travail. La discussion qui s'y trouve est cependant centrale, à savoir qu'une technique de modélisation centrée sur des objets est intrinsèquement meilleure, ne serait-ce que d'un point de vue esthétique.

L'enquête sur les SIG a révélé que des choix faits pour la représentation de l'information a eu des répercussions dans les contraintes placées sur les techniques numériques de modélisation sensées inter-agir avec l'outil de conception. En particulier, l'utilisation dans certains cas de courbes NURBS a provoqué l'analyse de ces formes pour l'AEM.

Beaucoup reste à étudier en relation aux progrès détaillés ici, en particulier quand aux

choix opérés pour la représentation et le stockage d'information variant dans l'espace de façon continue. Quelques extensions possibles sont décrites dans la conclusion ; on espère que certains trouveront là matière à recherche.

1.2 De la Notation et des symboles

Dans les mémoires qui traitent de la méthode des éléments analytiques, la notation devient souvent élaborée, parce que nombre de choses doivent être numérotées, ordonnées et classées. Cependant, le code informatique est souvent trivial, principalement grâce à la notation de contexte : le premier sommet d'un segment S_j peut être dénoté e.g.$\overset{1}{z}_j$ dans la littérature, mais dans le code informatique, une variable $z1$ sera définie dans le contexte du segment Sj pour contenir $\overset{1}{z}_j$ et n'aura de sens que dans les limites de ce contexte. Ainsi, lorsque l'ordinateur opère sur le segment Sj, il ne lui est pas nécessaire de se préoccuper des premières extrémités des autres segments, qui n'existent pas dans le contexte local : le nom $z1$ est suffisamment explicite pour être satisfaisant.

Considérant qu'un ordinateur est essentiellement stupide, tout aussi rapide qu'il puisse être, il a été décidé pour le présent mémoire de garder la notation aussi légère que possible en applicant le même concept de contexte, puisque le lecteur humain ne sera pas mis à mal par un concept que même son compagnon digital peut apprécier. Cela permet la réutilisation de symboles, chose fort précieuse compte tenu du nombre limité de symboles disponibles dans les alphabets grec et romain.

On porte également l'attention sur les symboles utilisés pour représenter des variables couramment utilisées dans la description des écoulements souterrains. Bien que ce mémoire soit soumis à une institution française, la norme choisie est celle utilisée dans le champ des éléments analytiques. Le potentiel d'écoulement est noté Φ, la charge piézométrique ϕ, la porosité ν et l'écoulement est caractérisé par le flux spécifique -parfois intégré-, plutôt que par la vitesse. Ces choix influencent l'aspect de la Loi de Darcy, qui est exprimée d'une façon peu orthodoxe pour les Français. Elle est offerte sous cette forme pour le besoin d'intégration du présent travail dans l'AEM.

1.3 De l'utilisation de l'Anglais

Le choix de la langue pour cette thèse ne fut pas facile. Le besoin d'un texte publié en Français sur la méthode des éléments analytiques, méthode pratiquement ignorée en France, semblait nécessiter l'utilisation du Français, maximisant ainsi l'audience du présent mémoire. Cependant, le niveau de confort de l'auteur en Anglais par rapport au Français en matière de rédaction technique, le fait que la plupart -sinon la totalité- de la recherche gravitant autour de l'AEM est publiée en Anglais, et le fait reconnu que les scientifiques français sont à l'aise à la lecture de l'Anglais, ont conduit au choix final de la langue de Shakespeare. Par un désir de clarté, et pour faciliter la compréhension de cette thèse, les passages suivants sont fournis dans les deux langues : cette introduction, la conclusion, et le résumé en tête de chaque chapitre.

Chapter 2

GIS and Modeling in hydrogeology

Synopsis

Purpose: This chapter focuses on a description of the use of GIS in hydrogeological modeling. It brings a logical argument for a shift in using the GIS as an input and design interface to making numerical models an analysis tool among many.

Outcome: The AEM is an important piece of a puzzle that should enable the creation of models centered on geographic features, objects. In order to improve the link between AEM and GIS in that context, a new element type along splines must be developed.

The focus of the work of the scientist is moving towards a resource, outcome centered model. Methods based on vectorial description of data and results might therefore be preferred because they offer an object perspective. The processes involved might be required in advanced analyses, but for many common problems where the flow controls the decision, a simpler representation of the process is sufficient. The limitation on the required number of parameters of the numerical model allows for a complexification and an increased amount of detail used in the representation of the geographic setting. Thus, the tool used for the management of geo-referenced information, the GIS, gains a central importance in modeling, as a design tool, as well as a repository of the information from field data and simulation results.

Object oriented numerical method for the resolution of the flow problems exist: Boundary

methods, as discussed in chapter 3. They can be linked to the GIS without forcing the loss of the object structure.

GIS are intrinsically object oriented because they were conceived for vectorial data. Raster data has gained a predominance in recent years, and some sources of information are only available in this object unfriendly format. Other than contouring of information by polylines, the only method available in popular GIS packages for translating continuously varying information into object representations produces a spline surface. Any method considered for the process modeling must handle spline geometries. Such capabilities are added to the analytic element method in chapter 4.

Résumé en Français

Objectif : Ce chapitre se concentre autour d'une description de l'utilisation des Systèmes d'Information Géographiques -SIG- en modélisation hydro-souterraine. Il apporte un argument logique à la redirection de l'utilisation des SIG d'outils de conception et de création de données d'entrées ar rôle de clef de voûte, dont les modèles numériques ne sont qu'un outil parmis d'autres.

Résultat : L'AEM est une pièce importante d'un puzzle qui devrait permettre la création centrée sur les caractéristiques, ou éléments, géographiques. Afin d'améliorer le lien entre AEM et SIG dans ce contexte, un nouveau type d'élément le long de courbes spline doit être développé.

L'intérêt du travail du scientifique se déplace vers des modèles centrés sur la ressource, ses sorties. Les méthodes basées sur des déscriptions vectorielles des données et des résultats peuventt par conséquent être préférables parce qu'elles offrent une perspective objet. Les processus impliqués peuvent être obligatoires pour les analyses les plus avancées, mais pour de nombreux problèmes communs où l'écoulement controle la décision finale, une représentation plus simple du processus physique est suffisante. La limitation du nombre de paramètres requis pour le modèle numérique, permet la complexification et l'augmentation du détail utilisé

dans la représentation de l'arrangement géographique local. Ainsi, l'outil utilisé pour la gestion de l'information géo-référencée, le SIG, gagne une importance centrale dans l'activité de modélisation, comme outil de conception, de même qu'en tant qu' entrepot de l'information obtenue par observation sur le terrain et des résultats de simulation.

Des méthodes numériques orientées objet existent pour la résolution de problèmes d'écoulements : les méthodes aux frontières, présentées au chapitre 3. Elles peuvent être liées au SIG sans avoir à forcer la perte de la structure objet.

Les SIG sont intrinsèquement orientés objet parce qu'ils sont originellement conçus pour de l'information vectorielle. Les données *Raster*, en grille, ont tendance à prédominer dans les dernières années, et certaines sources d'information ne sont plus disponibles que dans ce format peu amical pour les objets. Autre que la production de lignes de niveau, la seule méthode disponible dans les outils SIG les plus populaires pour traduire de l'information variable continue dans une représentation objet est de produire une surface spline. Toute méthode considerée pour modéliser le processus physique d'écoulement doit pouvoir gérer ces géométries. Une telle capacité est ajoutée à la méthode des éléments analytiques dans le chapitre 4.

2.1 Tools of hydrogeological modeling

The modeling of hydrogeology, as in most natural sciences, involves many different fields of science, each requiring different tools.

2.1.1 The three sides of modeling groundwater flow

Unlike in industrial sciences, where an object can be produced and re-produced, the geologist and geo-technical engineers are not at liberty to operate destructive testing, like disections and plasticity tests, on the main object of their work. Instead, much like medical doctors, they learn from experience, individually evaluate each modeling challenge from indirect observations, classify it, and choose a method to face this challenge according to their experience. The hydrogeologist finds help from three colleagues:

- the physicist and mathematician provide descriptions of the movement of groundwater, either using deterministic mathematical models based on mechanics that are tested at some scale with laboratory physical models, or using advanced statistical tools.
- the computer scientist makes the product of the physicist's work usable in the form of numerical tools meant to solve the mathematical model.
- the geographer offers means of organizing and handling information as it relates to the site of the model, and to derive knowledge from the numerical model with respect to the specific site.

Aside from his knowledge of geology, he must therefore understand and use the techniques of these three fields. Some hydrogeologists specialize in one or the other of these areas as well, making sure that the state of the art in each discipline is applied to hydrogeology.

Mathematical modeling

The mathematical modeling of groundwater flow can be done via:

- Stochastic models, which deal with the identification and quantification of the variability of model parameters. They provide a probabilistic representation of the solution; they are better used for pollution and transport problems, estimating vulnerability, than to quantify flow.
- Deterministic models, which attempt to provide quantitative analysis of the characteristics of the flow. Most models provide a set of quantitative equations linking unknowns -head, discharge, etc.-, parameters -permeability, porosity, density, etc.-, and variables -location.

The scope of this thesis is limited to deterministic modeling of the flow of groundwater. The mathematical model to be used is described in 3.1.2.

Numerical modeling

Within this thesis, numerical modeling is understood as a discipline of computer science which creates the tools necessary for the accurate solution of the differential equations provided by

the mathematical modeling of the physics and mechanics of groundwater flow.

The numerical model sometimes has the drawback of forcing hypotheses that the mathematical model did not include for the purpose of efficiency, either in the amount of input needed, or in terms of computational cost -time necessary to compute a solution.

Popular numerical models for groundwater flow include ModFlow -see [38]-, FeFlow -see [20]- or WhAEM -see [33].

Geologic setting modeling

Here, the model of the geologic setting -or geologic model- is the description, through digital means, of the setting where the numerical model is to be applied. The components of the geologic model fall into two categories:

- Hard data:
  - the field collected data
  - pre-existing data maps as relevant to the area of study.
- Inferred data:
  - the geologic parameters relevant to the model in a manner that accounts for their spatial distribution and eventual variability.
  - the types and locations of the boundaries of the model, whether internal or external, and the constraints on the variables at those boundaries.

It is important to note that the inferred data are the result of an inverse model. For example, permeability and storativity obtained from a pumping test may actually yield the coefficients that allow a best fit of the specific analytic function, e.g. the Theis solution -see e.g.[59].

Because of the increased complexity of models, the management of these forms of data, and the need to perform spatial analysis on them, has required the hydrogeologist to make use of new software tools. Geology handles information that is by nature related to a location on the earth: Geographic Information Systems -GIS- are these tools.

2.1.2 GIS: Geographic Information Systems

A GIS is a system that handles geo-referenced information and can produce spatial analysis on that information [8]. Two different types of GIS can be identified, though many software implementations seamlessly include both:

- Vectorized GIS. According to [60], the oldest type of GIS were meant to handle vectorized information, that is information whose localization could always be described as points, polygons, or polyhedra. Vectorized GIS is well suited for human geography, and land use analysis in particular.

- Raster GIS. This more recent form of GIS owes its popularity to two factors: firstly, the method used to store information, as large arrays or *grids*, is appealing to the computer scientist of the late 1970's and early 1980's; secondly, the advent of remote sensing and telemetry, including satellite imagery, favored systems that could readily be automated: the human presence required for digitation was made unnecessary by the use of scanning methods. It is interesting to note that [60] proposes that the raster methods were made necessary by the attempt to integrate the representation of two dimensional continuous data and processes.

The use of GIS in combination with flow models, deterministic or stochastic, is well documented in the literature. A review was found in [34], from which the authors propose two categories of links between numerical model and GIS, and further review supports their point: models that are either developed directly inside the GIS -see e.g. [46]-, or external models that interact with the GIS through input and outputs -see e.g. [3, 16]. The research presented in this thesis concerns principally the latter.

2.1.3 An Observation - Modeling: process centered activity

The purpose of modeling groundwater is to allow a decision maker or a stake-holder to acquire the information they request on the response of an aquifer to a given set of stresses. Because it is driven by the expected output, rather than by the available inputs, the choices made for modeling do not take the available data as the limiting factor. The desired output, as

expressed by the end user -stake-holder-, drives the choice of mathematical model, the set of physical processes to be simulated. The choice of mathematical model drives the choice of numerical model, and defines the set of parameters that need to be informed with data.

Thus, the characteristics of an individual site is ignored in favor of the expectation of a few individuals. The paucity of information, the quality of available data occasionally force a lowering of expectations, but more often than not, three dimensional models are used when $2+\frac{1}{2}$-Dimensions would be enough, transient when steady state would suffice.

2.2 Object centered modeling

The use of Geographic Information Systems -GIS- raises an interesting issue for the hydrogeologist. Unlike his surface water colleague, the hydrogeologist does not benefit to a great extent from the satellite collected raster data, because a plan view offers little information with respect to the sub-surface. In fact, once that data has been transformed into vector maps that describe the locations of most water features, the raster format is not usually needed to store the information needed by a groundwater model. The popular Finite Difference modeling tool Visual-MODFLOW, which is composed of a Graphical User Interface for model building and ModFlow -[38]-, as a computational engine, actually used zones of constant transmissivity to characterize the aquifer; the preprocessor is in charge of informing individual cells of the model what is their actual transmissivity value. This eases the sensitivity analysis and the inverse modeling. The hydrogeologist handles data which the original tools of Vectorized GIS were meant to represent: points, lines and polygons are sufficient to describe the input data of a groundwater model.

2.2.1 Concept

It is proposed that the modeling focus in hydrogeology could be shifted from an increased complexity of the mathematical representation of the physical phenomena and processes to an increased complexity of the geographic representation of the modeled area.

By mathematical complexity, it is not meant reducing the level of mathematics necessary to represent of compute the solution: that is inherent to the solution itself and can therefore not

be the choice of the modeler. Instead, this complexity implies increased number of parameters, variables and unknowns, number and order of interacting differental equations, etc.

2.2.2 Advantages and drawbacks

The implications of this shift are multiple.

- In the context of deterministic modeling, the reduction in the mathematical complexity implies a reduction in the number of parameters, to which the model is often very sensitive. Sensitivity analysis is a key of efficient modeling. By reducing the number of parameters, the modeler will get a better chance to understand the behavior of the model with respect to each of those he chose to keep, thus furthering the quality of his judgment in supporting or making decisions based on his model.

- By focusing on the objects, the features, of the model rather than the physical phenomena, the logical link between data, flow feature, and the results of the model will be more intuitive: beyond the use of GIS as a handy Graphical User Interface that serves the model, this object centering provokes a shift in logic where the model serves the information management tool and its user.

- Objects have been a means of improvement in computer science at large. Even computer languages like FORTRAN, traditionally procedural and array based, have had to insert object orientation facilities in their most recent versions. The transfer of information through the web has become object centered with the advent of the eXtensible Markup Language -XML-: as computer programs evolve to integrate such advances, it is possible to envision a situation where the GIS and model have no facilities explicitly defined for the inter-operation, and yet would be able to communicate because they each understand an externally defined language based on XML.

The main limitation to such a change in the practice of modeling is that the modeling tools must still understand objects. Whether XML is used or not, the actual software must be able to understand objects and translate them into its native mode: a gridding for finite difference software, a tessellation for finite elements. In both of these cases, considerable effort would

need to be invested in modifying the software, not only to handle the format change of the Input/Output in XML, but also to make sense of the object centering. The only alternative is for the GIS to know which tool is going to use its output and do some of the work for it.

2.2.3 A method for object centered modeling of groundwater flow

Methods for the object centered modeling of groundwater flow must therefore natively contain the notion of object and be able to handle the elementary features produced by a GIS: points, polygons, and arcs. Boundary methods -see 3.1.1- natively use these internal representation. One in particular, the analytic element method, fits the requirements. In recent research, object oriented frameworks were proposed that classify the elements in these three categories. In [5], elements are defined along precisely those geometries, and a few others -circle and disks in particular. In [56], elements are either located on points, lines, or collection thereof; polygons can be viewed as collections of lines. AEM software manuals -[58, 33, 32]- also show that this basic organization of data is part of the structure of the cómputer tools. The AEM is indeed able to handle the three types of elementary features.

One type of data, continuously varying in two dimension, is used to justify representation on grids -see [60]. Although this projection on arrays of the information is convenient to operate, the following shows that it is not necessary, despite being a valid choice.

Parameters varying in two dimensions

Many parameters in hydrogeology are inferred from values obtained at points scattered around the domain of interest; this includes information on precipitation -rain gauges- or depth to bedrock -from bore logs. The value of a parameter at any given point may be interpolated by many methods: nearest neighbor produces polygonal area of constant values; linear interpolation produces a triangular mesh.

Interesting methods for the production of smooth data exist in two popular GIS software packages, Arc/INFO and GRASS, but their aim is for the production of raster data from the point values: the function Spline fits a spline through the data points that has minimum curvature.

Such a function is particularly appealing because it produces a geometric object, the spline surface, that fits within an object centered view. The parameter is estimated at point where no observation was made as the elevation of the spline surface. In the case of GRASS, an open-source software, it is possible to preserve the geometric description of the spline used to produce the raster map of the parameter. This implies that for the description of complex parameters that vary continuously in two dimensions, splines can be added to the vectorized data types to extend the capabilities of polygons.

Importing raster data

Despite the value of the object centered approach, the current state of the modeling practice imposes to a certain extent the use of raster data. On national scales, large data sets and maps are controlled by a limited number of organizations whose choices may become standards. This is the case in the United States in particular with respect to geological maps stored and sold as Digital Elevation Models -DEM, grids- by the U.S. Geological Survey; it is noteworthy that the USGS is the principle funding agency of ModFlow, a Finite Difference tool. Similar situations exist in Europe: Elevation data is centralized in France by the IGN, who solely decides of the formats in which they are willing to sell the data with which they have been entrusted. Some information, maps of permeabilities, historical piezometric maps, elevation of substratum from geophysical analysis, etc. may be available only in a grid format.

Both ARC/INFO or GRASS provide global functions that allow the processing of a grid to produce contours -isopleths- as vector information. It is then possible to assume that the represented parameter is constant, or to use an interpolator between two consecutive contours. Although these may be sufficient for some parameters, the loss of information is substantial. A solution is to increase the number of contours, but this would produce a large number of objects. Again, the splines function can be used to represent the data: from the grid, a series of contours is obtained, and from the contours, which are vector data, a spline surface can be constructed and preserved, as in 2.2.3.

Conclusion

In order to account for continuously varying information with the GIS tools currently available, the numerical modeling technique should handle information passed as spline surface.

These surfaces are bounded by spline curves; any subdivision of such surfaces would also carry this type of bounds. Their isopleths are spline curves as well. Thus, for the numerical method to be able to make use of the spline surface, it must first be able to handle boundaries shaped like spline curves.

In the following, the analytic element method is presented in chapter 3, and the required elements, along spline shaped boundaries, are developed in chapter 4, along with the innovations necessary to make them usable in practice.

Chapter 3

The Analytic Element Method

Synopsis

Purpose: This chapter introduces the Analytic Element Method, abbreviated AEM, outlining the background concepts, and focusing on both the most recent developments, and the method's intrinsic limits. Examples of practical nature are referred to or provided.

Outcome: The limits and limiting features of the AEM are detailed, thus bringing forth the needs for new development related to the AEM in the context of interfacing with GIS.

As previously pointed out, the AEM is largely ignored in France; it is often dismissed for invoked reasons such as an incapacity to handle complex processes or simply the steep learning curve involved. Based on the principle of superposition, the method has the advantage of providing information over a 2-D or 3-D domain while containing unknowns along the internal or external boundaries only. This property makes it a natural favorite as a tool linked to vector-oriented data representations. Recent developments have allowed the models to achieve greater precision and efficiency, without adding much requirements on the data inputs. Some of these developments will be referred to or detailed in the present chapter. However, one must concede that the method is intrinsically limited by the range of phenomena that it can handle. The consequence is that in order to make it more attractive as a tool for groundwater modeling, a number of improvements are required. These are twofold: improvements related

(1) to increased complexity of the modeled phenomena, (2) to more sophisticated data representations. The former will only be introduced in the present work, as it is not crucial to the subject and constitutes a field of study in and of itself; recent developments and leads will only be mentioned. The latter is a topic of this thesis and new elements will be provided in chapter 4.

This introduction to the AEM is accompanied by examples meant mostly for the novice.

Résumé en Français

Objectif : Ce chapitre introduit la Méthode des Eléments Analytiques, abrégée AEM, en soulignant les concepts fondamentaux et en se concentrant sur les développements récents et les limites intrinsèques de la méthode. Des exemples de nature pratiques sont référencés ou fournis.

Résultat : Les limites et caractéristiques limitantes de l'AEM sont détaillées, mettant ainsi en évidence le besoin de nouveaux développements liés à la méthode dans le contexte de l'interfaçage avec le SIG.

Comme précédemment mis en avant, l'AEM est largement ignorée en France ; elle est souvent écartée pour des raisons invoquées telles que son incapacité à manipuler des processus complexes, ou simplement que la courbe d'apprentissage associée est difficile à gravir. Basée sur le principe de superposition, l'AEM a l'avantage de fournir de l'information sur un domaine en deux ou trois dimensions en ne manipulant de l'information que sur les frontières internes ou externes du domaine. Cette propriété en fait un favorit naturel comme outil lié à des représentations de données vectorielles, ou orientées vecteurs. Des développements récents ont permis aux modèles d'achever une meilleure précision et efficacité, sans ajouter trop de contraintes sur les données entrées. Certains de ces développements seront référencés ou détaillés dans le présent chapitre. Cependant, on doit concéder que la méthode est intrinsèquement limitée sur l'étendue des phénomènes qu'elle peut manipuler. Il en résulte que pour pour la rendre plus attrayante comme outil de modélisation, un certain nombre d'améliorations sont requises. Elles sont de deux catégories : améliorations liées (1) à un accroissement dans la complexité des

phénomènes modélisés, et (2) à des représentations plus sophistiquées de données. La première ne sera qu'introduite dans le présent travail, car elle n'est pas cruciale au sujet, et constitue un champ d'étude à part entière ; des développements récents et des pistes de recherche ne seront que mentionnées. La seconde est un sujet de cette thèse, et de nouveaux éléments seront fournis dans le chapitre 4.

Cette introduction à l'AEM est accompagnée d'exemples conçus pour le novice.

3.1 Fundamental concepts of the AEM

As mentioned in chapter 2, a description of the Analytic Element Method is required in order to understand one of the principal tools that will allow an Object-Oriented description of data to produce usable models. In the present section, the founding concepts of the method are depicted, following an outline of the placement of the AEM with respect to other numerical techniques.

3.1.1 Position of the AEM compared to other numerical techniques

Like other numerical techniques, the AEM is used to approximate the solution of a partial differential equation based on a distribution of error. It is related to the Boundary Element Method, and models produced with the AEM may often be connected to models produced by other methods. A classification of these methods is proposed so as to introduce similarities and differences between them.

A classification of techniques

Modeling techniques may be classified into three different categories, following e.g. [10] or [12]. In all boundary value problems, the problem is set based on:

- a differential equation
- a set of boundaries and associated boundary conditions

When a numerical tool is needed to solve the problem, either one or both of the following have to be performed:

- the domain is discretized: a set of points is created inside the domain. A set of relationships between the unknowns and the parameters at these points is also formulated so as to represent the differential equation. The points that fall on or closest to the boundaries are constrained using the boundary conditions instead of these relationships.

- the boundaries are discretized and the boundary conditions approximated in a functionally appropriate manner. The discretization of any boundary must be operated using geometrically relevant tools, such as pieces of straight-lines to approximate a one-dimensional object or closed planar polygons for a two-dimensional object.

The classical methods of Finite Differences -FDM- or Finite Elements -FEM- fall within the first category of methods, known as domain methods, where the domain only is discretized and the boundary conditions are represented exactly. With these methods, the boundary conditions are met exactly, although not always at the precise location of the boundary, but the governing equations are not met inside the domain. However, it is important to notice that, in practice, domain methods hardly accommodate for conditions located at infinity, and thus, boundaries are sometimes artificially inserted to replace such conditions. These methods provide an approximate solution to the original equation and spread the error throughout the domain.

Originally, the Analytic Element Method falls in the second category. It is a boundary method as it meets the differential equation exactly inside the domain but meets the boundary conditions only in an approximate fashion and at approximate locations. As a consequence, for each differential equation, a complete set of solutions has to be provided for the method to produce a usable result. That remains its principal drawback, as such solutions, the Green Functions for the particular equation, are potentially hard to find, when it is not impossible.

In recent developments, the AEM has moved towards a third category, known as mixed methods: although the domain is not discretized in the traditional sense associated to the FDM or FEM, the introduction of numerous polygonal elements for the representation of leakage between aquifers may be regarded as a splitting of the domain. Also, the organization of aquifer

and aquitard units in parallel horizontal entities is reminiscent of a discretization in the vertical direction. Furthermore, in the particular application of leakage, the differential equation is not exactly met. As a consequence, and in anticipation of future developments, it seems more suitable to place the AEM in the mixed methods, bearing in mind that it is the solution domain that is discretized rather than the physical domain. Therefore, the problem is still reduced to one with unknown located solely along the boundaries; the error in approximation is spread both over the boundaries and the domain.

Other boundary or mixed techniques exist that may compare or be included under the description of AEM. the most popular are the method of Distribution of Singularities, also known as the Boundary Elements Method -see e.g. [21], [10],[43].

In practice, the AEM has been applied to groundwater modeling in The Netherlands with NAGROM [15, 17, 14], at Yucca Mountain in Nevada [4], in Minnesota with the Metropolitan Groundwater Model described in [47] and used in [28]. The method seems particularly attractive at regional scales, and [30] suggests its use prior to local modeling with domain methods as a screening model.

Relationship between the Boundary and the Analytic Element Methods

In essence, a brief review of the literature shows that the Boundary Element method relies on the transformation of the differential equation into a boundary integral equation. This is made possible by the use of Greens Identities and the Divergence theorem which relate domain integrals involving a vector field to boundary integrals. Thus, the problem is reduced to evaluation of the latter integrals. This first step brings the Boundary Integral Equation Method, BIEM. The BEM itself revolves around the approximation of the boundary by a set of polygons or polyhedra, and the use of a linear combination of the fundamental solutions to the equations: the Green Functions, named after mathematician George Green. The coefficients of the combinations are determined by collocation, that is by forcing its value -Dirichlet Problem- or the value of its derivative -Neumann Problem- at certain points along the faces of the polygon or polyhedron.

As shown in [51], relying on Cauchy Singular Integrals in the two-dimensional case, the Analytic Element Method is actually a more general technique that completely includes the

BEM solutions within its own. Since the AEM also used solutions produced by other techniques, such as conformal mapping -see [52]-, it may be argued that the BEM is a direct subset of the AEM. However, in the three-dimensional case, where neither of these two techniques is available, the AEM may be perceived as limited to the BEM. One must then consider the elements created by Haitjema [26], Steward [49], or Luther [37] for the representation of partially penetrating wells to be convinced otherwise: their use of imaging techniques -[26], [49]- and superposition of circular sinks outside of the flow domain -[37]- are examples of means of achieving usable basis functions for the AEM outside of the framework of the BEM.

To summarize, the Analytic Element Method is a superset of the Boundary Element Method. The AEM has all of the advantages of the BEM, but removes some of its main drawbacks, as will be shown in the section 3.2.

The Analytic Element Method is therefore a boundary or mixed method. Exact solution to the differential equations are used in linear combination to approximate the specified boundary conditions. This general statement is further developed in the following.

3.1.2 Foundations of the method

As mentioned in 3.1.1, the Analytic Element Method is used to provide approximate solution to boundary-value problems defined by a differential equation and a set of boundary conditions. An introduction to the principles that govern the AEM may be found in [52, 54]. A different yet similar one is proposed here, focusing mainly on the principle of superposition, and Helmholtz Theorem.

Hypotheses for modeling groundwater flow

It is assumed, throughout this thesis, that by *modeling of groundwater flow* one refers to the production of a flow field describing the movement of water in a geologic rock formation represented as a porous medium. Although other types of flow may be included, such as fracture flow for karstic aquifers, they are set outside of the scope of the present work. As a result of this definition, it is always possible to describe the flow field in the subsurface as a continuous vector field of the variables of space (x, y, z) and time t.

Darcy's Law

The first works published on the flow of fluid through a porous medium are due to Henry Darcy -[13, Appendix D]. There, He derives an experimental law relating by a law of proportionality the discharge of water through a pipe filled with sand with the hydraulic heads [1] applied upstream and downstream from the pipe. This law is referred to as Darcy's Law. Modern expressions of it may be found in [51], [18] or [7], and appear as:

$$\vec{q} = -K \cdot \vec{\nabla}\phi \tag{3.1}$$

where $\vec{q}$ is the specific discharge in [m/s], ϕ is the hydraulic head in [m] and K is a symmetric square matrix of the hydraulic conductivities in [m/s]. It is alway possible to find the eigenvectors of the matrix K and to operate a change of variable based on these vectors to reduce the problem to that where K is a diagonal matrix. Furthermore, the ratios of the diagonal terms are often assumed to be constant in space, so that, using an appropriate non conformal change of variable, Darcy's Law may be rewritten as:

$$\vec{q^*} = -k \cdot \vec{\nabla}^* h^* \tag{3.2}$$

where k is a scalar function of space with dimensions [m/s] referred to as the hydraulic conductivity, and the space variable do not actually relate directly to the physical coordinate system -stretching has occurred-. Since it is always possible to bring oneself back to this situation, it is assumed throughout this thesis that the hydraulic conductivity matrix K is limited to $k * I$ where I is the identity matrix. For the sake of simplicity of notation, Darcy's law will be written as:

$$\vec{q} = -k \cdot \vec{\nabla} h \tag{3.3}$$

Equation 3.3 is the form preferred for the presentation of the AEM.

[1] The hydraulic head is in essence a representation of pressure in terms of equivalent water column elevation, just as pressure may be measured in millimeters of Mercury. The formula linking head ϕ, pressure p, elevation z, gravitational constant g and fluid density ρ is: $\phi = z + \frac{p}{\rho g}$. See e.g. [51] for details

Helmholtz Theorem

Evaluation of the specific discharge vector field is the purpose of most modeling techniques, although many achieve it indirectly through the approximation of the hydraulic head, followed by a differentiation to obtain the discharge. As recently pointed out by [52], a theorem known for over 150 years in electromagnetism may be used to separate the specific discharge vector field: Helmholtz Theorem. It states that any vector field may be separated into two vector fields, the first being divergence-free, and thus deriving from a vector-potential, the second being irrotational, and thus deriving from a scalar potential. Thus:

$$\exists \left(\Phi, \vec{\Psi}\right), \vec{q} = \vec{\nabla}\Phi + \vec{\nabla} \times \vec{\Psi} \tag{3.4}$$

and, alternatively to finding a head distribution that satisfies the differential equation, one may solve for the scalar and vector potentials.

A principal of the AEM which sets it apart from the other modeling techniques is to look for these function in a closed form, thus allowing the exact rather than numerical differentiation required to get the flow field.

Conservation of mass

In order to produce a usable differential equation, one considers the law of conservation of mass:

$$\vec{\nabla} \cdot \vec{q} = N(x, y, z, t) \tag{3.5}$$

where the right hand side is a source term, representing all intake or out-takes of fluid from the system: wells, rivers, infiltration, release from phreatic storage, etc. Some are known independently of the flow or head in the medium, such as wells, others are related by an equation, such as release from storage: $N = -\frac{S_s}{k}\frac{\partial h}{\partial t}$, others still constitute a boundary condition, e.g. head imposed along river boundary.

Using equation 3.4 in equation 3.5, and bearing in mind that the divergence of the curl of

a vector field is zero, the scalar potential Φ is the solution of the following Poisson's equation:

$$\vec{\nabla} \cdot \vec{\nabla}\Phi = \Delta\Phi = N(x, y, z, t) \tag{3.6}$$

Similarly, applying the curl operator to equations 3.3 and 3.4:

$$\vec{\nabla} \times \left(\vec{\nabla} \times \vec{\Psi}\right) = \Delta\vec{\Psi} \tag{3.7}$$

$$\vec{\nabla} \times \vec{q} = -\vec{\nabla}k \times \vec{\nabla}h = \vec{\nabla}ln(k) \times \vec{q} \tag{3.8}$$

For the scope of this thesis, the permeability k will be assumed to be constant by part. Thus, with equation 3.8, the specific discharge vector field may be assumed to be piecewise irrotational.

Although these derivations may be operated in three dimensions as has been the case thus far, the application of the flow equations in practice often require the use of two dimensional horizontal flow models, which are faster and easier to handle. This approximation may take place by using the Dupuit-Forcheimer assumption: in the case of an aquifer bounded at the bottom, although a vertical component of flow exists, the resistance to flow in the vertical direction is neglected: the variation in head in the vertical direction is then negligible. Thus, the head along any vertical line defined by $x = x_0, y = y_0, z \in \mathbb{R}$ is constant along that line. It is then possible to assign a unique value of head to any point in the horizontal plane.

In this case, a two-dimensional discharge vector may be defined as the total amount of water flowing through the aquifer at point (x, y) by integrating the specific discharge vector over the wetted thickness of the aquifer -the smallest of the total thickness of the geologic layer H and the water table elevation h:

$$\vec{Q} = (Q_x, Q_y) \tag{3.9}$$

$$Q_x(x, y) = \int_0^{min(h,H)} q_x(x, y, z)dz \tag{3.10}$$

$$Q_y(x, y) = \int_0^{min(h,H)} q_y(x, y, z)dz \tag{3.11}$$

Using Darcy's law, restricting oneself to the two-dimensional differentiation operator and

considering the assumption that k is constant by parts, the discharge vector may be expressed in each zone of constant hydraulic conductivity as:

$$\vec{Q} = -k \cdot min(h, H) \cdot \vec{\nabla} h \tag{3.12}$$

and introducing the function Φ defined as:

$$\Phi = \begin{cases} kHh - \frac{1}{2}kH^2 & H < h \\ \frac{1}{2}kh^2 & H \geqslant h \end{cases} \tag{3.13}$$

the discharge vector may be written as deriving from a potential:

$$\vec{Q} = -\vec{\nabla}\Phi \tag{3.14}$$

As a result, following all these assumptions the governing equation for horizontal flow throughout this thesis reduced to Poisson's Equation:

$$\Delta\Phi = \vec{\nabla} \cdot \vec{Q} = N(x, y, t) \tag{3.15}$$

The source term $N(x, y, t)$ may be obtained from data, model, or assumption. Because of the non-linearity involved with the time-dependent source terms such as release from phreatic storage, the rest of this thesis will focus on steady-state phenomena, or phenomena that may be considered as piecewise steady-state.

Linear operators and the principle of superposition

As can be observed in equations 3.14 and 3.15, the differential operator involved in the problem at hand are well known and fairly simple: the Laplacian and the Gradient operators are known as linear operators, because their operations on a linear combination of functions is a linear combination of their operations on the functions. In other words, for the Laplace operator:

$$\Delta\left(\sum_{n\in\mathbb{N}} a_n\Phi_n\right) = \sum_{n\in\mathbb{N}} a_n\Delta\Phi_n \tag{3.16}$$

See e.g. [11],[61]

This property of linearity is essential for the AEM to be used to solve the boundary value problem: for any linear operator, assuming that a set of solutions $\{\Phi_n, n \in \mathbb{N}\}$ exists that solves the differential equation exactly, then a particular solution that solves the problem may be built by linear combination of the solutions, in a manner that will minimize the distance between the constructed function at the boundaries and the boundary conditions.

A simple example may be considered here. For instance, the one-dimensional wave equation:

$$\frac{d^2 f}{dt^2} + \omega^2 f = 0 \tag{3.17}$$

with boundary conditions: $f(0) = 1, \frac{df}{dt} = 0 att = 2\pi$ the set of solutions is $\{sin(\omega t), cos(\omega t)\}$. A complete solution is written as $f(t) = a \cdot cos(\omega t) + b \cdot sin(\omega t)$ where a and b are unknown. A system of linear equations is set up by applying the boundary conditions:

$$f(0) = a = 1 \tag{3.18}$$

$$\frac{df}{dt}(t = 2\pi) = -a\omega \sin(2\pi\omega) + b\omega \cos(2\pi\omega) = 0 \tag{3.19}$$

so that the final solution is $f(t) = \cos(\omega t) + \cot(2\pi\omega) \cdot \sin(\omega t)$. The AEM works in the same fashion: (1) identifying the set of solutions to the governing equations, which will be referred to as the basis functions, and (2) combining the basis functions in linear form. This latter step is called *superposition.* A set of unknowns is then created, which is solved for by establishing a linear system of equations linking the values of the function at the boundary to the values of the boundary condition. Originally, as in the BEM, these coefficients were solved for based on a system of equations arising from collocation: as many points as there were unknowns were chosen along the boundary where the boundary conditions were enforced. It will be shown in section 3.2 that the system of equations may be built in a different way so as to minimize the overall error in the approximation.

Combining 2D and 3D models

As noted above, two-dimensional are sometimes preferable to three dimensional models, commonly for reasons of speed of execution as well as ease of representation of solutions. However, in some cases, the third dimension is essential to the appropriate representation of the problem, as is the case for *horizontal collector wells* -see e.g. [50]. The inclusion of such features in models is of interest for a specific problem to be studied. Such embedding of locally 3D solutions within otherwise 2D models have been achieved -see e.g. [27]. The embedding is made possible by the facts that:

- any 2D element actually produces a 3D specific discharge vector, although the third component is zero. The principle of superposition still holds.
- 3D elements usually approach 2D representation some distance away from the element. If 3D elements are far enough from the 2D ones, the latter are not significantly disturbed and their resolution process remains valid.

Three dimensional solutions are a topic of their own, which falls outside of the scope of the present document. The remarks given here only intend to show that the work achieved on analytic element method in 2D has value even in the case of problems for which local 3D effects must be accounted.

Intrinsic limitations

The AEM is intrinsically limited by the principle of superposition to the case of linear equations. This limitations may sometimes be lifted if the equations are linearized, as is often the case for transient and unconfined flow: the best example of this is the common usage of the Theis solution for the evaluation of aquifer properties through pumping tests.

The main limitation of the AEM in practice is due to the necessity for a complete base of solutions for each new differential equation: the amount of investigative research required to produce such a base is important, and the limited community of researchers in the AEM cannot produce bases as fast as others produce variations on differential equations. In some cases, a differential equation will already be known and be heavily studied in a different field

of physics, so that a solution base exists, but the practical use of such a base could be limited by the implementation of the computation of the functions, or of the linear combinations of these functions. An obvious example of this phenomenon is the evaluation of series of Bessel functions for series of small coefficients for low orders, and large coefficients at high orders: a classical forward Clenshaw recurrence fails -see [45], requiring the use of an alternate method of computation. These issues of stability of computational algorithms may undermine the AEM as the effort involved in resolving them may appear as overwhelming to the beginner.

However, the Analytic Element Method does remain a practical tool for modeling many groundwater flow problems, with many basic solutions already existing. These solutions are introduced in the following, and the most recent advances are discussed in section 3.2.

3.1.3 Basic elements

The purpose here is to introduce the basic concepts and solutions used in the most basic of solution bases for elementary problems in groundwater flow, so as to produce the framework of the building blocks around which the most recent advances were built.

Introduction to 3D-elements

In most of this thesis, the focus is placed on two-dimensional models only, but as is discussed in Chapter 2, the issue of three-dimensions may be conceptually taken into account: this is necessary to create a framework that will remain acceptable in the near future, as more elaborate solutions become available in 3D or transient settings.

The basis of three dimensional elements is that they generate a fully 3D specific discharge, that may not be approximated everywhere using the Dupuit-Forccheimer assumption. What may be assumed however, is that the functional basis of solutions approaches the basis of the corresponding 2D problem as the functions are evaluated further from the element, as pointed out above, if the aquifer or the water table elevation are somehow bounded.

3D-solutions generally involve the use of the fundamental solution of Laplace's equation in three dimensions $\Delta\Phi + \Delta^k = 0$ where Δ^k is a function equal to zero everywhere except at point $P_k = (x_k, y_k, z_k)$, and such that $\int_{\mathbb{R}^3} \Delta^k d\tau = Q$, where Q is the discharge of water drawn from

the aquifer at point P_k. This solution is expressed as:

$$\Phi(x,y,z) = \frac{1}{4\pi r}, \quad r = \sqrt{(x-x_k)^2 + (y-y_k)^2 + (z-z_k)^2} \tag{3.20}$$

the flow results from application of Darcy's Law, and is expressed as:

$$\vec{q}(X) = -\frac{1}{4\pi} \cdot \frac{\overrightarrow{X - P_k}}{r^3} \tag{3.21}$$

This solutions is then imaged across the relevant impermeable boundaries to create a solution which approaches the 2D solution as x and / or y grow large -see [26].

Another approach, taken by Steward in his PhD dissertation -see [49]-, is to compute the flow field using a three dimensional solution of the vector potential, rather than a scalar potential. This method has the advantage of allowing future incorporation of rotational flow, which might be more relevant in three dimensions than divergent flow: in 3D divergent flow occurs because of elastic release from storage, which is generally small, while rotation in the flow would be inserted by phenomena as common as variable hydraulic conductivity.

General solutions are obtained through integration of the solution for a given distribution of singular points.

A review of the literature reveals that the 3D solutions are generally cumbersome to use, with each author often choosing his or her own notation to derive a solution. This makes them difficult to integrate within the present work, which relates not only to mathematical solutions for practical problems, but also to the organization of data structures for the modeling of groundwater flow. It should also be mentioned that 3D data structures are thus far quasi inexistent in common GIS tools: these structures generally rely on a 2D+$\frac{1}{2}$ dimension representation, where the third dimension is approximated by layers, which amounts to a discretization. As a result 3D solutions are set outside the scope of the present work.

This reduction of the problem to 2D settings only implies that specific tools may be introduced which use the assumption of independence of the solution from the third, vertical, dimension. In some cases, these solution may also be used for 2D-flow in the vertical plane, where solutions are assumed to be independent of one of the two horizontal coordinates instead.

The complex variable for 2D flow

One of the most interesting tools is complex calculus. It is based on the existence of a number, noted i such that $i^2 = -1$. This number falls outside of the set of real numbers, and it is possible to construct a complete field $\mathbb{C} = \{z = x + i * y, (x, y) \in \mathbb{R}^2\}$, with additive and multiplicative laws appropriately defined; such definitions may be found in most complex analysis textbooks, such as [48, 1]. The variable $z = x + i \cdot y$ is called the complex variable for 2D flow; it is in no way related to the elevation above the confining layer of an aquifer.

In the case of an aquifer with constant anisotropy of hydraulic conductivity, z may be defined in a slightly different way, so as to account for the anisotropy and yet reduce the flow equation to those of the isotropic case: see [51, p211] for the definition of a new referential (X, Y), and define $z = X + i \cdot Y$.

The advantage of using the complex variable is that, in the case of non-divergent irrotational flow, the scalar potential and the third component of the vector potential that solve equation 3.4, are conjugate harmonics -see e.g. [51], [7] or [61]-, so that they may be written as the real and imaginary part respectively of a complex function of the variable z, named the complex potential:

$$\Omega(z) = \Phi + i \cdot \Psi \tag{3.22}$$

As a result, all superpositions may take place in the complex plane, rather than in the $\mathbb{R}^2$-plane, which in practice is much easier to perform. also, the isopleths of Psi turn out to be the streamlines of the flow, so that existing contouring algorithms may be used to trace them. Finally, a function W may be defined as:

$$W(z) = -\frac{d\Omega}{dz} = -\frac{\partial \Phi}{\partial x} + i\frac{\partial \Phi}{\partial y} = Q_x - i \cdot Q_y \tag{3.23}$$

which renders the computation of the discharge vector extremely easy to perform analytically, thus reducing numerically errors commonly associated to differentiation. These benefits may be perceived as outweighing the drawbacks of the assumptions required for the complex potential to exist, and justify their use in the present work.

Functions associated to elements

The following three basic solutions are provided here to illustrate the ease with which basic functional bases may be found. An example follows, showing a practical possible use of the solutions.

- Wells and dipoles

  Also referred to as point singularities, wells and dipoles originally derive from the fundamental solution of Laplace's equation in 2D, with withdrawal of water at discharge Q located at point $z_k = x_k + i \cdot y_k$:

$$\Delta\Phi + \Delta^k = 0 \tag{3.24}$$

  with:

$$\forall z \neq z_k \in \mathbb{C}, \Delta^k = 0 \tag{3.25}$$

$$\int_{\mathbb{R}^2} \Delta^k d\sigma = -Q \tag{3.26}$$

  the real scalar solution to this problem, as provided by e.g. [10] or [43] , is:

$$\Phi = \frac{Q}{2\pi} \ln(r) + C, r = |z - z_k|, C \in \mathbb{R} \tag{3.27}$$

  which may also be expressed as the real part of the following complex potential:

$$\Omega(z) = \frac{Q}{2\pi} \ln(z - z_k) + C, C \in \mathbb{C} \tag{3.28}$$

  A dipole is derived from the solution of the well problem. Detailed descriptions may be found in e.g. [51] or [35]. The principle is to superpose the complex potentials of two wells of opposite discharge rate, placed symmetrically about a point z_p, and to define the complex potential of the dipole as the limit of the sum as the distance between the wells and the point reduces to zero. In the limit, the product of the discharge by the distance to the point is assumed constant:

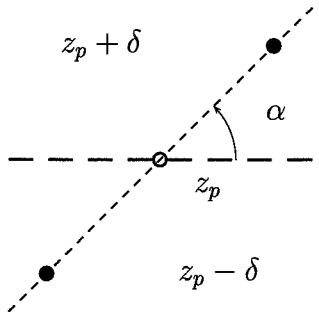

Figure 3.1: Setup for derivation of a line dipole

$$\Omega(z) = \lim_{|\delta|\to 0, Q\cdot\delta=-\sigma} \frac{Q\cdot\delta}{\pi} \cdot \frac{\ln(z-(z_p+\delta)) - \ln(z-(z_p-\delta))}{2\delta} = \frac{\sigma}{\pi}\cdot\frac{1}{z-z_p} \tag{3.29}$$

Dipoles are used to locally direct the flow, as they create a singularity by absorbing water on one side and producing the same amount on another, at an angle $\alpha = \arg(\sigma)$, thus producing a local preferential channel. Mostly, dipoles are used in distributions along a line, to create such local flow modifying features as cracks or barriers. A major difference between the well and the dipole is their behavior as z becomes large: this *behavior at infinity* is an important characteristic of analytic elements as it informs the modeler on the global effect of an element on his model. Wells produce an infinite response at infinity, but in a weak [2], logarithmic manner; this logarithmic behavior is observed for all elements that draw water out of an aquifer. Dipoles on the other hand tend to zero as z gets large. It is a characteristic of very local features.

- Uniform Flow

It is possible to construct an element analogous to the dipole, but at infinity. The derivation is almost identical, except for the fact that δ as defined in figure 3.1 grows to infinity, and the ratio $\frac{Q}{2\pi\delta}$ is kept constant at $-\overline{Q_0} \in \mathbb{C}$. Equation 3.30 gives the result of the computation to the limit, up to an imaginary constant, which may always be ignored.

$$\Omega(z) = -\overline{Q_0}\cdot z + C, C \in \mathbb{C} \tag{3.30}$$

[2]The choice of the term weak is made here because the logarithm is weaker than any power of z, i.e. $\forall\beta \in \mathbb{R}^*, \lim_{|z|\to\infty} \frac{\ln(z)}{z^\beta} = 0$

The complex discharge function W may also be computed, following equation 3.23:

$$W = \overline{Q_0} \tag{3.31}$$

It is a complex constant, and corresponds to a constant discharge vector at infinity. In modeling, this element is used to represent a uniform flow field, which may constrain elements. It is commonly used by researchers to test new elements. It may also be particularly useful in small studies of the interaction between a small well and the aquifer: A uniform flow may be determined by three non-aligned measurements, thus providing a general field of flow, upon which a well may be superposed. Figure 3.2 shows the flow-net produced by such a setting. Dashed lines are piezometric contours, solid lines are streamlines.

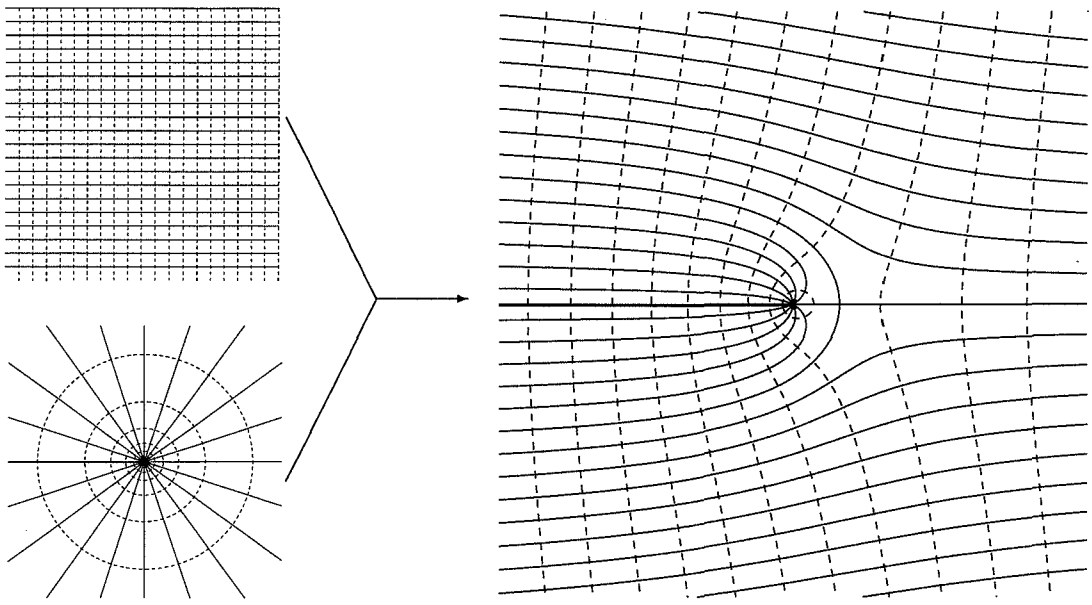

Figure 3.2: A well in uniform flow, produced by superposition of solutions 3.30 and 3.28

- Line elements

Line elements are the third type of basic line element relevant with the present dissertation. Others exist, such as area elements used for representation of ponds and such elements that produce divergence over specific areas; The reader is referred to [51] or [31] for details on these elements.

The concept of line elements is to derive the complex potential for singularities distributed along lines. This is achieved by considering the superposed influence of many similar elements placed along that line: a line-dipole can thus be seen as a string of dipoles along line. If the strength of each elementary dipole located at point $\delta \in [z_1; z_2]$ is $\frac{-1}{2i}\lambda(\delta)d\delta$, then the principle of superposition relates the complex potential of the line dipole to the Cauchy Singular Integral:

$$\Omega(z) = -\frac{1}{2\pi i}\int_{z_1}^{z_2} \frac{\lambda(\delta)}{z-\delta} d\delta \tag{3.32}$$

It is possible to introduce a local variable complex variable Z which maps the segment $[-1; +1]$ in the complex plane to $[z_1; z_2]$ in the physical plane. A simple linear transformation suffices whenever $z_1 \neq z_2$.

$$Z = \frac{z - \frac{z_2+z_1}{2}}{\frac{z_2-z_1}{2}} \tag{3.33}$$

Applying this transformation to both z and δ in eq.3.32, the complex potential of a line dipole may be written as:

$$\Omega(Z) = -\frac{1}{2\pi i}\int_{-1}^{1} \frac{\lambda(\Delta)}{Z-\Delta} d\Delta \tag{3.34}$$

In the present work, upper case lettering will refer to the local plane while lower case will refer to the global physical coordinates, unless specified otherwise. For the sake of simplicity of notation, no distinction in symbols is given between functions that act on various representations of the same variable. Thus, the complex potential Ω generated by any element at a point defined by $(x, y) \in \mathbb{R}^2$ in the traditional cartesian coordinate system or by $z \in \mathbb{C}$ in the physical complex plane or by $Z \in \mathbb{C}$ in the local complex plane will be designated by the same letter regardless of the chosen representation: $\Omega(x, y) = \Omega(z) = \Omega(Z)$

As proven in [51], assuming $\mathcal{D}$ is the domain of analyticity of λ, it follows that:

$$\exists q \in \mathbb{C}^{\mathbb{C}}, \forall z \in \mathcal{D} \cap \{\mathbb{C} \setminus [z_1; z_2]\}, \quad \Omega(Z) = \frac{1}{2\pi i} \cdot \left[\lambda(Z) \cdot \ln\left(\frac{Z-1}{Z+1}\right) + q(Z)\right] \tag{3.35}$$

The function q depends on the jump function λ only. It guarantees that the behavior of

the complex potential as $|Z|$ gets large remains consistent with the expected behavior: a sum of poles behaves at infinity like a pole, and therefore:

$$\Omega(z) \underset{|z|\to\infty}{\propto} \frac{1}{Z} \tag{3.36}$$

Similarly, it is possible to consider a sum of wells along a line segment; the elements thus constructed is called a line sink. However, as argued in [35], most arguments made based on the line dipole carry over to the case of a line sink by considering an integration by parts on the complex potential of the line sink of strength σ:

$$\Omega(z) = \frac{1}{2\pi}\int_{z_1}^{z_2} \sigma(\delta)\cdot \ln(z-\delta)\, d\delta \tag{3.37}$$

$$= \frac{1}{2\pi}\cdot\left[\lambda(z_2)\ln(z-z_2) - \lambda(z_1)\ln(z-z_1) + \int_{z_1}^{z_2}\frac{\lambda(\delta)}{z-\delta}d\delta\right] \tag{3.38}$$

$$\text{with } \left.\frac{d\lambda}{dz}\right|_{z\in[z_1;z_2]} = \sigma(z) \tag{3.39}$$

The last integral in eq.(3.38) is of the same form as eq.(3.32), thus establishing the link between line sinks and line dipoles.

Traditionally, line-sinks were used with constant strength, a single coefficient which was adapted to fit the boundary conditions at a single point in the middle of the element. With faster computers came a better representation of the strength σ with linear and quadratic approximations, using the end points as locations for meeting the boundary condition as well as the mid-point for the quadratic case. This logically resulted in the method of collocation, popular in boundary methods, for representation of higher degree: the coefficients of a polynomial of degree N representing the strength were chosen to fit the boundary condition exactly at N uniformly spaced points along the line. This method produced accurate results at the time, but became intrinsically limited and did not benefit from the improvement of computers as much as domain methods, which may explain why many people lost interest for boundary methods.

3.2 Recent Advances

The purpose of this section is to introduce some of the recent concepts and advances in the field of the analytic element method. This section neither claims to be an exhaustive or a *best-of ...* list, but instead introduces such concepts as are either discussed or used in chapter 4.

3.2.1 Over-specification

The concept of over-specification is to be contrasted with collocation, mentioned in 3.1.3. It is a method related to the solving mechanism of high degree elements, with 20 or more degrees of freedom.

The failings of the collocation method

The collocation method fails when the number of unknowns gets large: as they are fitted to meet the specified values exactly at the specific locations, error appears between the collocation points and at the ends of the fitting interval. This is particularly problematic for the analytic element method, because it relies heavily on the correct representation of singularities at the tips of its elements. Particularity pathologic is that increasing the degree of the element, i.e. adding degrees of freedom does not always reduce the error, and often even increases it -see fig. 3.3 for a simple example, and [6] for an excellent demonstration with inhomogeneities.

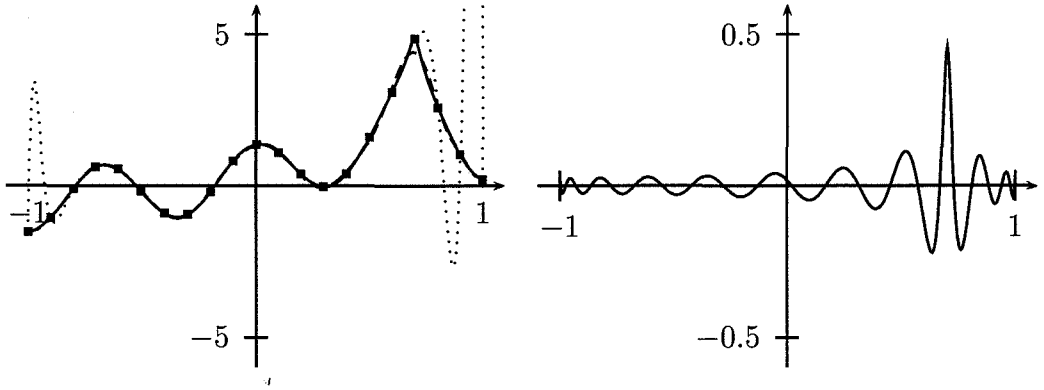

(a) fitted curve (b) overspecification error, zoom ×10

Figure 3.3: a function and fitted polynomials of degree 21, (a) function $F(x)$ -solid-, collocation fit $P_C(x)$ -dotted-, over-specification fit $P_O(x)$ -dashed-, (b) error $F(x) - P_O(x)$

To resolve this problem, Janković, in [31], proposes several tools to improve the overall error between the fitted and actual curves:

- orthogonal functional bases, which are more accurate for fitting problems
- solve the problem in the least square sense, by spreading the error throughout the fitting interval. This is achieved by setting a system of equations similar to that used in collocation but with many more points than unknowns: the system is over-specified; the points are called control points, rather than collocation points since the functions do not usually coincide there.
- optimized location of control points.

Solving for unknowns in the least squares sense

The principle of solving in the least square sense is well known in fitting theory, as is evident by its presence in popular numerical analysis books -see e.g. [45]. It is even mentioned in a few boundary element texts - see [12, 43]-, but usually as a side note, a point of interest that is rarely implemented. Solving for the unknowns in the least square sense is achieved by establishing an over-specified equation system -see 3.2.1- relating the vector of N unknowns λ to the M values to attain $\mathbf{v}$ by an M by N matrix $\mathbf{S}$:

$$\mathbf{S}\lambda = \mathbf{v} \tag{3.40}$$

The inversion of this system may not be operated exactly, since $\mathbf{S}$ is not square. This problem is circumvented by left multiplication by the transpose $\mathbf{S}^T$, and inversion of the square matrix $\mathbf{S}^T\mathbf{S}$, so that:

$$\lambda = \left(\mathbf{S}^T\mathbf{S}\right)^{-1}\mathbf{S}^T\mathbf{v} \tag{3.41}$$

It is possible to impose a value at any given point -collocation at that point- using the technique of Lagrange multipliers -see [31, 11]. This is particularly helpful for the purpose of obtaining the correct singularity at the tips of line elements. Figure 3.3(b) shows the error between a function and a polynomial fitted with over-specification, to be compared with fig.3.3(a). More

details on over-specification are offered in 4.5.2, where it is used in the context of the presented research.

3.2.2 Superblocks

The concept of superblocks is detailed in [41]. Their purpose is to increase both the capacity [3] and the speed of computation of analytic elements models.

Superblocks rely on the fact that the superposition of analytic functions is an analytic function itself. It can therefore be expanded as a Laurent series outside of the smallest circle that contains all the singularities that generate the function. It can be expanded as a Taylor series within any disk that does not contain any singularities.

The approach in [41] allows the use of superblocks for all element geometries known in the AEM, at the step of evaluation of the complex potential and discharge function, as well as during the phase of resolution of unknown coefficients.

In principle, the complex potentials associated with each element that falls strictly within a given square block of the physical domain to be modeled have their sum represented outside of the circle that circumvents the square as a Laurent series. The sum of the potentials of the elements outside of that circle is represented inside as a Taylor series.

Thus, for a point inside the block, the total complex potential is evaluated as the sum of complex potentials generated by all the elements that are not outside of the circle plus the value of the Taylor series. Outside, the value of the Laurent series is added to the influence of all the elements not inside the circle.

In large models, the capability to locally represent the influence of a large number of elements as a single series can dramatically reduce computational time, thus allowing either refinement -thus increasing model capacity-, or faster response time of the model -i.e. increasing speed.

3.2.3 Curvilinear elements

Curvilinear elements are elements defined along one dimensional features that are not necessarily straight. Traditionally, such boundaries are replaced by a string of lines, usually chosen as

[3] number and degree of elements in the model

chords of the actual locus of the boundary. This has a major drawback, as the number of line segments rapidly becomes large, as demonstrated by the Weierstrass Approximation Theorem -see [9, 22]. This is especially true in the case that the boundary has a small radius of curvature.

In order to reduce the number of line segments used to represent a boundary, or to obtain smooth boundaries, elements were created that have non-straight geometries. Prior to the research presented in this thesis, the published available geometries are circular and hyperbolic arcs. Some of the latter's applications include the modeling of leaky walls [29], and of a free surface [19].

These elements are discussed in detail in the chapter 4.

3.2.4 *Not-So-Analytic* Elements ?

In many cases that fall outside of the scope of the present work, elements may be defined and used in the context of the analytic element method that do not have an analytic complex potential.

Indeed, elements with analytic complex potential are available only in the case of Laplace's equation, which would be truly limiting for the modeling of actual flow problems.

Most notably is the case of the *Area-sink* -see e.g. [52], [51]-, used to represent an area where infiltration occurs. These elements do have a real potential, which fits the definition of a real analytic function -see [9]: they possess derivatives at all orders and agree with their Taylor series locally.

The realm of problems that these functions make accessible include problems with specified infiltration, leakage between aquifer layers, flow with continuously varying fluid density, in aquifer with continuously varying hydraulic conductivity, etc.

The two points below are offered as insights in the current developments on some of the fundamental research on the analytic element method. The published material is very limited, as they regard on-going research; they provide a sense of the direction taken and of the extended capabilities that the method should reach in practice in the near future.

Using Helmholtz's Theorem

As mentioned in eq.3.4, the specific discharge, like any vector field, may be represented as the sum of the gradient of a scalar function, the potential in irrotational flow, and the curl of a vector function, the vector potential in divergence free flow -see [52]. In two dimensions, the latter reduces to a scalar function as well, which identifies with the stream-function in the case of Laplace's equation.

Producing area elements for divergent types of flow is already possible, but has remained a topic of research as the complexity and range of modeling needs has expanded.

Rotational flow had been dismissed until the implications of Helmholtz's theorem in the AEM were fully realized. Functions developed for divergent flow will be readily available for rotational flow, as, in two dimensions, only a multiplicative factor of the imaginary i separates the two classes of problems. This *re-discovery* widens the scope of the AEM while reusing previous work.

Using Wirtinger Calculus

The functional analysis method by which a complex variable $z = x + i \cdot y$ and its conjugate $\bar{z} = x - i \cdot y$ are taken as independent variables is known as *Wirtinger Calculus*, as communicated by Barnes -personal communication,2000- and Strack [55].

One of the features of this analysis is that the Laplacian operator may be expressed as:

$$\Delta = \frac{\partial^2}{\partial x^2} + \frac{\partial^2}{\partial y^2} = 4 \frac{\partial}{\partial z} \frac{\partial}{\partial \bar{z}} \tag{3.42}$$

This identity was used in [39] to derive the potential associated with a circular area sink where the infiltration was represented as a polynomial of the variables $(z, \bar{z})$, although the research was initiated prior to the realization of the link between 3.42 and Wirtinger Calculus.

The value of this method is in the ease it offers to create elements with non-zero divergence or rotation. Indeed, if the divergence $\gamma = -\Delta\Phi$ is known, then the potential is:

$$\Phi = \frac{1}{4} \int \int \gamma dz d\bar{z} \tag{3.43}$$

up to an harmonic function.

The combination of Helmholtz's theorem and Wirtinger calculus will enable the creation of new solution and elements that will enable the expansion of the AEM within the field of modeling of groundwater flow as well as to areas of engineering where the accurate representation of 2D vector fields is required.

3.3 Examples of basic elements

The following is a set of flownets produced using basic analytic elements. Solid lines are lines of constant stream function, dashed lines are piezometric contours, unless specified otherwise.

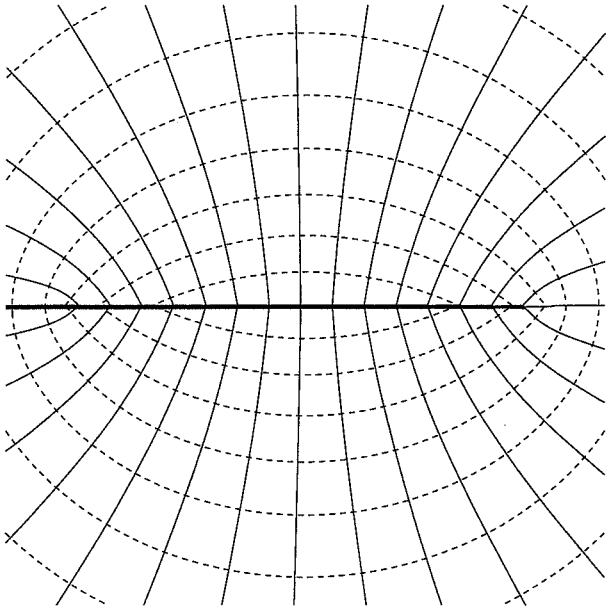

Figure 3.4: Isolated constant strength line-sink

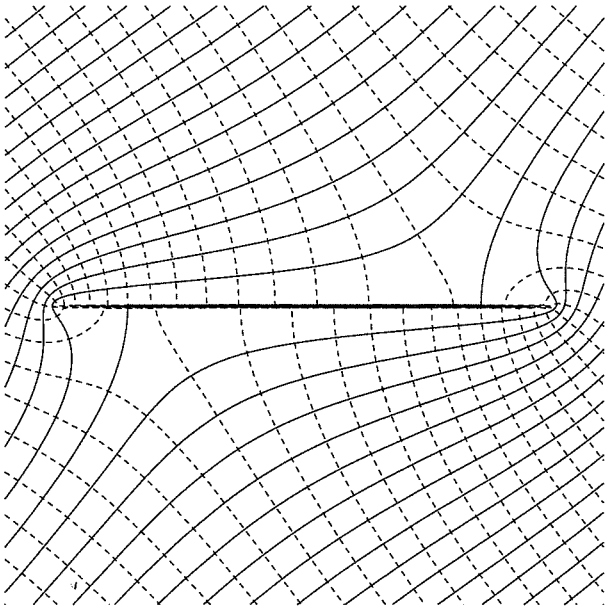

Figure 3.5: Impermeable barrier in uniform flow

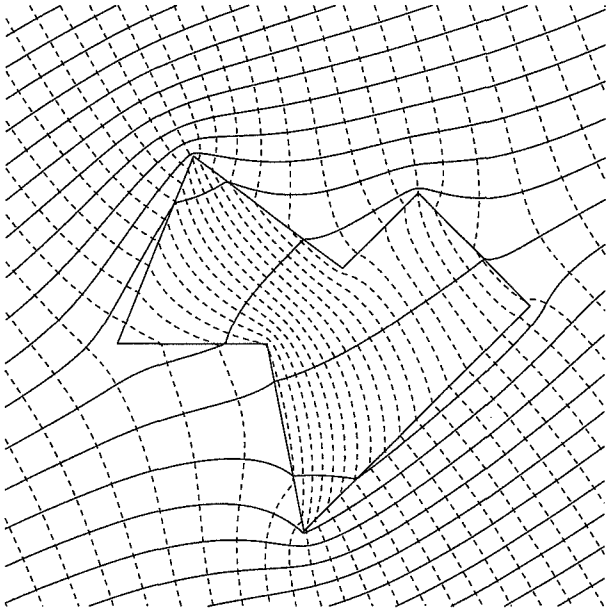

Figure 3.6: A zone of low permeability ($\frac{k_{in}}{k_{out}} = .1$) in uniform flow

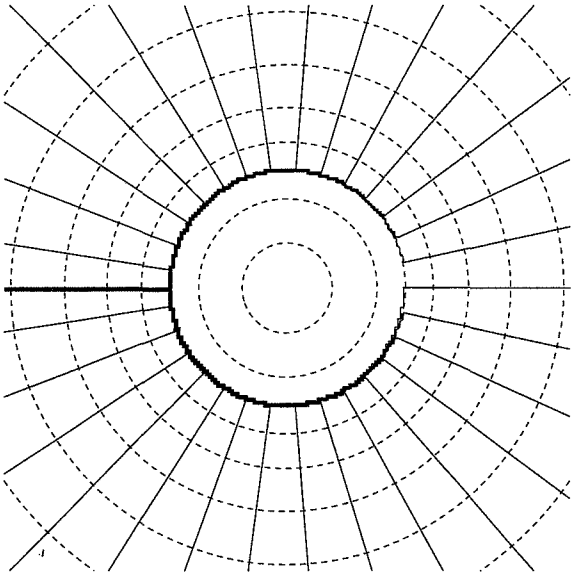

Figure 3.7: A circular area of infiltration. The stream function is not defined inside.

Chapter 4

Analytic elements along curved shapes

Synopsis

Purpose: This chapter details the geometry and use of curvilinear elements in the Analytic Element Method. It provides an extended set of geometric description for data, allowing a richer object description to be used in the AEM.

Outcome: General and existing geometries are represented in a concise format, the Rational Bézier curves. Solutions and algorithms are provided for that specific case and a methodology is derived for resolution of coefficients for the process model. The computation of these functions is slow and requires improvements to enable them as practical tools, provided in chapter 5.

The choice of managing information for the modeling of groundwater flow with GIS tools leads to the introduction of complex geometries for the representation of some features. In particular, smooth boundaries, such as those that may be obtained as the output of a GIS, are appealing to model designers. A new set of boundary shapes is offered that satisfies the appeal of smooth shapes and does not disrupt the boundary value problem. This implies:

- providing a detailed description of the capabilities of such a new geometry and showing how it can be used to incorporate existing boundary shapes, such as straight line and circular or hyperbolic arcs.

- deriving the complex potential, which is needed to incorporate the element within the analytic element method.

- offering a method for the local resolution of the boundary value problem which is not disruptive to the global solution of a model.

Thus, this chapter provides a description of the geometry and modeling capabilities of Rational Bézier Splines, and relates them existing curvilinear elements. Mathematical functions and algorithms necessary for the computation of a complex potential associated with these elements is provided for their implementation into AEM code. Results are illustrated by textbook examples, with a validation of the mathematics in an ideal setting.

Résumé en Français

Objectif : Ce chapitre détaille la géometrie et l'utilisation d'éléments curvilinéaires dans la méthode des éléments analytiques. Il fournit un ensemble étendu de descriptions géométriques pour des données, permettant une description objet plus riche à utiliser avec l'AEM.

Résultat : Les géométries générales et existantes sont représentées dans un format concis, les courbes rationelles de Bézier. Solutions et algorithmes sont fournis pour ce cas, et une méthodologie est dérivée pour la résolution des coefficients pour le modèle de processus. L'évaluation de ces fonctions est lente et requière des améliorations pour permettre leur utilisation dans la pratique, améliorations fournies au chapitre 5.

Le choix de gérer l'information pour la modélisation des écoulements souterrains avec des outils SIG conduit à l'introduction de géométries complexes pour la représentation de certains traits du domaine physique à modéliser. En particulier, les frontières lisses, telles qu'obtenues en sortie de SIG, sont attirantes pour certains concepteurs de modèles. Un nouvel ensemble de formes est offert qui satisfait le critère attirant des courbes lisses, et ne perturbe pas le problème de valeur aux limites. Ceci implique :

- la fourniture d'une description détaillée des possibilités d'une telle géométrie, et la démonstration

de la façon dont elle incorpore les formes déjà existantes, telles que segments de droite et arc de cercle ou d'hyperbole,

- la dérivation du potentiel complexe associé, nécessaire à l'incorporation de l'élément dans l'AEM,
- la proposition d'une méthode pour la résolution locale du problème de valeur aux limites qui ne perturbe pas la solution globale d'un modèle.

Ainsi, le présent chapitre fournit une description de la géométrie et des capacités de modélisation des splines Rationelles de Bézier, et les relie aux éléments curvilinéaires existants. Les fonctions mathématiques et algorithmes nécessaires pour le calcul du potentiel complexe associé à ces éléments sont fournis pour être implémentés dans tout code informatique des AEM. Les résultats sont illustrés par des exemples *d'école*, avec une validation des mathématiques dans une situation idéalisée.

4.1 Curvilinear shapes in the Analytic Element Method

Commonly, the Analytic Element method relies on the use of pieces of straight lines to represent the boundaries where a condition is imposed. There is no actual restriction to such shapes however, since the potentials for line-sinks and line-poles are actually derived from the Cauchy Singular Integral, which may be operated on any Jordan curve - smooth, compactly supported contour: see [40]. In [51], a statement is made admitting the limited relevance of non-straight elements in the context of regional modeling, but specific applications may make such elements desirable.

4.1.1 Reason for existence

The main purpose of curvilinear elements, elements along non-straight pieces of lines, seems to be used as connectors between regular line elements when an abrupt corner is unacceptable. In such a situation, the velocity of the flow is locally forced to infinity, because the direction of flow changes abruptly. This behavior is consistent with the exact analytical behavior, as may be illustrated by the flow around a corner; however, the way in which infinity is reached, the type of the singularity at the corner, is not usually represented exactly. Although this behavior

is acceptable for the mathematician, it is not for the modeler. Not only does it imply a local violation of Darcy's law, which is only valid for low Reynold's numbers and thus low velocities, it may also make the results of the model unusable in the vicinity of the singularity located at the corner point. In regional modeling, this may be inconsequential, because of the focus on the *big picture* rather than on the details, but in local modeling, this behavior may result in false interpretation of the model, and thus lead to wrong decisions in water management projects. Two solutions are available to the modeler, which both stem from the need to better represent the boundary: firstly, one may choose to use many more line segments locally, thus improving the resolution of the representation of the boundary, but at some scale, the issue of undesired singularities still exists. Secondly, one may choose a better, smoother geometry to represent the boundary, in the hope of removing the singularity from the velocity field. Focusing on the latter, elements have been provided that may be used to replace the tip of line elements and allow their smooth connection. Two such elements have come to the attention of the author: pieces of circular arcs, and pieces of regular hyperbolae, herein referred to as hyperbolic arcs. The most used AEM program, MLAEM, makes use of the latter.

4.1.2 The circular arc

The circular arc element is detailed extensively in [51], section 41, based on the work of [19]. To summarize, a bilinear -and therefore bijective- transformation is derived that maps the line-segment $[-1, 1]$ in the ζ-plane into the desired circular arc in the physical domain.

By placing a standard straight line element in the ζ-plane, such as a line-dipole, a circular arc element is obtained in the physical domain - up to a constant. The jump across the arc, in the direction normal to the arc at each point is directly related to the jump across the line element at the corresponding point in the ζ-plane, thus allowing control of the boundary condition along the arc at the same precision as can be achieved with line elements.

Circular arcs are a powerful tool to achieve the connection of two straight line elements, limited only by their fixed radius of curvature.

4.1.3 The hyperbolic arc

The hyperbolic arc is the more sophisticated of the two curvilinear elements presented here. It is arguably more *tricky*. Detail on these elements may be found in [42] and [53].

The elements relies on a quadratic mapping that links the *normalized* Z-plane and a ζ-plane in which most calculations occur:

$$\zeta = \Gamma\left(Z^2 - 1\right) + Z \tag{4.1}$$

In the case of the hyperbolic arc, the desired curve maps onto the line segment $[-1, +1]$ -as is becoming customary-, but there is no unique mapping back from that segment onto the Z-plane. Indeed, the line segment maps back not only to the desired boundary, but also to a second piece of hyperbola, symmetric to the original with respect to its origin. Because of arbitrary limitations placed upon the element -namely the fact that the hyperbola is regular-, the following can be demonstrated:

- the desired boundary is always included within the unit circle in the Z-plane - see [35]

- the second possible image of the line segment is outside of the said unit circle. This is a consequence of the above-mentioned symmetry.

It follows that the complex potential associated with the element is associated to the complex potential of a line element in the ζ-plane when Z is within the unit circle, and that an analytic continuation can be provided as a Laurent series in Z outside, a *far-field* expansion. Thus, an element is constructed that is analytic everywhere but along the desired piece of hyperbola. Using the theorem of unicity, the derived solution is the only possible solution.

The element is limited by the acceptable representations for the jump function, and by the fact that improvements to the line element cannot be carried through directly to this hyperbolic arc element without some analysis, particularly for the far-field expansion.

4.1.4 Remarks

Mapping based elements

The general concept behind the derivation of the complex potential for the existing curvilinear analytic elements is the use of a conformal map -i.e. a bijective complex function- that transforms the chosen boundary shape into a straight line segment: the circular arc uses a bilinear transformation, while the hyperbolic element rests a particular quadratic map and one of its two possible inverses. The direct consequence is the difficulty in producing varied shapes; controlling both the map and its inverse often requires implementation for each specific type of shape, and generalization is difficult.

Another issue is that the correction function is related directly to the type of representation chosen for the jump function as well as to the mapping used for the representation of the boundary. As a result, improvement accomplished in computing the straight line element with various representations of the jump functions may not be directly applicable to the curvis, because the correction function must be re-derived for the new representation. In all likelihood, a curvi will still use the power basis functions, and force any other representation to be projected on that basis before using it. As a result, all the limitations of the power basis functions will still apply to the curvis. It is also possible to envision using alternate representation for the jump function along a hyperbolic arc, such as rational functions: in that case, a correction function would have to be derived specifically for the arc, without regard for the correction function already derived for the straight line case.

Geometric limitations

Given two lines that have to be joined with a smooth corner, either one of the representations allows at most one choice, and sometimes requires the use of more than one element. Indeed, in order to achieve continuity of the boundary, the end points are fixed, and the orientation of the lines to be connected determine the directions of the tangents to the curvi at the end points, thus using the two degrees of freedom available in either case. Regarding strings of curvilinear elements, the modification of a single parameter on one of the pieces of the structure impacts every piece of the string: this renders such construction somewhat cumbersome.

Other branches of engineering have been faced with issues, of limited geometric capabilities for design, and alternative solutions have been found: the automotive industry in particular has been innovative in providing new shapes classes to its designers that could still be properly handled by its engineers. One must recognize the need in such industry for designer artistic freedom, because it usually leads to better sales, which does not exist in groundwater: the look of the boundary is far less consequential in a groundwater model than the shape of the body is in a car, in terms of customer approval. However, by limiting the capacity of the model designer to implement his conception of reality, his conceptual model, the results of the groundwater model are only approximately the answers sought by the decision maker. If a *better* answer is to be provided, a better implementation of the conceptual model - that is one less limited by the intrinsic restrictions of a tool or another- should be sought. By enhancing the number of shapes available to represent the boundaries of a problem, thus offering the possibility of a better fit of the conceptual boundaries, one allows the construction of better models. The following details the development of such elements, along geometrically diverse boundaries, which do not suffer from the restricting limitations of the current curvilinear elements.

4.2 B-Splines shaped boundaries

The purpose here is not to give an exhaustive description of the geometry of B-Splines, but instead to introduce them and to show their relevance in the design of groundwater analytic element models. For details on the actual geometry and versatility of these shapes, the reader is referred to [22] for a textbook-like introduction and to [44] for a complete presentation. Instead, the following focuses on introducing B-Splines, on showing how the most mathematically complex category of such splines may be represented using a simpler class of curves, and on the geometric features that they provide.

4.2.1 An introduction to B-Splines

Splines originally stood for *Smooth Polynomial Lines*, although this is actually debated. What is commonly accepted is that splines are continuous smooth parametric curves or surfaces defined by a piecewise polynomial parametric function. Smoothness has actually become optional:

many curves have the ability to *break*, that is have an abrupt jump in the direction of their tangents at any given location. The functional basis used to define the curve has been expanded from polynomials to include all rational functions, i.e. ratios of polynomials.

The most widespread splines are used to model one dimensional functions in terms of their variable. For example, computing a numerical integral using Simpson's method uses piecewise quadratic representation of the integrand. Commonly used in function fitting are the Hermitian and cubic splines. In the one dimensional case, the parameter of the spline is replaced with the variable of the function.

For $n > 1$ n-dimensional splines are defined using n functions of the same parameter, usually named u or v. In the case $n = 2$, a point (x, y) on a spline would be defined by:

$$\forall u \in [u_0, u_1], \begin{bmatrix} x = x(u) \\ y = y(u) \end{bmatrix} \Leftrightarrow z = x + iy, z = z(u) \tag{4.2}$$

so that the two real functions may be replaced by a single complex parametric map. This feature is extendable to three and four dimensions, using quaternions; it is one of the keys to implementation of modern splines -see [44]-. Being able to represent the set of points on a curve as a complex parametric function is the feature that allows the derivation of the complex potential associated to spline shaped elements. This point is emphasized in 4.3.

History

Splines were originally designed for the automotive industry. Unlike most technical advances, they were derived not for the benefit of engineers, but to allow designers to expand their ideas onto a framework that could later be used to actually manufacture a vehicle. The new, more complex curves, first developed by French engineer Pierre Bézier for Renault, allowed the introduction into the market of smoother, rounder cars, that followed closely the vision of the designers.

Since the *liberation* of the automotive designers, Bézier curves and their successors have enabled the representation of many objects where a designer uses a computer tool: Graphic arts, notably for the entertainment industry, architecture, molding industry, and so on have all

integrated these curves to some degree.

Even in geomatics, the science behind modern GIS, these curves are sometimes used to represent linear information. Topographic maps, for example, may include contour levels defined as NURBS curves. It is therefore logical that applications seeking to inter-operate with GIS would attempt to incorporate NURBS shaped features as part of their input; this argument is reinforced in the case of groundwater modeling, as the expansion of the shapes available to the model designer may free him the way it freed his counterpart in the automotive industry.

Geometric considerations

The range of shapes that splines can represent is vast, if not infinite. Any continuous curve which can locally be represented as a polynomial parametric function can be associated with a spline that will match it up to an arbitrary precision; this is a consequence of Weierstass's approximation theorem - see [9]. Notable exceptions are fractal curves.

Although it is not always the best choice, because of storage requirement or because of the time necessary to display them through direct evaluation, splines are usually preferred in applications where the representation of the curvature of the curve matters as much as its location; as shown in [22], a spline converges faster to a desired continuous curve than a string of line segments whose vertices are constrained to lie on the curve.

Splines are described mathematically as parametric curves in an n-dimensional space with an array of piecewise polynomial functions, as outlined above. The shape of the spline is controlled through many parameters; all splines have a set of control points and a degree. Below, the exhaustive list of controlling parameters is detailed for NURBS, the most general instance of splines.

Geometrically, the main consideration is that the designer of a spline may control not only locations through which the spline must pass, but also the slope of the spline. This allows for the creation of such shapes as circles, general closed curves -sometimes referred to as *potatoids*-, looping elements, or even straight lines. Not all these shapes are acceptable in the context of the analytic element method: indeed, an hypothesis of the method used in the following to compute a complex potential is that the curve be of Jordan type -see [40]- which excludes self intersecting curves. Looping elements, or folding elements, in the sense defined in [35], are both

explicitly prohibited for the following derivations to hold true. It is pointed out that the same solution as the case of intersecting line segments is acceptable: the element may be broken up into pieces that do not cross each other; a node must be inserted at the intersection -see figure 4.1 for an example.

Categories of Splines

There are many categories of splines. The most common are presented in the following list, along with a few comments as to their relevance in this dissertation:

- Hermitian splines -often used in their cubic forms-, are piecewise polynomial lines forced to pass through specific points. They are largely used to represent injective functions, and are usually parametrized by the variable x, so that $y = y(x)$. Little control is provided on the derivatives. These splines offer a smooth curve passing through given locations, and are sometimes used in curve or data fitting. Such splines have little interest in the present context. They can be represented by any other type of spline if required; issues specific to these splines are ignored in the rest of the dissertation.

- Bézier curves are the original tool invented by Pierre Bézier. They are parametrized using the *Bernstein Polynomials* - see [35, eq. 3.10]. The most common type of Bézier splines is the cubic form, controlled by 4 points, which allows the definition of the end points and the tangents at those points. These polynomials are independent of the curve. Derivation of the complex potential associated with Bézier splines of degree 3 or less is found in [35]

- Rational Bézier Curves are an extension of the previous. Instead of the Bernstein polynomial, the basis functional set is extended to specific rational functions which depend

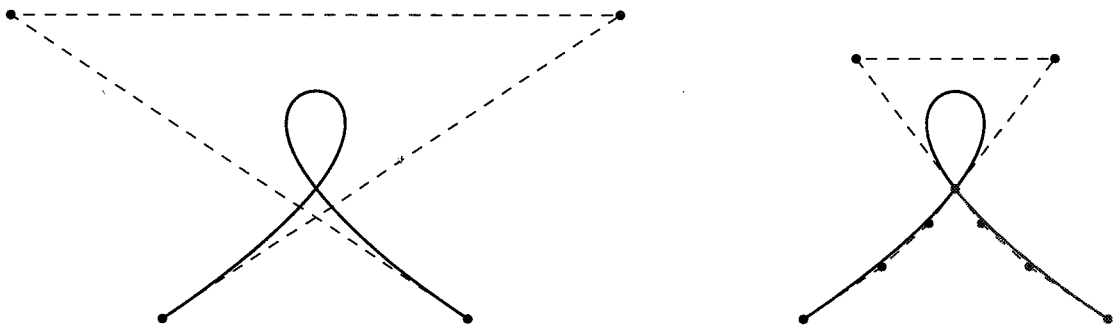

Figure 4.1: A looping spline and the three element used instead to represent the same boundary

on a set of weights, making the functional base dependent on the curve. Such curves offer great flexibility. For practical purposes, such a curve of degree three allows the modeler enough flexibility to represent most boundaries.

- B-splines are inspired from Bézier curves, which they extend by using a different piecewise polynomial basis. A set of values of the parameter, called the knots, is associated to each curve. The polynomials are computed iteratively using a recurrence relation seeded with step functions -see [22] or [44] for illustration.

- Non-Uniform Rational B-Spline curves, or NURBS curves are the most general category of spline to date. They combine the characteristics of both branches of splines evolved from the original Bézier curves: they are parametrized by piecewise rational functions. They have both a set of knots, and a set of weights. All other types of splines may be represented and stored as NURBS: they are the generalized spline.

The two categories of splines considered in this dissertation are the NURBS and the Rational Bézier curves: the former for its versatility in the design process, the latter because its particular mathematical representation allows the -relatively- easy derivation of a complex potential for a singularity distribution along such a shape.

4.2.2 Relating NURBS curves to Rational Bézier curves

The array of the capabilities of Non-Uniform Rational B-Splines far exceeds the scope of this dissertation, and implies a more complex mathematical description. Although such curves are geometrically comparable to simpler classes, especially in terms of the algorithms used to display them via a computer, their representation in mathematical terms requires much care of indices and local parameters which are not relevant to a groundwater model. The following shows how a NURBS curve may be represented as a sequence of Rational Bézier curves, thus allowing the generalization of results obtained for the latter to be applied to the former, should one decide to implement NURBS curve boundaries in a groundwater modeling program.

The parameters of NURBS curves

NURBS curves are determined by many more parameters than any other spline classes. They require all the following:

- an integer, called either the degree or order. This parameter defines the degree of the polynomials to be used as the numerator and denominator of the parametric representations. The degree of either may actually be smaller, for particular choices of other parameters; these *degenerated* cases do not warrant a change in the way the spline is defined or displayed, and are therefore practically inconsequential. All splines have a degree. Any spline may be represented without loss of its shape using a spline of larger degree

- a sequence of control points, with cardinal larger than or equal to the degree of the spline plus one: Bézier splines -standard or rational- have as many control points as degree plus one, B-Splines have more. All valid NURBS are contained within their *convex hull*: the smallest convex polygon constructed with its control points.

- a sequence of weights, one for each control point, all positive for valid splines; a negative weight in an otherwise positive sequence leads to the loss of the complex hull property: the spline may extend beyond its hull. Rational Bézier splines also have weights. NURBS with a constant sequence of weights, i.e. all weights equal, reduce to B-splines.

- a sequence of knots: it defines intervals within which the parametric function used to represent the spline is of the same continuity as the degree d of the curve, i.e. it is d-times continuously differentiable. B-Splines also have a sequence of knots. NURBS of degree d with a sequence of knots of cardinal $2d$, defined such that the first d knots are zero and the last d are 1, reduce to Rational Bézier curves.

Splines of any type may be represented as a special case of a NURBS.

Equivalent sequence of Rational Bézier curves

Rational Bézier curves are NURBS whose knots are all equal to zero or one. It is possible to obtain a list of such curves to represent any NURBS by using the following sequence of

operations, each detailed in [44]:

1. the NURBS curve is subdivided: this is performed by knot multiple insertion at each of the knots of the original curve. For a NURBS of degree p, each of the knots must appear $p+1$ times. Thus, for a regular knot at u_k, which appears once, u_k is inserted p times; for a double knot, u_k is inserted $p-1$ times, and so on. Clamped curves -curves which pass through their first and last control points- already have the correct multiplicity for their first and last knots. This operation results in a new set of control points $\{Q_m\}$; at each of its knots u_k, the curve passes through one of its control points, $Q_{k\cdot(p+1)}$. Sub-curves are defined between each of the original knots: considering knots $\{u_k, u_{k+1}\}$, a new curve $C_k(u)$ is defined by a knot sequence of $p+1$ times u_k followed by $p+1$ times u_{k+1}, and by the control point subset $\{Q_{k\cdot(p+1)}, \ldots, Q_{(k+1)\cdot(p+1)}\}$

2. each sub-curve is rectified by linear reparametrization: its parameter is affinely transformed using $v = \frac{u-u_k}{u_{k+1}-u_k}$. The new curve, defined by the above subset of control points and the parameter v is a Rational Bézier curve.

The operation presented in figure 4.1 made use of this technique, along with knot insertion at the crossing point. It is a good example of subdivision and reparametrization.

4.2.3 Existing curvilinear shapes as Bézier curves

Extensive study of the representatibility of quadratic curves -circular arcs and conics in particular- can be found in [44]. Quadratic rational Bézier splines are shown to enable the representation of pieces of conics. As a result, both the circular and hyperbolic arcs geometries, which have analytic elements associated to them may actually be represented in the framework of splines. Here is presented a summary for these specific shapes. Indeed, consider a conic C defined in the two dimensional plane by the quadratic form:

$$\forall X = \begin{bmatrix} x \\ y \end{bmatrix} \in C, f(X) = X^T A X + B^T X + c = 0 \tag{4.3}$$

where the 2 by 2 symmetric matrix A is defined as: $\begin{bmatrix} \alpha & \beta \\ \beta & \gamma \end{bmatrix}$

and the 2 by 1 vector B is: $\begin{bmatrix} a \\ b \end{bmatrix}$

Such definitions of conics are commonplace, and may be found in most early university level geometry books. One is referred in particular to textbooks used in the French *classes préparatoires*, such as [25]. Using this representation for the conic, and defining the following parameters:

- X_0 and X_2 two points on a conic
- X_1 the intersection of the tangents to the conic at $X0$ and $X2$
- $w_1 = \sqrt{-\frac{f\left(\frac{X0+X2}{2}\right)}{f(X1)}}$, $w_0 = w_2 = 1$

the rational Bézier curves B defined as follows:

$$\forall X \in B, \exists u \in [0,1], X = \sum_{k=0}^{2} w_k X_k R_{k,2}(u) \tag{4.4}$$

exactly coincides with C between X_0 and X_2. This may be verified by substitution of 4.4 into $f(X)$ as defined in 4.3. One should note the restrictions that result from the previous definitions: conic pieces must have end points where the tangents are non-parallel -this implies that a half-circle may not be represented in this fashion- and the particular conic branch represented by the rational Bézier spline is the shortest piece of the conic that connects the two endpoints. An interesting fact is that w_1 may be replaced by its opposite, $-w_1$ to obtain the longer branch, but in doing so one would include a large curve that reaches infinity twice in the case of hyperbolae; splines are traditionally defined for positive weights, so the particular case of negative w_1 is ignored, although it might become useful in the future for the representation of truncated ellipses.

The benefits of having such a representation are twofold:

- firstly, the availability of this representation means that special cases of single isolated features can be developed for comparison with existing solutions. This step of comparison

of solutions is crucial in the Analytic Element Method, as it offers a validation of the newly developed element

- secondly, programmers can consider replacing the existing representation of curvilinear elements with the new, more flexible spline elements while preserving the existing functionality: models using the legacy elements may be reused with the new definition without requiring more effort from the modeler. This backward compatibility feature is necessary before such elements can even be considered for inclusion in existing programs.

The geometric capabilities of NURBS are extraordinary, explaining the success they have had in many fields where human design and perception is involved. From engineers to artists, they have found an audience to make use of their flexibility. However, in the context of groundwater flow, they are not meant to be used only to represent results, but for the modeler to actually define the aquifer features. Given a NURBS curve and the equivalent sequence of Rational Bézier splines, the following provides the derivations needed to effectively solve the Laplace equation with such shaped boundaries.

4.3 Complex Potential of Spline-shaped elements

Computing the complex potential associated with a linear feature is achieved through the computation of the Cauchy singular integral. Several texts may be cited here, but the reader is directed especially to [51] for a description of the use of the singular integral in the specific context of the Analytic Elements Method, and to [40] for proofs and conditions of integrability. The complex potential is defined to solve the Laplace equation exactly within the domain, while satisfying a specific boundary condition, along a specific boundary. Approximation of the actual solution in the AEM is due not to a discretization of the domain, as in the FDM or FEM, but to the choice of the shapes used to represent the boundary, and to the choice of functional bases onto which the boundary condition is projected.

[40] provides the proof of existence of a solution for the case of smooth, non-self-intersecting boundaries - Jordanian curves. However, details for derivation are not provided, since it depends heavily on the curve and its mathematical representation. The present section provides those

details for the case of Rational Bézier curves or sequences of such curves, such as general NURBS curves.

4.3.1 The line-dipole

For the purpose of the present dissertation, only the specific case of the line-dipole along Rational Bézier curves will be provided, as the extension of the derivation to line-sinks is analogous to the case of straight line-segments. Extensions using Wirtinger calculus are also possible, following the guidelines provided by [55] for straight line elements, but such extensions have only been tested by the author for very particular cases and are therefore not reported here; they are considered as beyond the scope of the present work.

The complex potential for a line-dipole may be obtained by integrating the complex potentials of superposed dipoles of elementary strength $\lambda d\delta$ along a curve $\delta \in C$; see 3.1.3 for comparison with the straight line. Since the potential for a dipole of such strength at location δ is:

$$\Omega_{pd}(z) = \frac{-1}{2\pi i} \frac{\lambda(\delta)\, d\delta}{z - \delta} \tag{4.5}$$

the continuous summation can be expressed as the *Cauchy singular integral*:

$$\Omega_{ld}(z) = \frac{-1}{2\pi i} \int_C \frac{\lambda(\delta)}{z - \delta} d\delta \tag{4.6}$$

Equation 4.6 is valid for a straight line segment, and was used as such in 3.1.3. Passing from a discrete sum of point dipoles to a continuous one - an integral - is in fact possible as long as the curve C is smooth and the differential $d\delta$ is defined. The consequence is that the Cauchy Singular integral is defined everywhere except on the boundary itself, as long as C is a Jordanian curve, as defined in [40]. The concept is valid for any strength distribution λ along the curve, whether real -thus providing the line-dipole as defined by Strack-, pure imaginary -giving the line-doublet-, or a general complex function -considered in the present dissertation as leading to the *generalized line-dipole*, or line-dipole in short-.

If the curve C is defined by a parametric function, i.e.:

$$\exists \Gamma \in \mathbb{C}^{[u_l,u_u]}, \delta \in \mathbb{C} \Rightarrow \exists u \in [u_l, u_u], \delta = \Gamma(u) \tag{4.7}$$

the smoothness condition implies the differentiability of the function Γ -if only by parts- along $[u_0, u_1]$, and as a result, the differential $d\delta$ may be expressed as:

$$d\delta = \frac{d\Gamma}{du} du \tag{4.8}$$

so that the singular Cauchy integral may be rewritten as:

$$\Omega_{ld}(z) = \frac{-1}{2\pi i} \int_{u_0}^{u_1} \frac{\lambda(\Gamma(u))}{z - \Gamma(u)} \frac{d\Gamma}{du} du \tag{4.9}$$

$$= \frac{1}{2\pi i} \int_{u=u_l}^{u=u_u} \lambda(\Gamma(u)) \, d[\ln(z - \Gamma(u))] \tag{4.10}$$

If the curve is defined by parts, that is, if there is a sequence $\{u_k, k \in [0, N]\}$ such that $u_0 = u_l$ and $u_N = u_u$, the integral may be expressed as:

$$\Omega_{ld}(z) = \frac{1}{2\pi i} \sum_{k=0}^{k=N-1} \int_{u=u_k}^{u=u_{k+1}} \lambda(\Gamma(u)) \, d[\ln(z - \Gamma(u))] \tag{4.11}$$

in which the function Γ is continuous and differentiable in each of the integration intervals. Applied to the case of NURBS, this implies that the Cauchy singular integral for a singularity distribution along a NURBS may be evaluated as the sum of the singular integrals over each segment of the curve included between the images of its knots. Since a NURBS can be decomposed into Rational Bézier curves between its knots -see 4.2.2-, the capability of evaluation of the Cauchy Singular Integral along such splines would be extensible to the case of NURBS, by superposition as shown in 4.11.

In certain cases, the integral 4.10 may be formally evaluated. The following shows how the integration is performed in the case of Rational Bézier Curves.

4.3.2 Cauchy Singular Integral over Rational Bézier curves

Considering the Rational Bézier Curve B of degree n defined by its set of control points z_k and weights w_k, with parameter u defined between 0 and 1, the function $\Gamma(u)$ is defined as:

$$\Gamma(u) = \sum_{k=0}^{k=n} w_k z_k R_{k,n}(u) \tag{4.12}$$

with

$$R_{k,n}(u) = \frac{B_{k,n}(u)}{D(u)} \tag{4.13}$$

$$D(u) = \sum_{p=0}^{p=n} w_p B_{p,n}(u) \tag{4.14}$$

with $B_{k,n} = \binom{k}{n} u^k (1-u)^{n-k}$ the Bernstein Polynomial of order k and degree n - see [44]. The denominator $D(u)$ is independent of the summation parameter k.

Equation 4.10 may be modified to account for the particular parameterization of B. Indeed:

$$N(u) = \sum_{k=0}^{k=n} w_k z_k B_{k,n}(u) \tag{4.15}$$

$$P(u,z) = z \cdot D(u) - N(u) = \sum_{k=0}^{k=n} w_k (z - z_k) R_{k,n}(u) \tag{4.16}$$

$$z - \Gamma(u) = \frac{P(u,z)}{D(u)} \tag{4.17}$$

so that,

$$\ln(z - \Gamma(u)) = \ln(P(u,z)) - \ln(D(u)) \tag{4.18}$$

A well known result of algebra is that all complex polynomials of degree n may be expressed as a product of n monomials and a complex constant: the field of polynomials with complex coefficients is a splitting field: all polynomials in $\mathbb{C}[Z]$ can be expressed as a product of linear polynomials. $P(u,z)$ and $D(u)$ are both polynomials in u. Defining the roots of D as the set $\left\{\overset{*}{\zeta}_k, k \in [1, n_d] \bigcap \mathbb{N}\right\}$ and the roots of $P(.,z)$ as the set $\{\zeta_k(z), k \in [1, n_p] \bigcap \mathbb{N}\}$, the

polynomials may be expressed as:

$$P(u,z) = P_0(z) \prod_{k=1}^{k=n_p} (u - \zeta_k(z)) \tag{4.19}$$

$$D(u) = D_0 \prod_{k=1}^{k=n_d} \left(u - \overset{*}{\zeta}_k\right) \tag{4.20}$$

Thus, defining $\Lambda = \lambda \circ \Gamma$, the Cauchy Singular integral becomes:

$$\Omega_{ld}(z) = \frac{1}{2\pi i} \int_{u=0}^{u=1} \Lambda(u)\, d\left[\ln\left(\frac{P_0(z)}{D_0}\right) + \sum_{k=1}^{k=n_p} \ln(u - \zeta_k(z)) - \sum_{k=1}^{k=n_d} \ln\left(u - \overset{*}{\zeta}_k\right)\right] \tag{4.21}$$

$$= \frac{1}{2\pi i}\left[\sum_{k=1}^{k=n_p} \int_{u=0}^{u=1} \frac{\Lambda(u)}{u - \zeta_k(z)} du - \sum_{k=1}^{k=n_d} \int_{u=0}^{u=1} \frac{\Lambda(u)}{u - \overset{*}{\zeta}_k} du\right] \tag{4.22}$$

The strength may be expressed as a polynomial in u along the boundary, there exists a set of complex coefficients Λ_k such that:

$$\Lambda(u) = \sum_{k=0}^{k=n_L} \Lambda_k P_k(2u-1) \tag{4.23}$$

where P_k is the k^{th} Legendre polynomial. Considering the equality linking Legendre polynomial to Legendre functions of the second kind through the Cauchy singular integral -see [2] :

$$Q_k(z) = \frac{1}{2} \int_{-1}^{+1} \frac{P_k(t)}{z - t} dt \tag{4.24}$$

it follows that the complex potential for the line-dipole along a Rational Bézier Curve may be expressed as:

$$\Omega_{ld}(z) = \sum_{k=1}^{k=n_p} \mho_{ld}(2\zeta_k(z) - 1) - \sum_{k=1}^{k=n_d} \mho_{ld}\left(2\overset{*}{\zeta}_k - 1\right) \tag{4.25}$$

$$\text{where} \quad \mho_{ld}(\chi) = -\frac{1}{\pi i} \sum_{k=0}^{k=n_L} \Lambda_k Q_k(\chi) \tag{4.26}$$

This complex potential can be viewed as the superposition of the complex potential generated by a line-dipole located in $[-1,+1]$ evaluated at $n_p + n_d$ locations. This observation is

particularly interesting because it implies that all equivalences established for straight line elements may be carried over to curvilinear elements without the need for supplementary work. All and any research yielding improvement for the straight line-dipole will provide improvements for the Rational Bézier curvilinear elements as well.

It remains to be defined whether some practical limitations follow from the preceding derivation. It involves the roots of polynomials $P(u,z)$ and $D(u)$ thus naturally bringing the issue of root finding. It is detailed in the following discussion.

4.3.3 Computing the discharge function

The discharge function is defined, following [51], as the opposite of the derivative of the complex potential with respect to z, the complex variable related to the physical plane. By definition, the derivative of an analytic function exists throughout the domain of definition of the complex potential itself. See previous arguments in Chapter 3.

Thus, at any point z such that all the roots ζ_k satisfy $\Gamma'(\zeta_k) = \left.\frac{d\Gamma}{d\zeta}\right|_{\zeta_k} \neq 0$, the discharge function associated with NURBS is:

$$W_{ld}(z) = -\frac{d\Omega_{ld}}{dz} = -\sum_{k=1}^{k=n_p} \left.\frac{d\mho_{ld}}{d\chi}\right|_{\chi=2\zeta_k-1} \frac{d(2\zeta_k-1)}{dz} \tag{4.27}$$

$$= 2\sum_{k=1}^{k=n_p} \frac{\tau_{ld}(2\zeta_k-1)}{\Gamma'(\zeta_k)} \tag{4.28}$$

$$\text{where} \quad \tau_{ld} = -\frac{d\mho}{d\chi} \tag{4.29}$$

and points not satisfying the condition, the critical points of the mapping Γ, are handled below.

4.4 Evaluation issues

Upon numerical implementation, the following issues arose:

- Special points and possible singularities, weak or strong, introduced by the use of the parametric function $\Gamma(\delta)$ must be identified and handled by the software program. This is a common issue in the Analytic Elements Method, since it rests on the proper use of singular functions.

- The evaluation requires the finding of roots of polynomials.
- The speed of computation using a straightforward direct implementation is slow.

The following provides a discussion of the first two issues. The third is addressed in chapter 5.

4.4.1 Special points

Roots and poles of the mapping

The mapping $u \in [0,1], z = \Gamma(u)$ define each section of the spline and may be extended analytically, for a complex variable $\zeta \in \mathbb{C}$. This extension is defined by replacing $u \in [0,1]$ with $\zeta \in \mathbb{C}$ in equation 4.12. $\Gamma(\zeta)$ is then defined by a rational function of the complex variable, and as such has a set of specific points associated with it: roots -the roots of its numerator- and poles -the roots of its denominator.

In general, the roots do not cause any specific issue, either analytically or numerically. It suffices to notice that they map to the point $z = 0$, the origin.

The poles are no greater concern since they are mapped to infinity in the z-plane. The complex potential at infinity is never numerically evaluated because infinity is always outside of machine range. Analytically, it is pointed out that the roots of the polynomial $P(u, z)$ as z goes to infinity include all the poles of Γ, and that if the degree of $N(u)$ is larger than the degree of $D(u)$, the remaining roots have infinite modulus. Referring to equation 4.25, the influence of these poles is removed in the second member of the right hand term of the equation: the only influences left are those of the other roots which sums to zero, since all these roots have infinite modulus.

As a result, the roots and poles of the mapping do not require special handling.

Critical points

As demonstrated in 4.3.3, a special case arises wherever $\frac{d\Gamma}{d\zeta} = 0$. At these locations, the general form of computation for the complex potential still holds, but the computation of the discharge function breaks down. Because the complex potential was derived using the Cauchy singular integral, it is analytic everywhere outside of the boundary: Unless a critical point occurs on the

boundary itself -which would violate the smoothness condition and may therefore be ignored- the derivation guarantees that the discharge function is not singular at these points. A method is offered to achieve a numerical result at the critical points. This method fails in one very uncommon situation, which can be identified at the time of modeling and is detailed below. Such a case -called multiply critical point- is so rare and unlikely that it was decided to exclude the case from the implementation: curves presenting such critical points would be rejected and the modeler required to modify the input to the model - usually, adding a control point to the NURBS without actually modifying the shape was enough to remove the problem.

At any point $z \in \mathbb{C}$ -including at a critical point-, the sum of the roots of the polynomial $P(u,z)$ is related to its coefficients by the relationship -see e.g. [2]:

$$\sum_{k=1}^{k=n_p} \zeta_k = -\frac{a_1(z)}{a_0(z)} \tag{4.30}$$

$$P(u,z) = \sum_{k=0}^{k=n_p} a_k(z)\, u^{n_p-k} \tag{4.31}$$

The denominator $a_0(z)$ is never zero, since it is the leading coefficient of the polynomial of degree n_p. Taking the differential of 4.30:

$$\sum_{k=1}^{k=n_p} d\zeta_k = -\frac{d\frac{a_1}{a_0}}{dz} dz \tag{4.32}$$

At a regular critical point $\overset{c}{z}$, some of the roots ζ_k of $P\left(u, \overset{c}{z}\right)$ equal one and only one of the roots $\overset{c}{\zeta}_n$ of $\frac{d\Gamma}{d\zeta}$ [1].By Taylor expansion of Γ about its critical point, it can be shown that if $\overset{c}{\zeta}_n$ is of multiplicity m_n in $\frac{d\Gamma}{d\zeta}$, the m_{n+1} roots of $P(u,z)$ converge to it as z approaches $\overset{c}{z}_n = \Gamma\left(\overset{c}{\zeta}_n\right)$. Reordering the set $\{\zeta_k\}$ such that the roots that do so are first, the derivation of the discharge function at the critical point may be modified as follows.

[1] when the ζ_k include more than one such root, the critical point $\overset{c}{z}$ is multiply critical. Solution for this case is similar to the one proposed here, using more of the relationships between roots and coefficients of a polynomial. Such cases are extremely rare.

From 4.27:

$$\begin{aligned} -d\Omega_{ld} &= 2\tau_{ld}\left(2\overset{c}{\zeta}_n - 1\right)\sum_{k=1}^{k=m_n+1} d\zeta_k + \sum_{k=m_n+2}^{k=n_p} 2\tau_{ld}\left(2\zeta_k - 1\right)d\zeta_k \\ &= -\tau_{ld}\left(2\overset{c}{\zeta}_n - 1\right)\frac{d\frac{a_1}{a_0}}{dz}dz \\ &\quad +2\sum_{k=m_n+2}^{k=n_p}\left[\tau_{ld}\left(2\zeta_k - 1\right) - \tau_{ld}\left(2\overset{c}{\zeta}_n - 1\right)\right]d\zeta_k \end{aligned} \tag{4.33}$$

$$W\left(\overset{c}{z}_n\right) = -\tau_{ld}\left(2\overset{c}{\zeta}_n - 1\right)\frac{d\frac{a_1}{a_0}}{dz} + 2\sum_{k=m_n+2}^{k=n_p}\frac{\tau_{ld}\left(2\zeta_k - 1\right) - \tau_{ld}\left(2\overset{c}{\zeta}_n - 1\right)}{\Gamma'\left(\zeta_k\right)} \tag{4.34}$$

Even in the most complex cases, $\frac{d\frac{a_1}{a_0}}{dz}$ is easy to compute. The numerous special cases are therefore not listed here; the reader can effortlessly consider them following the derivation for the two most common cases:

- when $\deg\left[N\left(u\right)\right] = \deg\left[D\left(u\right)\right] = \deg\left[P\left(u, \overset{c}{z}_n\right)\right] = n_p$, the polynomials N and D may be factored using their roots into:

$$N\left(u\right) = \alpha_N \prod_{k=1}^{k=n_p}\left(\zeta - \mathring{\zeta}_k\right) \tag{4.35}$$

$$D\left(u\right) = \alpha_D \prod_{k=1}^{k=n_p}\left(\zeta - \overset{*}{\zeta}_k\right) \tag{4.36}$$

and therefore:

$$a_1\left(z\right) = -\alpha_D \sum_{k=1}^{k=n_p} \overset{*}{\zeta}_k z + \alpha_N \sum_{k=1}^{k=n_p} \mathring{\zeta}_k \tag{4.37}$$

$$a_0\left(z\right) = \alpha_D z - \alpha_N \tag{4.38}$$

$$\left.\frac{d\frac{a_1}{a_0}}{dz}\right|_{z=\overset{c}{z}} = \frac{\alpha_N}{\alpha_D}\frac{\sum_{k=1}^{k=n_p}\left(\overset{*}{\zeta}_k - \mathring{\zeta}_k\right)}{\left(\overset{c}{z} - \frac{\alpha_N}{\alpha_D}\right)^2} \tag{4.39}$$

- when $\deg[D(u)] = 0, D(u) = \alpha_D$, and $deg[N(u)] > 1$

$$a_1(z) = \alpha_N \sum_{k=1}^{k=n_p} \mathring{\zeta}_k \tag{4.40}$$

$$a_0(z) = -\alpha_N \tag{4.41}$$

$$\frac{d\frac{a_1}{a_0}}{dz} = 0 \tag{4.42}$$

It is pointed out that throughout this section, the assumption that the curve is smooth and regular leads to the necessity that no critical point may be located on the curve itself. The resolution process could not take place otherwise, without special handling.

4.4.2 Roots of polynomials

For each evaluation of the complex potential at any point z in the physical plane, the polynomial in u $P(u, z)$ must be decomposed, which requires the determination of its roots. For a Rational Bézier curve of degree n, this polynomial is generally of degree n as well and therefore has n roots. At one specific location, and one at most, the polynomial degenerates and its degree is reduced. This special case is described in 4.4.1; in the following, it is assumed that $P(u, z)$ is of the degree of the spline.

The root finding issue is twofold:

- Firstly, for $n \geq 5$, a numerical algorithm must be used to compute the roots: There is no closed form analytic method for finding the roots of a polynomial of degree larger than 4. This poses an apparent philosophical problem, since the elements fit within the *Analytic* Element Method. The notion of using a numerical procedure for finding the roots suggests that it might be impossible to analytically differentiate the function, which is one of the main advantages of the method. However, since the complex potential for these elements is determined via the Cauchy Singular Integral, the analytic differentiation is guaranteed: all derivatives exist, up to an infinite order, wherever the complex potential itself exists as well.

  The ability to compute efficiently the discharge function $W = Q_x - iQ_y = -\frac{d\Omega}{dz}$ is paramount for in the context of the AEM. The technique used for curvilinear elements

was shown above, in 4.3.3. It can be observed that no new root finding was necessary.

- Secondly, the process of finding roots of a polynomial is slow. For high-precision elements, for which the jump function is approximated with a polynomial of degree 20 or smaller, a spline of degree 5 implied that more than 90 percent of the computational time was spent on finding the roots for any location in the z-plane; in other words, the evaluation of the potential of the spline was equivalent to evaluating a string of 10 straight line elements, each of degree eqaul to that of the spline. This phenomenon is worse for low degree elements, when up to 99 percent of the computational effort is spent on the root finding step.

The issue of root finding is therefore linked to the issue of speed of computation. The method proposed in chapter 5 will provide a mean to reduce the need of using the actual roots only in the close vicinity of the curvilinear element.

4.5 Solving a boundary value problem along a spline

The resolution of the boundary value problem is very similar to the method used for the advanced line elements mentioned in chapter 3.

A matrix is established by evaluation the influence of each individual component of the complex potential or the discharge function at points located along the element. A linear system of equations is then defined that relates this influence matrix, the vector of unknown coefficients of the jump function, the influence of other features at the chosen locations, and the intended value. The linear system is then solved in the least squares sense.

The issue is in correctly building the influence matrix.

The present section details this procedure in the case of a relevant boundary condition: the head specified element. The choice of the Dirichlet boundary condition is argued and justified for its representativeness. The Matrix is then built, and flow nets are presented, showing that the condition in Laplacian flow is indeed fulfilled.

4.5.1 Representativeness of the Dirichlet problem

In the applications defined as the focus of this thesis, the problems to be solved were limited to potential flow. In such a flow, two principal boundary conditions exist: Dirichlet -corresponding to the constraining the solution to a particular function along the boundary- and Neumann -the gradient of the solution normal to the boundary is specified.

The Neumann problem is very similar to the Dirichlet problem, except that the influences to consider are in the discharge function -projected on a direction normal to the boundary- instead of the complex potential. Thus, the method required to solve the one is extensible to the other: only one must be presented to provide the resolution scheme.

It was argued that the results of 4.3 are transferable from line-dipoles to line-sink with minimal efforts. The Dirichlet problem implies the use of line-sinks, and thus offers the opportunity to show the similarity between the two cases.

Considering these two facts, the Dirichlet problem is solved here along a Rational Bézier curve.

Other boundary conditions exist, which may involve the jump along the element directly, as discussed in 4.5.3. A general description of possible boundary conditions can be found in [31].

4.5.2 Setting up the resolution matrix

The resolution matrix is dependent on the influence functions, which differ from the case of straight line elements. The case of the Dirichlet problem requires the use of Line-sink instead of line dipoles to represent the element.

Line-sinks and branch cuts

The line-sinks imply the addition of two logarithmic singularities at the tips of the element. Unlike the straight line elements, there is no obvious default orientation for the location of the cuts created by these singularities; placed in the ζ-plane, their location is not easily predictable. The endpoint singularities are therefore located in the physical plane.

They are arbitrarily defined to lie tangential to the curve at the endpoints in the z-plane,

in the direction of the tangent; see figure 4.2. This definition makes it easy to track the cuts and to cancel out cuts in the case of smooth strings of Rational Bézier curves.

From 4.25 and 4.26, the complex potential for a line-sink may be expanded into:

$$\begin{aligned}\Omega_{ls}(z) &= \sum_{k=1}^{k=n_p} \upsilon_{ld}\left(2\zeta_k(z)-1\right) - \sum_{k=1}^{k=n_d} \upsilon_{ld}\left(2\overset{*}{\zeta}_k - 1\right) \\ &+\frac{\Lambda(0)}{2\pi i}\ln\left(\frac{z-\Gamma(0)}{-\Gamma'(0)}\right) - \frac{\Lambda(1)}{2\pi i}\ln\left(\frac{z-\Gamma(1)}{-\Gamma'(1)}\right) \\ &+\frac{1}{2\pi i}\left[\Lambda(0)\ln\left(-\Gamma'(0)\right) - \Lambda(1)\ln\left(-\Gamma'(1)\right)\right]\end{aligned} \tag{4.43}$$

Another possibility is to ensure that the cuts always lie along horizontal lines passing through each endpoint. In this case, the complex potential is:

$$\begin{aligned}\Omega_{ls}(z) &= \sum_{k=1}^{k=n_p} \upsilon_{ld}\left(2\zeta_k(z)-1\right) - \sum_{k=1}^{k=n_d} \upsilon_{ld}\left(2\overset{*}{\zeta}_k - 1\right) \\ &+\frac{\Lambda(0)}{2\pi i}\ln\left(z-\Gamma(0)\right) - \frac{\Lambda(1)}{2\pi i}\ln\left(z-\Gamma(1)\right)\end{aligned} \tag{4.44}$$

The former is preferred over the latter in most cases, because the argument of the logarithms are, in essence, scaled to account for the curvature of the element at the tips. The numerical evaluation of the complex potential close to the tips, which involves a singularity -in the line dipole component- and its removal -through the logarithm-, seems more reliable in practice with the former expression. This observation was made empirically over a limited number of cases and for the evaluation of an element with known coefficients; it corresponds to similar experience for the case of straight elements, where the singularities are preferably removed in

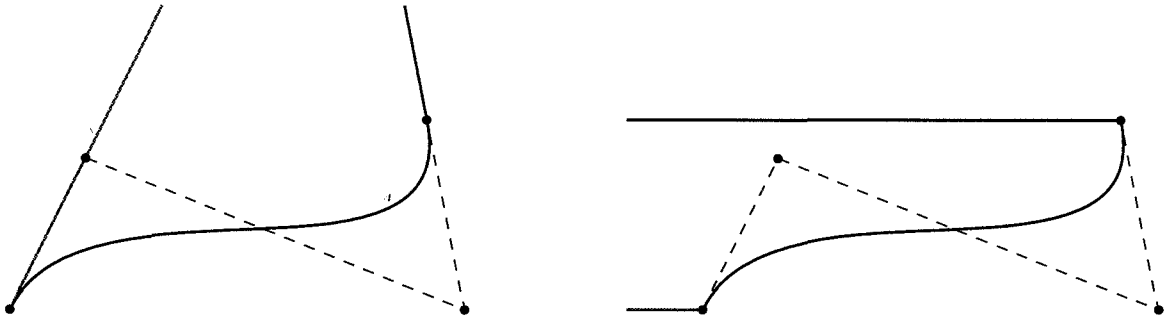

Figure 4.2: Line-sink and possible locations of the branch cuts

the Z-plane than the physical plane. It may be noted that the last term of 4.43 is a constant which is optional since all complex potentials are known up to a constant; its inclusion eases the connection of elements in a string.

Influence functions

Reorganizing 4.44 so as to express the complex potential in terms of a series with coefficients Λ_k, using 4.26:

$$\Omega_{ls}(z) = \sum_{n=0}^{n=n_L} \Lambda_n \overset{n}{\Omega}_{ls}(z) \tag{4.45}$$

$$\overset{n}{\Omega}_{ls}(z) = \frac{1}{\pi i}\left\{\sum_{k=0}^{k=n_p} Q_n(2\zeta_k - 1) - \sum_{k=0}^{k=n_d} Q_n\left(2\overset{*}{\zeta}_k - 1\right) + \frac{(-1)^n}{2}\ln\left[z - \Gamma(0)\right] - \frac{1}{2}\ln\left[z - \Gamma(1)\right]\right\} \tag{4.46}$$

where the $\overset{n}{\Omega}_{ls}$ are the influence functions of the line-sink. It is pointed out that the singularity associated with the Legendre functions of the second kind is removed in each of the influence functions, so that their imaginary parts are defined at the endpoints -the real parts are multi-valued because of the branch cuts.

Matrix construction

Given the influence functions associated with an element, construction of the matrix used in the resolution scheme depends only on the type of boundary condition to be achieved and on a choice of a set of control points on the spline curve:

$$D_{cp} = \left\{\overset{m}{z} \in \mathcal{C}, m \in [1, M] \cap \mathbb{N}, M > N_L\right\} \tag{4.47}$$

The control points are chosen in a manner similar to that suggested in [31]: points are selected in $[-1, +1]$ in the ζ-plane, according to a particular distribution, usually a uniform or a Chebychev distribution. The images of these points are found by applying the mapping Γ, and the resulting set is the set of the control points. It may be noted that one of the roots of each of these control points is known and lies in $[-1, +1]$; this fact should be used in implementing the element, to

speed up the assembly of the matrix, and to avoid the insertion of numerical errors linked with the root finding process. It is pointed out that the dominant factors of the matrix were found to be the contributions from the functions evaluated at the roots located between -1 and +1; numerical error in these results in significant loss of accuracy in the solution. Thus, the following set of control points is defined, where $M \geq N_L$ is an arbitrary integer:

$$D_{cp} = \left\{ \overset{m}{z} = \Gamma\left(\overset{m}{u}\right), \overset{m}{u} = \cos\left(\pi \frac{m - \frac{1}{2}}{M}\right), m \in [1, M] \cap \mathbb{N}, M > N_L \right\} \tag{4.48}$$

In the case of the Dirichlet problem, a head specified condition is imposed. This implies that the real part of the complex potential along the curve is imposed, following the definition given in chapter 3; the value imposed at any point z on the curve is defined as $\overset{\odot}{\Phi}(z)$. The coefficients $\Lambda_k = i\mu_k$ are purely imaginary; the cancellation of the leading i's yields expressions of the complex potential that match those of [51] and [31]. Thus, defining as $\overset{\vee}{\Phi}(z)$ the influence of all analytic elements other than the one being solved, the following real linear equation may be established:

$$\forall \overset{m}{z} \in D_{cp}, \quad \sum_{n=0}^{n=n_L} \mu_n \Im\left(\overset{n}{\Omega}_{ls}\left(\overset{m}{z}\right)\right) = \overset{\odot}{\Phi}\left(\overset{m}{z}\right) - \overset{\vee}{\Phi}\left(\overset{m}{z}\right) \tag{4.49}$$

which leads to the matrix equation:

$$\mathbf{A} \cdot \mu = \mathbf{b}, \begin{cases} \mathbf{A} = (a_{m,n})_{\substack{m \in [1,\, M\,] \cap \mathbb{N} \\ n \in [0, N_L] \cap \mathbb{N}}}, \; a_{m,n} = \Im\left(\overset{n}{\Omega}_{ls}\left(\overset{m}{z}\right)\right) \\ \mu = (\mu_n)_{n \in [0, N_L] \cap \mathbb{N}} \\ \mathbf{b} = (b_m)_{m \in [1, M] \cap \mathbb{N}}, \; b_m = \overset{\odot}{\Phi}\left(\overset{m}{z}\right) - \overset{\vee}{\Phi}\left(\overset{m}{z}\right) \end{cases} \tag{4.50}$$

If $M = N_L + 1$, then the matrix $\mathbf{A}$ is square.It may be inverted, thanks to all the restrictions placed on the acceptable shapes of the boundary -non self intersecting, no critical point on the boundary, etc.-, and the system 4.50 has a unique solution vector μ. Otherwise, the system is over-determined and cannot be solved classically. It is solved in the least-squares sense instead, recognizing that the product of a matrix by its transposed is an invertible squared matrix:

$$\mu = \left(\mathbf{A}^T \mathbf{A}\right)^{-1} \mathbf{A}^T \mathbf{b} \tag{4.51}$$

Other conditions may be added to the problem, such as imposing the value of the jump at either endpoint. The method used to enforce such conditions is based on Lagrange multipliers, as introduced in [31] and is detailed in [35].

4.5.3 On Jump-specified elements

In some cases, the jump in the complex potential of the element is directly involved in the system of equations. This is the case in particular for elements used in joining domains of different physical properties, such as hydraulic conductivity, and for areas with rainfall.

The most common instance, a jump in hydraulic conductivity across the boundary, is introduced here. In that case, the real potential jumps, but the head must remain continuous. This implies that the coefficients of the jump function λ are real. Because of the choice of relationship between head and potential, the condition can be reduced to:

$$\frac{\Phi^+}{k^+} = \frac{\Phi^-}{k^-} \tag{4.52}$$

where $(.)^+$ indicates a the limit of a quantity as the evaluation location approaches the curve in the direction of the normal, and $(.)^-$ in the opposite direction. The value of the potential of the element on the boundary is not zero, unlike the case of the straight line element. Considering that if ξ is a point in the interval $[0, 1]$, and $z_\xi = \Gamma\xi$ is the corresponding point on the curve in the physical plane, the potential evaluates to:

$$\tilde{\Phi}(z_\xi) = \sum_{n=1}^{m=n_p} \lambda_n \cdot \Re\left(\overset{n}{\Omega}_{ld}(z_\xi)\right) \tag{4.53}$$

Defining the influence of all other elements at location z_ξ as $\overset{\vee}{\Phi}(z_\xi)$, eq.4.52 becomes:

$$\frac{k^+}{k^-}\left(\frac{1}{2}\lambda(\xi) + \tilde{\Phi}(z_\xi) + \overset{\vee}{\Phi}(z_\xi)\right) = \left(-\frac{1}{2}\lambda(\xi) + \tilde{\Phi}(z_\xi) + \overset{\vee}{\Phi}(z_\xi)\right) \tag{4.54}$$

Defining $\alpha = \frac{k^+ - k^-}{k^+ + k^-}$ and reorganizing:

$$\sum_{n=1}^{m=n_p} \lambda_n \left[P_n(2 * \xi - 1)\right] + \alpha \cdot \Re\left(\overset{n}{\Omega}_{ld}(z_\xi)\right) = -\alpha\overset{\vee}{\Phi}(z_\xi) \tag{4.55}$$

This equation is similar to eq.4.49 established for the Dirichlet problem. The resolution from that point is therefore similar and not repeated here.

The jump in potential across the element at z_ξ along the direction normal to the curve is exactly the value of the jump function $\lambda(\xi)$. A set of curvilinear line-sinks must also be added to guarantee continuity of flow across the boundary, in a manner similar to the straight case. As a result, if the curve is the boundary of an area-sink, the resolution of the unknowns is virtually identical to the case of straight line element, except that it takes place in the ζ-domain rather than the physical plane; it is therefore not repeated here. Instead, reference is made to [31] and [57], although the shape of the interpolator should be chosen differently.

4.5.4 Examples

Two examples are offered here to show the flownets obtained using the new curvilinear elements. The degree chosen was moderately high: $N = 32$ and the number of control points is 40. The solutions do well overall, but attention is drawn to the irregular patterns of some streamlines in figures 4.3(c) and 4.3(b). These are explained by the fact that the entire curvilinear element has only 36 degrees of freedom. Were there need for more precision, the elements should be broken into two pieces -by subdivision-, and resolved; this would significantly slow all computations.

Piezometric contours are dashed lines, stream-function isopleths are solid line and correspond to streamlines, up to the branch cuts.

Both examples were solved only once. The complex potential was evaluated for each figure, on a grid of 401 by 401. The figure were creating using Scilab[2], see [24].

[2]Scilab is produced by INRIA - www-rocq.inria.fr. It is an open source software for mathematical operations.

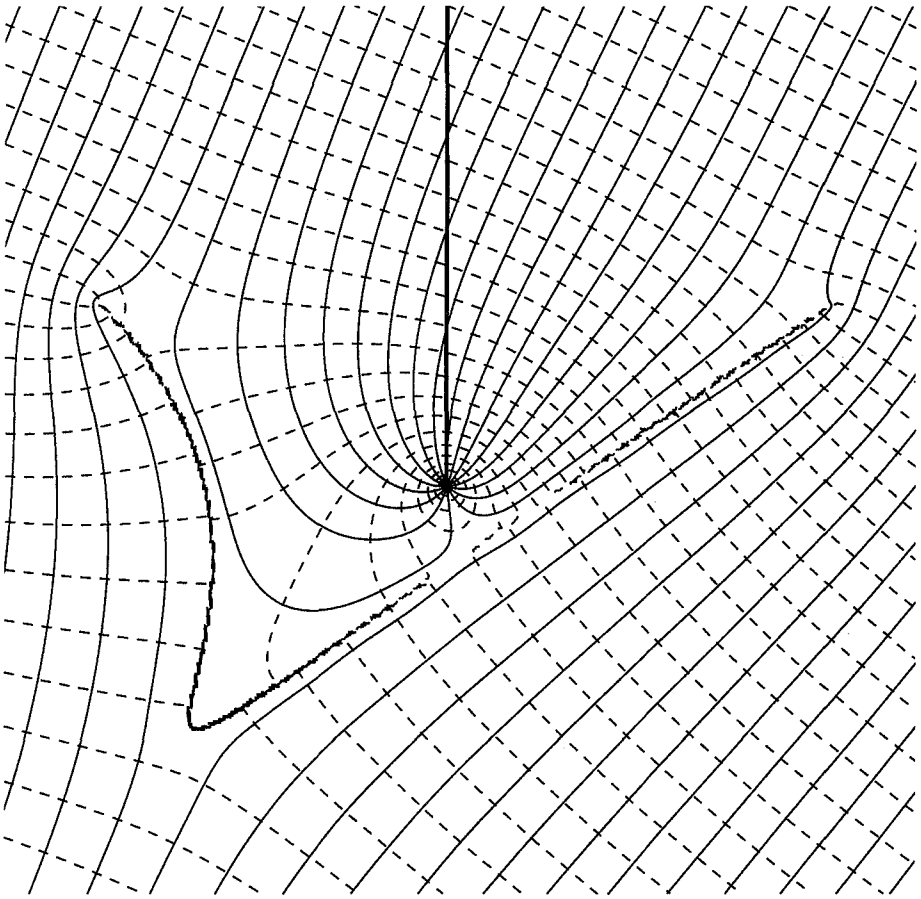

(a) general view

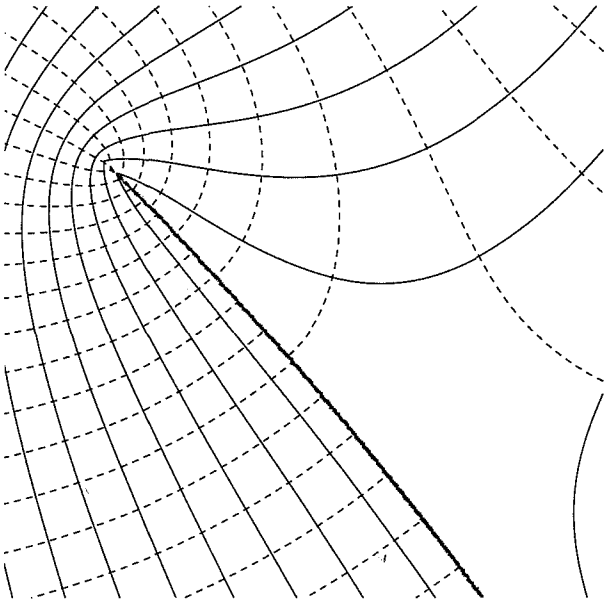

(b) zoom on tip

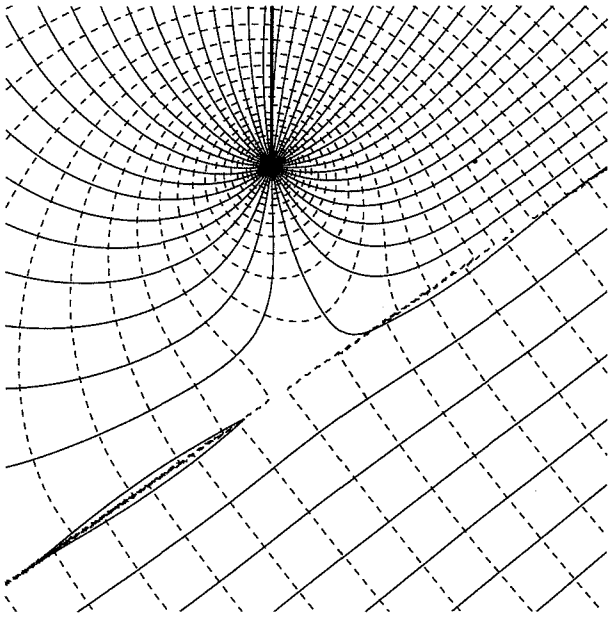

(c) zoom on well location

Figure 4.3: an impermeable barrier in uniform flow next to a well

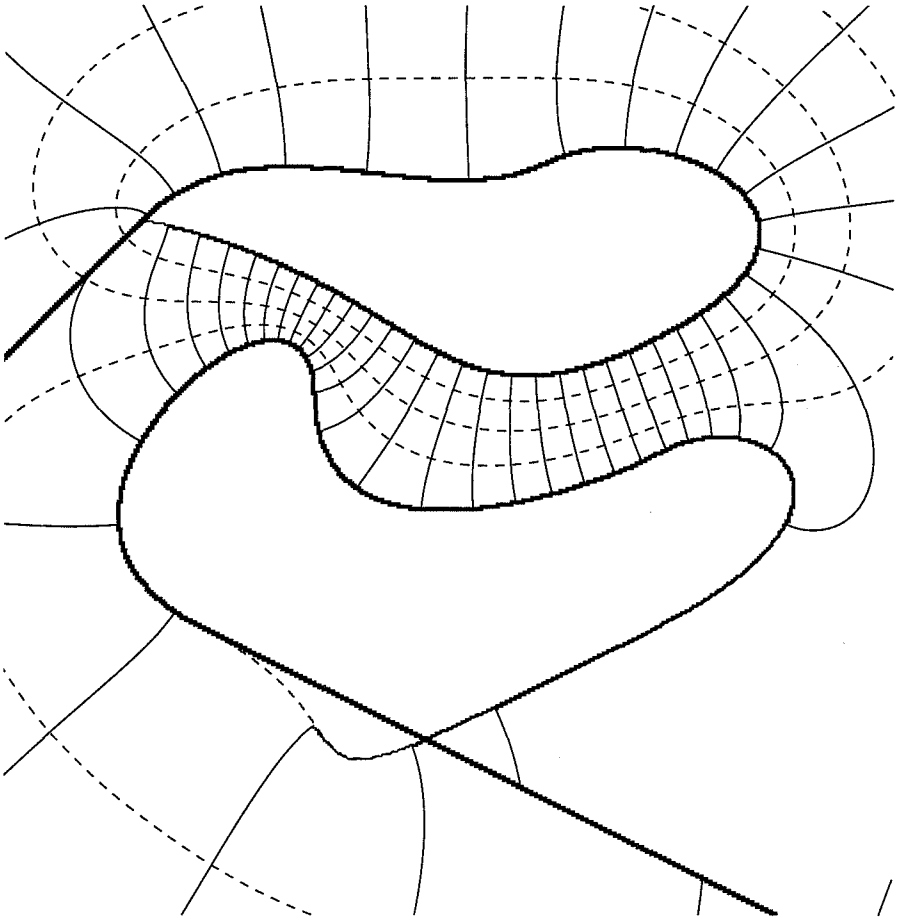

(a) general view

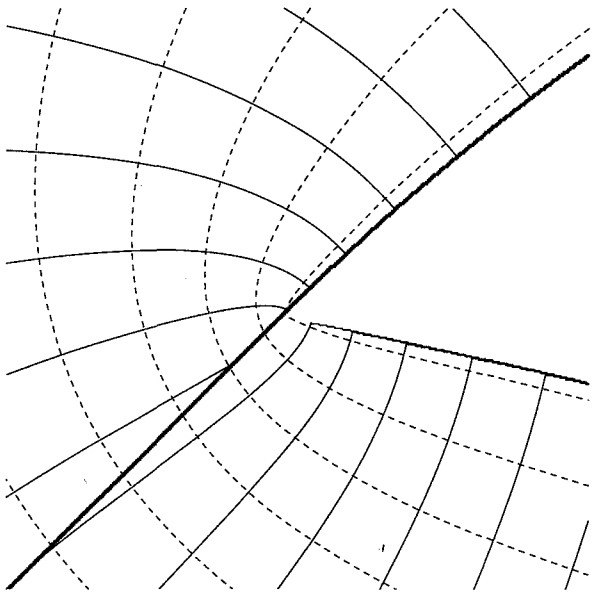

(b) zoom on western tip of northern lake

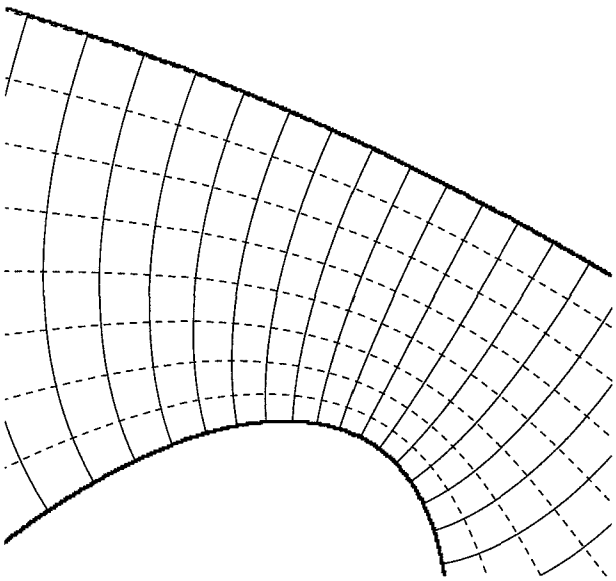

(c) zoom on narrow section between the lakes

Figure 4.4: Two head specified lakes in a field of uniform flow

Chapter 5

Computational efficiency of curvilinear elements

Synopsis

Purpose: The elements along NURBS curves derived in chapter 4 are too slow to be used in a practical modeling setting. This chapter provides a method for speeding up computations.

Outcome: A polygonal far-field, an approximation of a complex potential away from the boundary to which it is associated, and a method for creating line elements of very large degree are detailed.

As pointed out in 4.4.2, the speed of computation of the complex potential is hampered by the necessity to the find the complex roots of an n^{th} degree polynomial. A second issue, as apparent in eq.4.25, is that the complex potential requires the evaluation of n_p series of Legendre functions, thus making this second step comparable in speed to the evaluation of n_p standard line elements. As a whole, the evaluation process is therefore so slow that the elements seem of little worth in practice.

What is proposed here is a method to significantly speed up the evaluation -by an order of magnitude in most practical cases-, without adding complexity for the modeler; Thus, the design advantage of the Bézier shapes is preserved, with little added computational overhead compared

to standard line elements. This method relies on two concepts: (1) the complex potential can be approximated, using a direct boundary integral, outside any polygon surrounding the element by an analytic function that is faster to compute and does not require that the roots of the polynomial be found, and (2) the accuracy of the approximation can be chosen through the use of line elements of very large degree $N \geq 50$.

Résumé en Français

Objectif : Les éléments le long de courbes NURBS dérivés dans le chapitre 4 sont trop lents pour être utilisés dans un environnement réel de modélisation. Ce chapitre veut fournir une méthode pour accélérer ces calculs.

Résultat : Sont détaillés ici, (1) Un *champ lointain* polygonal, une approximation du potentiel complexe à distance de la frontière à laquelle il est associé, ainsi que (2) une méthode de création d'éléments linéaires de très haut degré.

Comme mis en évidence au point 4.4.2, la vitesse de calcul du potentiel complexe est gênée par le besoin de trouver les racines complexes d'un polynome de degré n. Un second problème, apparent au travers de l'équation 4.25, est que le potentiel complexe requière l'évaluation de n_p séries de fonctions de Legendre, rendant ainsi cette seconde étape comparable à l'évaluation de n_p éléments linéaires classiques. En totalité, le processus d'évaluation est par conséquent si lent que ces éléments semblent être de peu de valeur dans la pratique.

Ce qui est proposé ici est une méthode pour accélérer l'évaluation de façon significative -par un ordre de grandeur dans les cas pratiques-, sans ajouter de complexité pour le modélisateur ; ainsi, l'avantage des formes de Bézier à la conception est conservé, avec un faible surcoût de calcul comparé à l'utilisation de segments de droite. Cette méthode repose sur deux concepts : (1) le potentiel complexe peut être approché, en utilisant une intégrale frontière directe, à l'extérieur d'un polygone quelconque entourant l'élément par une fonction analytique plus rapide à calculer et qui ne nécessite pas la recherche des racines de polynomes, et (2) la précision de

l'approximation peut être choisie en utilisant des éléments linéaires de très haut degré $N \geq 50$.

5.1 Polygonal Far-Fields

The concept of Far-Fields rests on the principal that as distance away from a singularity increases, the complex potential associated with the singularity may be represented by an alternate function. Most notably is the use of a Laurent series expansion of the potential of straight line elements outside of the unit disk.

Whatever expansion is used, it must be defined in a domain free of the singularity distribution with which it is associated. In the case of curvilinear elements, the disk defined so that its diameter corresponds to the line between the end-points of the element does not, in general, contain the entire element: a Laurent series expansion of the complex potential is not usually a possible representation for such elements.

Considering the property of NURBS curves relating the location of the object to the smallest convex polygon constructed with its geometric control points, the convex hull, it is possible to surround any NURBS curve defined by $n+1$ control points with an $n+1$-sided polygon -in some cases, fewer than $n+1$ sides are needed. This type of boundary is always available, and the strict inclusion of the curvilinear element within such a polygon is guaranteed provided that all weights of the NURBS are non-negative -see [44, 22]. Using this polygon as boundary of the domain outside of which an expansion would be used is therefore general enough to be considered.

Two issues related to these shapes need to be resolved:

- Which expansion can be associated to polygons?
- If the convex Hull is too large, can a polygon be constructed with tighter fit?

5.1.1 Direct boundary integral over a polygon

Using the direct boundary integral method -see e.g. [36] for a description in real variables, [51] in complex-, it is possible to represent the complex potential generated by the curvilinear

element outside of the polygon by the sum of the potentials of line elements located along the sides of the polygon. This produces a sort of "custom fitted" far-field evaluation method, which removes the need to find the complex roots of 4.16 for any point outside of the convex hull, and does not add computational effort since the number of line elements used along the convex hull of a Rational Bézier Curve is equal to the degree of the spline. As a result, speed is greatly improved.

According to [51], a direct boundary integral in terms of complex variables over a simply closed contour $\mathcal{C}$ enclosing a domain $\mathcal{D}$ yields:

$$\forall z \notin \mathcal{D}, \Omega(z) = \frac{-1}{2\pi i} \int_{\mathcal{C}} \frac{\Omega(\delta)}{z-\delta} d\delta \tag{5.1}$$

Choosing $\mathcal{C}$ as the closed polygon $\mathcal{P} = \{z_k, k \in [0, n+1] \bigcap \mathbb{N}\}$, $z_{n+1} = z_0$, eq.5.1 becomes:

$$\forall z \notin \mathcal{D}, \Omega(z) = \sum_{k=0}^{k=n} \frac{-1}{2\pi i} \int_{z_k}^{z_{k+1}} \frac{\Omega(\delta)}{z-\delta} d\delta \tag{5.2}$$

which corresponds to the combined potentials of $n+1$ straight line elements, each along one side of the polygon and such that the jump $\overset{k}{\lambda}$ along the k^{th} side equals the value of the complex potential $\overset{\Gamma}{\Omega}$ of the curvilinear element along that line:

$$\forall z \in [z_{k+1}, z_k], \overset{k}{\lambda}(z) = \overset{\Gamma}{\Omega}(z) \tag{5.3}$$

Thus, given the potential to be approximated and the location of the polygon, a set of line elements may be obtained whose combined contributions will equal the potential of the curvilinear element outside of the polygon. When approximating the jump functions $\overset{k}{\lambda}$ with polynomials, the complex potential outside of the polygon is approximated as:

$$\forall z \notin \mathcal{D}, \hat{\Omega}(z) = \sum_{k=0}^{k=n} \frac{-1}{2\pi i} \int_{z_k}^{z_{k+1}} \frac{\overset{k}{\lambda}(\delta)}{z-\delta} d\delta \tag{5.4}$$

Associating a line element with each side of the polygon, the problem of approximation reduces to finding the $\overset{k}{\lambda}$'s. Fitting a complex polynomial to a known function is a well known problem of approximation theory and is not detailed here. Defining the complex potential associated

with side k as:

$$\overset{k}{\Omega}(z) = \frac{-1}{2\pi i}\int_{z_k}^{z_{k+1}} \frac{\overset{k}{\lambda}(\delta)}{z-\delta} d\delta \tag{5.5}$$

the approximation is:

$$\forall z \notin \mathcal{D}, \hat{\Omega}(z) = \sum_{k=0}^{k=n} \overset{k}{\Omega}(z) \tag{5.6}$$

5.1.2 Polygon refinement

The polygon can be refined using standard graphical techniques associated with NURBS curves, as described in e.g.[44]: knot insertion, knot refinement and/or curve subdivision in particular allow for the creation of a tighter polygon.

- *curve subdivision* is the principle by which a NURBS curve is described as a sequence of Rational Bézier curves, as described in 4.2.2: each section on the NURBS between to consecutive distinct knots is replaced by a RB curve -see Fig.5.1 for an example.
- *knot insertion* allows the NURBS to be replaced by an equivalent NURBS of identical locus, but described by more control points. -see Fig.5.2.
- *knot refinement* is similar to knot insertion, except that more than one knot is inserted. Refinement is more efficient than multiple knot insertions.

An issue with using the convex hull to produce a polygon surrounding each RB curve is that the resulting area has vertices on the curve or on its tips. Using the above mentionned refinement techniques produces vertices on the curve itself. The direct boundary integral described in 5.1.1 is meant to use line elements along which the complex potential is represented as a polynomial: the chosen polygon cannot intersect the curve. Such a polygon may be obtained by slightly *inflating* the convex hull via an homothety -a dilation about its center of gravity. Thus, if the polygon $\mathcal{P}$ is defined by vertices $\{z_n, n \in [1,N] \bigcap \mathbb{N}, N \in \mathbb{N}\}$, then the new polygon $\mathcal{P}'$ is defined by the set $\{z'_n, n \in [1,N] \bigcap \mathbb{N}, N \in \mathbb{N}\}$ obtained by:

$$z'_n = \alpha(z_n - z_c) + z_c \tag{5.7}$$

$$z_c = \frac{1}{N}\sum_{n=1}^{N} z_n \tag{5.8}$$

where α is a real number strictly larger than 1. Because $\mathcal{P}$ is convex, the newly created polygon contains the original, which contains the curve; therefore, the curve is necessarily strictly inside $\mathcal{P}'$ and the integral 5.2 may be operated. Figure 5.2 shows the inflated polygon for $\alpha = 1.2$. Such large inflation is required for the visibility of the figure only. In practice, for computation only, $\alpha = 1.01$ is sufficient.

Another method of refinement of the polygon is consecutive subdivision and merging of the polygons of each sub-curve. The common point of the polygons of two consecutive sub-curves lies on the curve. Inflation cannot be used on the merged polygons, since this shape is usually not convex. Instead, the following techniques can be applied:

- the polygons of each sub-curve are inflated and then merged. However, with this technique, the merged polygon often contains one or two very small sides relative to their neighbors, which results in inaccuracies in the evaluation of the complex potential, at a location that is very close to the curve. There is no simple technique for *cleaning-up* the polygon efficiently. This method is therefore abandoned.
- The vertices that fall on the curve itself are moved away:
  - if the vertex is at the tip, by stretching away from the centroid of the the vertex and its follower and predecessor -see Fig.5.3.
  - otherwise, in the direction normal to he curve at that point -see Fig.5.4(a). Note that the case of a vertex at an inflexion in the curve is only a minor issue, where care must be taken in the order of the control points only -see Fig.5.4(b).

It is also possible to design a custom fitted polygon by hand. The rules mentionned above are provided for handling by a computer while keeping the guarantee of inclusion of the curve inside the polygon.

5.1.3 Examples

The following examples were produced using customized Scilab scripts. In both examples, the curvilinear element is an impermeable barrier using 64 degrees of freedom to meet the boundary condition along a Rational Bézier curve of degree 5. It is placed in a field consisting of uniform

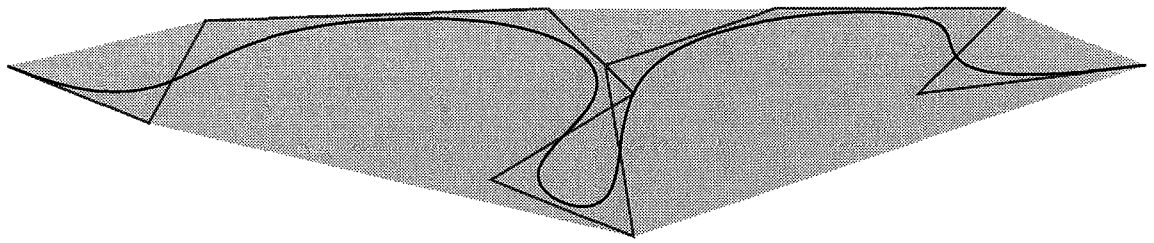

(a) general convex hull

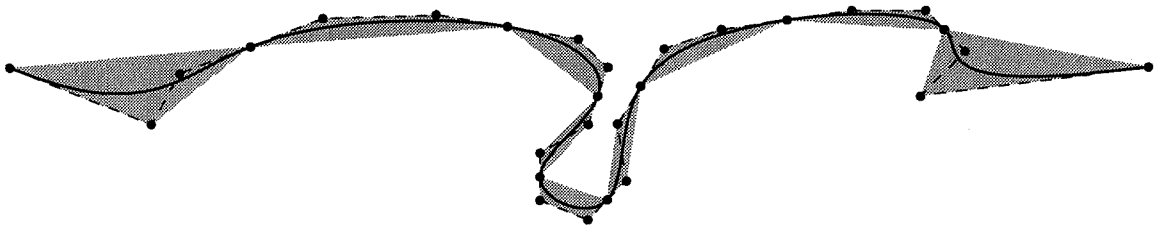

(b) hull refined by subdivision

Figure 5.1: Polygon obtained as the union of the convex hull of the subdivisions of a NURBS curve

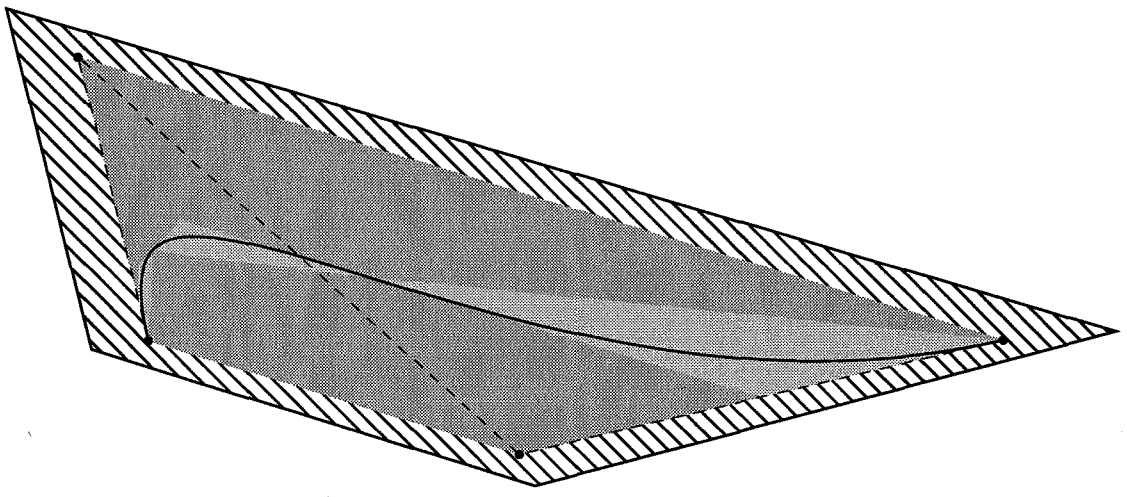

Figure 5.2: The convex hull of a Rational Bézier Curve, its inflated substitute, and the polygon obtained by further subdivision

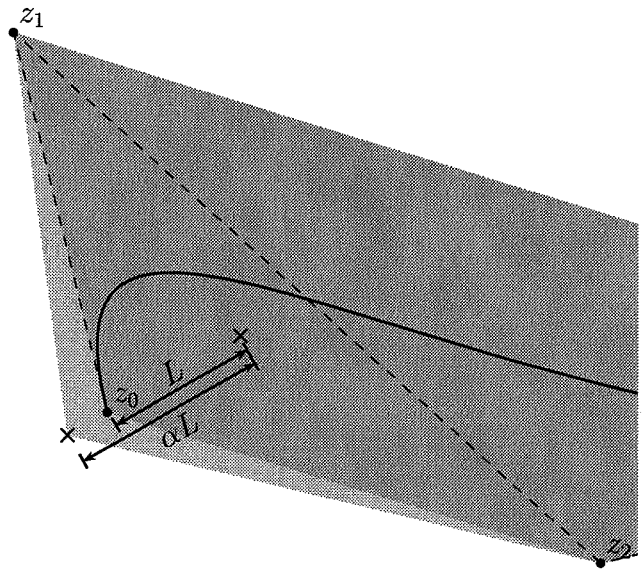

Figure 5.3: Changing the location of the endpoint vertex of the surrounding polygon

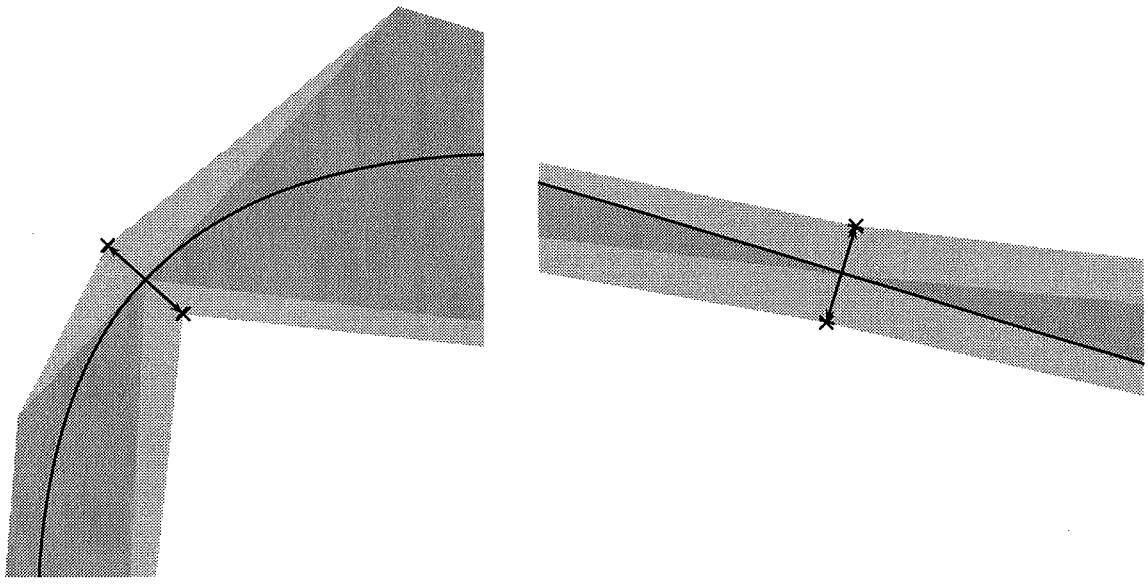

(a) regular points (b) inflexion points

Figure 5.4: moving polygon vertices away: (a) at regular points; (b) at inflexion points.

flow and a well. Figure 5.5 shows the undisturbed fields, before the impermeable element is added. Figure 5.6 represents the flow field after the impereable barrier has been added.

general polygonal far-field

In this case the chosen polygon is the convex hull inflated by 1 percent. Only 5 line elements are necessary: one of the control points of the spline is strictly inside the hull. Figures 5.8(a) and 5.8(b) show the complex potential as evaluated throughout the domain of interest, and restricted to the inside the polygon, without approximation. Figure 5.8(c) shows the approximation obtained outside of the polygon. Figure 5.8(d) shows the logarithm of the absolute error, which is zero inside, by design, and heavily concentrated around the polygon outside, reaching 10^{-4}. The computation of the influence of the curvilinear element was twice as fast with the polygon as without.

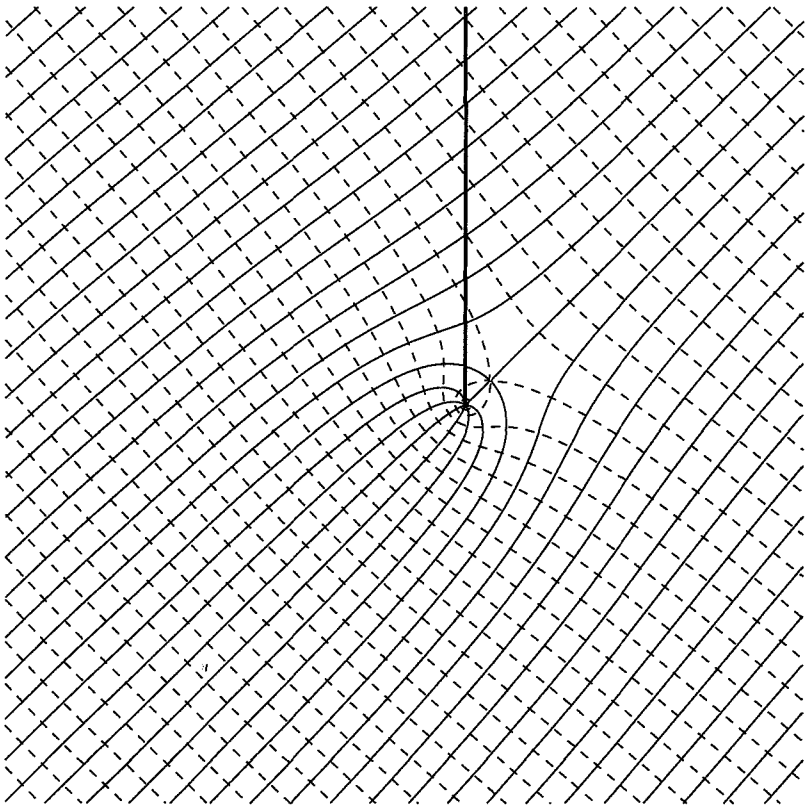

Figure 5.5: General flow field

refined polygon

In this situation the polygon is refined manually to include one extra side, and by moving the lower two points so as to get a closer fit. This manual choice is performed because in the case of this example, the automatic treatment is not necessary. The speed of the evaluation outside is reduced by 20 percent, due to the addition of a side. If the number of sides had been doubled, the evaluation speed would have been cut in half: the time of computation varies linearly with the number of sides. The overall gain is speed was minimal -around 3 percent-, as the reduction in the number of evaluation inside the smaller polygon is barely sufficient to offset the cost of an extra line element. Thus, it is suggested that polygon refinement should be limited to cases where the area of interest is limited to a region very close to the curvilinear line element. The error remains concentrated along the edges of the polygon -see figure 5.7.

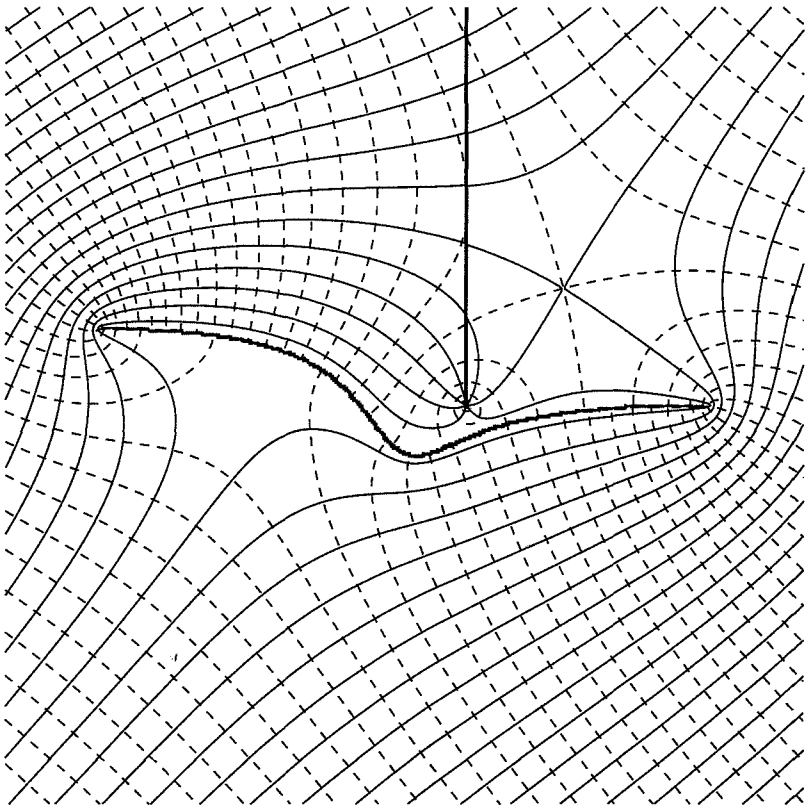

Figure 5.6: Flow field with the curvilinear barrier

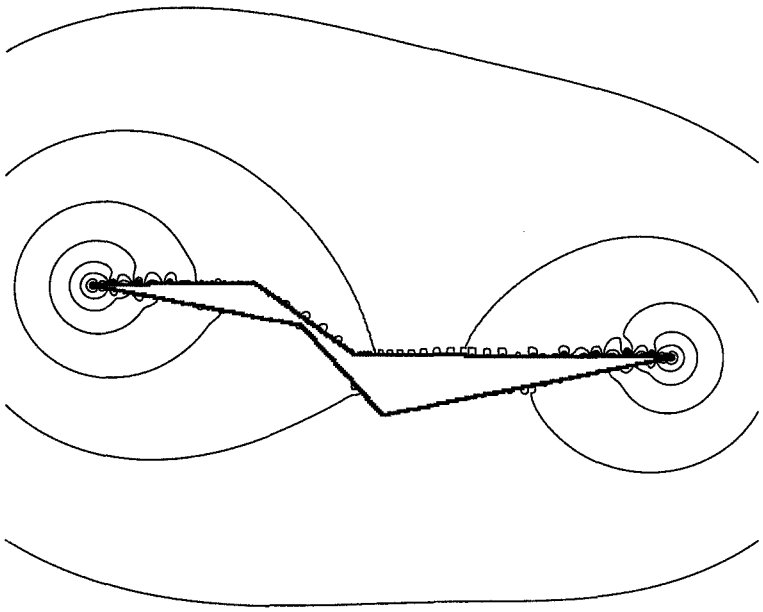

Figure 5.7: Logarithm of absolute error for a refined polygon

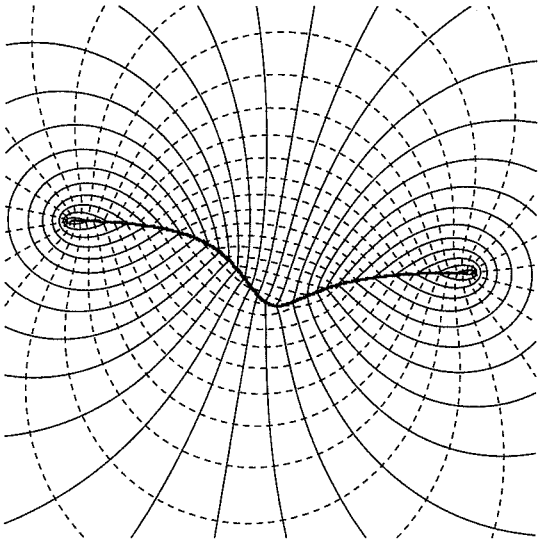

(a) complex potential of the element - No approximation

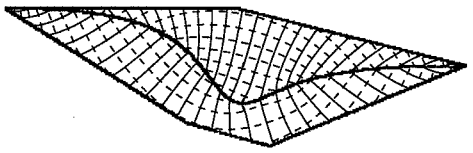

(b) same as 5.8(a), restricted to the polygon

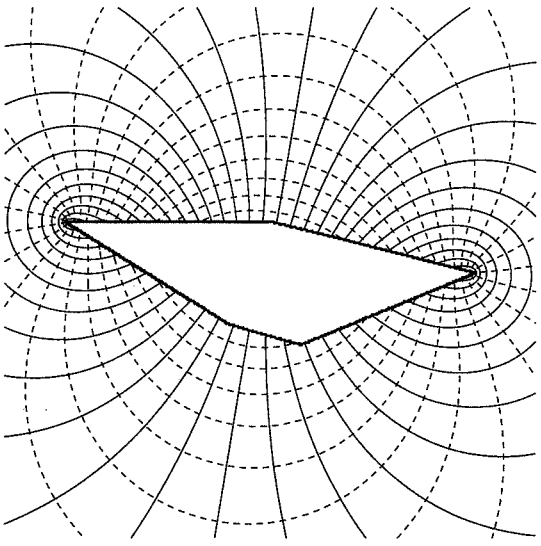

(c) approximation outside of the polygon

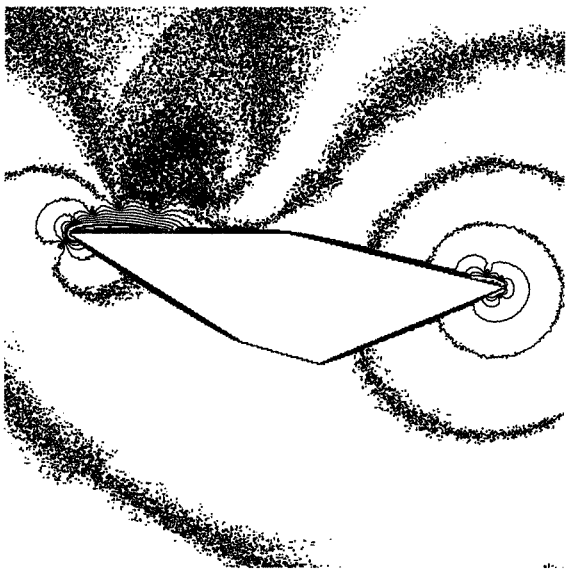

(d) absolute error log-plot

Figure 5.8: The complex potential of a curvilinear element and polygonal Far-Field approximation

5.2 Line Elements of very large degree

An issue must be raised with respect to the elements used in construction the polygonal far field expansions: although line elements of high degree are available for the modeling of groundwater flow, as shown in [31] and [6], these elements are made primarily for the purpose of matching boundary conditions of a groundwater flow problem; small local errors are acceptable, and these elements are not usually used at their highest settings, because errors of a few centimeters or millimeters for a condition of head specified to several meters is actually acceptable.

In the present context, these elements would be used for the evaluation of the complex potential of another element, essentially providing an analytic continuation of that potential outside of the polygon. This implies that the line elements are used based on the choice of the numerical engine developer, rather than on the wish of the modeler: they need to be able to match the potential to a great precision. It was found that these high-degree line elements [1] have intrinsic limitations, which reduce their usability in the present context: 40 to 45 degrees of freedom seem to impose a limitation, especially when these elements come very close to the boundary of the NURBS. For this reason, a new look is taken at two different type of line element, the classical element as well as the double root element -see [51]-, which will enable more control, and more precision in the vicinity of the polygon.

5.2.1 Double-Root line-elements

The double root element is presented in [51, pp.462-470]. The main characteristic of the double-root elements is that they rely on a map of the unit circle in the ζ-plane onto a slot in the Z-plane. This mapping may be introduced as:

$$Z = \frac{1}{2} \cdot \left(\zeta + \frac{1}{\zeta} \right) \tag{5.9}$$

[1] The authors of [31] and [6] actually refer to them as *high-order* line elements, but this is a slight misnomer, which could cause confusion in the future, when Wirtinger calculus is used to its fullest. The choice was made -as argued in [35] to rename them *high degree* line elements

Traditional view

This map is NOT bijective, and one may choose the reverse map as either one of the following:

$$\zeta = Z \pm \sqrt{Z^2 - 1} \tag{5.10}$$

This equation implies that there exist square root singularities at both extremities of the slot, thus the name of the element; another designation, referring to equation 5.9, could be *Hyperbolic Line Element.* In [51], Strack chooses to map the outside of the unit circle onto the slotted Z-plane.

The mapping chosen by Strack is called $\chi = Z + \sqrt{Z^2 - 1}$; thus, following Strack's expression for the complex potential [51, eq. (39.13)],

$$\Omega = \sum_{n=0}^{n=\infty} \omega_n \chi^{-n} \tag{5.11}$$

Revisiting the Double-Root Line element

For purely cosmetic reasons, and because no use of poles will be made, the opposite is chosen here, leading to the following reverse map:

$$\zeta = Z - \sqrt{Z^2 - 1} \tag{5.12}$$

This map has a major flaw when implemented innocently: It not only provides the jump required along the slot, it also contains a discontinuity along the imaginary axis inside the unit disk. Indeed, the square root jump whenever its argument is real and negative, which implies:

$$Z^2 - 1 \in \mathbb{R}^- \implies \{Z^2 \in \mathbb{R}\} \cap \{Z^2 \leq 1\} \tag{5.13}$$

$$\implies \{Z \in \mathbb{R}, |Z| \leq 1\} \cup \{(iZ) \in \mathbb{R}, |Z| \leq 1\} \tag{5.14}$$

This can be remedied by noting that inside the complex field, the square root may be defined as the bijective inverse of the square, by identifying it to the halving power function:

$\sqrt{Z^2} = Z^{2\frac{1}{2}} = Z$. Noting that:

$$1 - Z^{-2} \in \mathbb{R}^- \implies \{Z^2 \in \mathbb{R}\} \cap \{Z^2 \leq 1\} \cap \{Z^2 > 0\} \tag{5.15}$$

$$\implies \{Z \in \mathbb{R}, |Z| \leq 1\} \tag{5.16}$$

the mapping may be computed in the following manner:

$$\zeta = Z \cdot \left(1 - \left(1 - \frac{1}{Z^2}\right)^{\frac{1}{2}}\right) \tag{5.17}$$

Eq.5.17 has the drawback of requiring special handling of the case $Z = 0$.

Referring to [51] once again, it should be pointed out that the χ mapping was computed as $\chi = z + \sqrt{z+1}\sqrt{z-1}$, thus dubbing the elements as *double-root*, since each root singularity, present at each tip, was expressly used for the evaluation of χ.

One may note that $\zeta \cdot \chi = 1$. Applying it into equation 5.11,

$$\Omega = \sum_{n=0}^{n=\infty} \omega_n \zeta^n \tag{5.18}$$

As noted in [51], it is possible to include other expansions about particular points. However, with this choice of mapping, adding other Taylor expansions would be useless since they would all combine into one; therefore, the sum given above is sufficient to describe all sums of Taylor expansions. An additional term is needed to account for discharge or vorticity added by the element. The complex potential is then defined as:

$$\Omega = -\frac{Q}{2\pi} \ln \zeta + \sum_{n=1}^{n=\infty} \omega_n \zeta^n \tag{5.19}$$

Local resolution procedure

The expression in eq.5.19 reduces along the slot to a classic Chebychev polynomial series[2] when all the coefficients are real:

$$\Phi(X) = \Re\left[\Omega\left(X\right)\right] = \sum_{n=1}^{n=\infty} \omega_n T_n(X) \tag{5.20}$$

where T_n is the Chebychev polynomial of order n. Thus, the problem of fitting the head along the slot to a specified polynomial -a Dirichlet condition- becomes entirely trivial: one does not have to adapt the jump of the element to attain the target function $\overset{t}{\Phi} = \sum_{n=0}^{n=\infty} a_n T_n(X)$, as the orthonormality of the Chebychev polynomials guarantee that:

$$\forall n \in \mathbb{N}^*, \quad \omega_n = a_n \tag{5.21}$$

This equation begs the question of adapting the degrees of freedom of the element in a manner that will lead an objective function to achieve a minimum as proposed by Janković. Since these degrees of freedom are known exactly as soon as a target function is defined, it is sufficient to approximate a target function by combination of the condition imposed on the element and the influence of the other elements in the model. If the element is isolated, in the sense that no other element is crossing it, even at its tip, this is simply a problem of fitting a Chebychev series to the external influences, then adding the conditioning polynomial, and the degrees of freedom of the element will be exactly known.

In summary, if we define:

- The boundary condition, or value that should be observed along the element after resolution of the problem $\overset{BC}{\Phi}\left(X\right) = \sum_{n=1}^{n=\infty} \beta_n T_n(X)$
- The influence on the complex potential of all other elements in the model with respect to local coordinates $\overset{o}{\Omega}\left(X\right)$

[2] When examined in the ζ-plane, the Chebychev series turn into Fourier Cosine Series in terms of the argument of ζ.

then, following the suggestion of [31] on orthogonal bases:

$$\begin{aligned} \forall n \in \mathbb{N}^*, & \\ \omega_n &= \frac{2}{\pi}\int_{-1}^{+1}\left(\overset{BC}{\Phi}(X) - \Re\left(\overset{o}{\Omega}(X)\right)\right)\cdot T_n(X)\frac{dx}{\sqrt{1-X^2}} \\ &= \beta_n - \frac{2}{\pi}\int_{-1}^{+1}\Re\left(\overset{o}{\Omega}(X)\right)\cdot T_n(X)\frac{dx}{\sqrt{1-X^2}} \end{aligned} \tag{5.22}$$

Thus, if we approximate $\Re\left(\overset{o}{\Omega}(X)\right)$ as:

$$\Re\left(\overset{o}{\Omega}(X)\right) = \sum_{n=0}^{n=\infty}\overset{o}{\omega}_n T_n(X) \tag{5.23}$$

with:

$$\overset{o}{\omega}_n = \frac{2}{\pi}\int_{-1}^{+1}\Re\left(\overset{o}{\Omega}(X)\right)\cdot T_n(X)\frac{dx}{\sqrt{1-X^2}} \tag{5.24}$$

then:

$$\forall n \in \mathbb{N}^*, \quad \omega_n = \beta_n - \overset{o}{\omega}_n \tag{5.25}$$

and the only problem left is the issue of linking $\overset{o}{\omega}_0$ and β_0 to the pumping rate Q of the element. Two separate cases can be identified:

- The element is isolated and used to represent a crack or a barrier with no net discharge or vorticity: $Q = 0$
- The element does in fact draw or add water from/to the aquifer. Then Q depends on the other elements in the flow domain that also add/draw water, and the coefficient Q may only be computed with respect to the other discharges. This should be done through the use of a *reference point* as presented in Strack, and in Janković.

This applies in the case of a Dirichlet boundary conditions, and a similar computation may be operated in the case of a Neumann boundary condition. However, instead of solving for $\Im W(X) = -Q_n(X)$, it was found that better results are achieved with the double root element when adapting $\Im\frac{1}{2i}\left(\zeta - \frac{1}{\zeta}\right)W = \sin\left(\operatorname{acos}(X)\right)Q_n(X)$

Figure 5.9 shows the results obtained when representing a breaking impermeable wall with double root elements of degree $N = 350$, and a comparison with the results for the same

problem as generated by the program *SPLIT* set to maximum precision for the same problem. In the case of Neumann and Dirichlet conditions, the double root element provides much more control and therefore accuracy, than its standard counterpart.

Evaluation of Double-Root elements

The expression for the complex potential associated to a double-root element is a standard power series in ζ. Classical methods may be used to evaluate it, such as Horner's rule or Knuth's rule in the case of real or pure imaginary coefficients, as suggested by Barnes (personal communication). However, $\zeta = Z \cdot \left(1 - \sqrt{1 - Z^{-2}}\right)$ must be evaluated at every point which may slow down computations. A number of tricks may be employed to speed up computations as suggested by Barnes. One of them consists in choosing judiciously the number of terms used to compute the complex potential as a function of the location where it is evaluated. Barnes uses the Near-field/far-field approach, using a Laurent expansion when $|Z| \geq 1.1$. The problem of choice of cutoff thresholds is therefore identical with the Far-field approach as it is with the double root series. What is interesting however, is that the far-field coefficient are not optimized with respect to the boundary condition but rather with respect to reduction of the error at the connection to the Near-field; thus, in theory, nothing actually allows the cutoff to take place other that the fact that the error induced by the cutoff is negligible in practice.

In the case of a Dirichlet or Neumann problem, the coefficients of the double root element's complex potential are actually computed with respect to the Boundary Condition exactly, using an orthogonal functional basis; thus, a truncated series of N coefficients out of an original series of M is exactly the same series as what would be obtained if only N coefficients were calculated in the first place. If we designate the exact solution to the flow problem with the chosen boundary condition along the slot as:

$$\overset{\infty}{\Omega}(Z) = \overset{\infty}{\omega}_0 \ln \zeta + \sum_{n=0}^{n=\infty} \overset{\infty}{\omega}_n \zeta^n \tag{5.26}$$

then the error induced by a truncation at order N at ζ is exactly:

$$E_N(\zeta) = \left| \overset{\infty}{\Omega}(Z) - \overset{N}{\Omega}(Z) \right| = \left| \sum_{n=N+1}^{n=\infty} \overset{\infty}{\omega}_n \zeta^n \right| \tag{5.27}$$

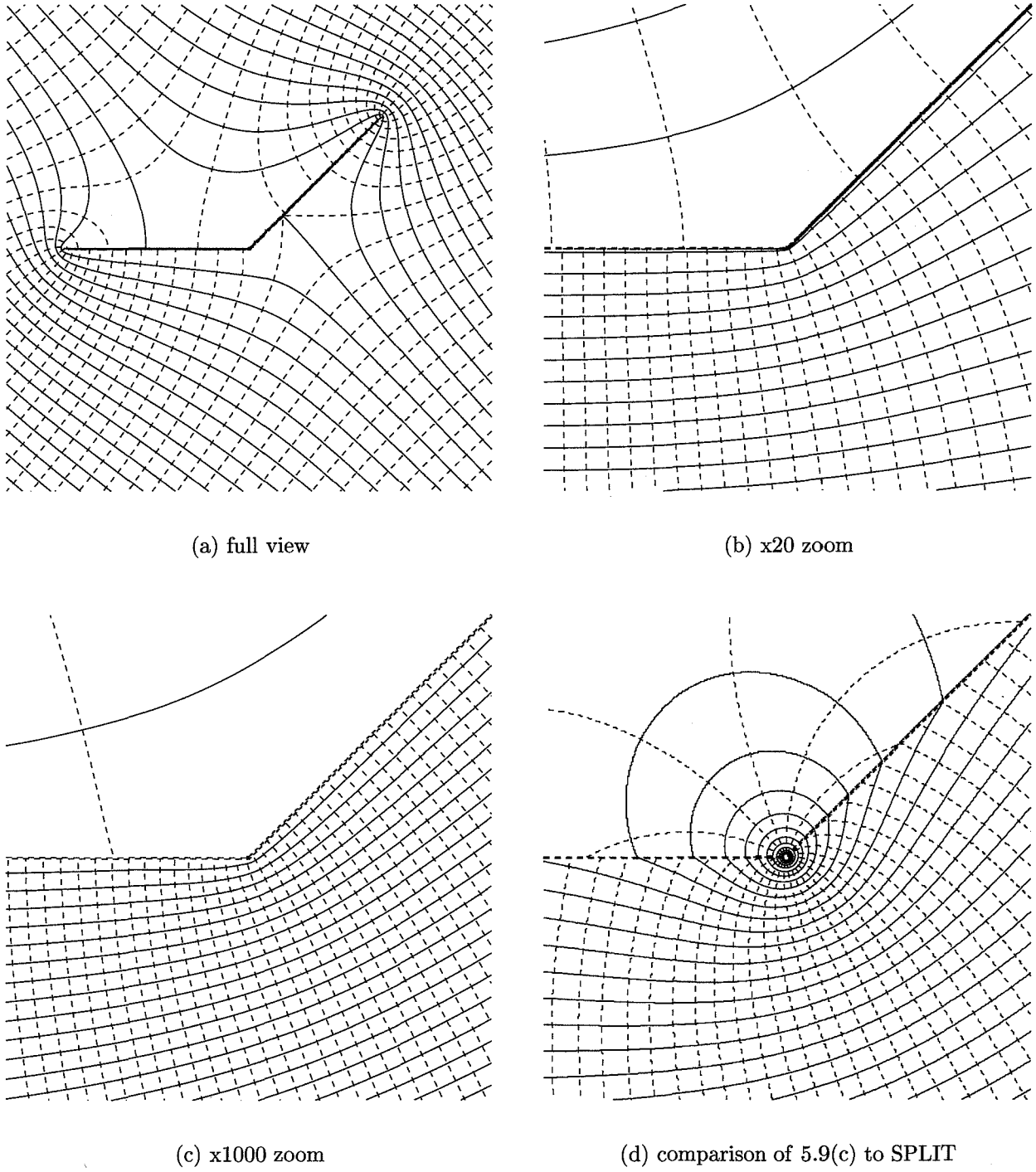

(a) full view

(b) x20 zoom

(c) x1000 zoom

(d) comparison of 5.9(c) to SPLIT

Figure 5.9: Double Root elements for connected impermeable barriers in uniform flow. $N = 350$

Defining $\mu = \sup_{n \geq N+1} \left| \overset{\infty}{\omega}_n \right|$, which always exists in practice, the error may be bound as:

$$E_N(\zeta) \leq \mu \cdot \left|\zeta^{N+1}\right| \cdot \left| \sum_{n=0}^{n=\infty} \zeta^n \right| = \mu \cdot \frac{|\zeta|^{N+1}}{1-|\zeta|} \tag{5.28}$$

If a relative error ϵ is defined, a threshold $\overset{N}{\tau}_\epsilon$ can be computed such that, for any Z where $|\zeta(Z)| \geq \overset{N}{\tau}_\epsilon$, the truncation error is less than $\mu \cdot \epsilon$:

$$\forall \epsilon \in \mathbb{R}, \exists \overset{N}{\tau}_\epsilon \in \mathbb{R}, \forall Z \in D = \left\{ Z \in \mathbb{C}, |\zeta(Z)| \geq \overset{N}{\tau}_\epsilon \right\}, E_N(\zeta) \leq \mu \cdot \epsilon \tag{5.29}$$

The domain D is an ellipse outside of which the sum may be truncated to the desired degree N. Figure 5.10 represents in dashed (resp. dotted) the ellipse inside which more that fifty (resp. twenty-five) terms must be used for the series in ζ and the disk inside which either a near-field or a Laurent expansion of more than fifty (resp. twenty-five) terms must be used in Z; also represented in this figure are the ellipse and disk corresponding to $N = 250$ (gray). The thresholds used for the Laurent series were provided by Dr. R. Barnes. Two means may be used for comparison of such domains where time of computation is similar, because the series have the same number of terms: firstly, one can compare the radius of the limiting disk for the Laurent expansion to the major axis of the limiting ellipse of the double root; secondly, as is apparent on the figure, a better means of comparison of the zones is the surface area that they cover. Table 5.1 shows the squared major axis/threshold values for different degrees, as well as the surface area of the corresponding disk/ellipse and the ratio of these areas for $\epsilon = 10^{-9}$. It is worthwhile noting that in practice, μ gets very small as N increases.

Jump-specified elements

The main disadvantage of the double root element is in problems where the jump in the complex potential along the element is specified as a polynomial. Indeed, if the Jump along the line $J(X), X \in [-1, +1]$ is known as a series of Chebychev polynomials:

$$J(X) = \sum_{n \geq 0} \mu_n T_n(X) \tag{5.30}$$

	Threshold squared		Exclusion ellipse Area		
Degree N	Double Root	Standard	Double Root	Standard	ratio
1	624942673.9969	2229361453.1191	1963315311.9728	7003745563.3154	3.56
2	460479.1793	1707402.2724	1446636.4361	5363962.4357	3.70
3	12520.9165	47324.5106	39334.0486	148674.3349	3.77
4	1443.9285	5515.9893	4534.6641	17328.9916	3.82
5	342.7416	1318.5594	1075.1826	4142.3767	3.85
6	122.9749	475.0441	384.7633	1492.3951	3.88
7	57.3685	221.1065	178.6508	694.6267	3.89
8	31.7899	122.0473	98.2878	383.4230	3.90
9	19.9086	75.8969	60.9540	238.4374	3.91
10	13.6345	51.4660	41.2334	161.6855	3.92
15	4.3884	15.2951	12.1142	48.0510	3.97
20	2.5759	8.0949	6.3295	25.4310	4.02
25	1.9237	5.4668	4.1876	17.1745	4.10
35	1.4399	3.4513	2.5002	10.8427	4.34
50	1.2104	2.4217	1.5853	7.6080	4.80
75	1.0943	1.8256	1.0089	5.7353	5.68
100	1.0538	1.5804	0.7478	4.9649	6.64
150	1.0245	1.3645	0.4979	4.2866	8.61
200	1.0141	1.2662	0.3750	3.9779	10.61
250	1.0091	1.2100	0.3014	3.8013	12.61

Table 5.1: *Comparison of squared thresholds and corresponding areas*

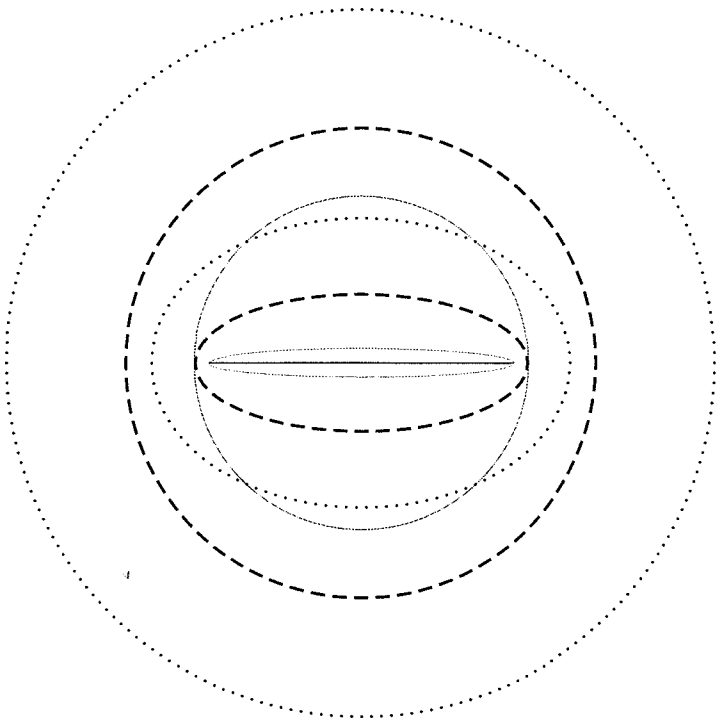

Figure 5.10: *exclusion ellipses for $N = 25$(dotted), $N = 50$(dashed) and $N = 250$(solid gray)*

and the potential of the double root element is defined following eq.5.19, then the following objective function may be defined and minimized with respect to the coefficients of the double root element, where $x = \cos(\theta)$:

$$\Psi = \int_0^{\pi} \left| Q\frac{i\theta}{\pi} - 2i\sum_{n\geq 1} \omega_n \sin(n\theta) - \sum_{n\geq 0} \mu_n \cos(n\theta) \right|^2 d\theta \tag{5.31}$$

This problem closely resembles the attempt to match a sine series to a cosine series. This would be impossible to resolve over an integration interval $\theta \in [-\pi, \pi]$, but may be achieved to some extend over $\theta \in [0, \pi]$. It was observed that the fit obtained is usually poor, forcing the use of several thousands of terms in the double root element to obtain an approximation of the jump to 10^{-7}, which is at the limit of the acceptable for the application described in 5.1.

This is due to the fact that the jump function of a Double-Root element always reaches 0 at its tips. In order to imitate a non-zero value, the element forces a type of behavior similar to a Gibbs phenomenon there. This uses many degrees of freedom. The use of double root elements in the case of jump matching problems leads to a high computational cost, thus going against the intended objective of the polygonal far fields. Although the number of terms can rapidly drop as distance from the polygon increases, the cost remains too high for most application.

5.2.2 Improving High Degree Line Element

Since double-root elements are prohibitively expensive for this particular application, a method is proposed to improve the High Degree Line Element so as to remove the limit to the maximum degree of the polynomial used to represent the strength.

The failings of High Degree Line Element

The main limitation of line elements of high degree is that the polynomial used to represent their jump function is limited to a degree $N \leq 45$. This restriction is induced a numerical -rather than an analytical- issue: for elevated orders, and for an argument inside the unit disk, the numerical evaluation of the complex potential requires either the use of a Clenshaw recursion -see [45]- to compute a series of Legendre functions, or, as proposed in [31], the multiplication

of a power series by a logarithm and subsequent subtraction of a correction polynomial. The former breaks down well within the unit disk, even for moderate degrees, as shown in Figure 5.11. The latter can be pushed to be satisfactory up do degree 45. Both break down because past their respective limits, their algorithms require the subtraction of very large numbers from very large numbers: the small numerical error relative to such large values are often what remains after the subtraction. The limit of 45 results from the observation that below that limit, it is possible to accurately compute the potential inside and a little beyond the unit circle and to switch to a Laurent series outside without any occurrence of numerical error; thus the function can be evaluated accurately throughout the domain of interest. It is pointed out that this limit is valid when using double precision computing; the limit is lower in single precision.

As a consequence, if a far-field expansion of the Legendre series, other than an Laurent expansion, can be provided to approximate the influence of the line element that satisfies the following conditions:

- can match the Legendre series to a chosen precision at a given boundary
- can be computed accurately and efficiently outside of the boundary
- is associated to a boundary within which the Legendre series can be accurately computed

then this expansion could be used to represent the Legendre series in place of the Laurent series.

It can be experimentally observed that the standard Clenshaw recursion provides an accurate result within ellipses with foci ± 1. Thus, an elliptical domain can be defined for each value of N within which the Legendre series can be directly evaluated using this recursion.

To determine the size of the ellipses, experiments were run to find their maximum extent: A Legendre series is used to represent a known function. The chosen series solves the problem of an isolated line element in uniform flow. The actual solution is the double root: $\Omega = Z - (Z^2 - 1)^{\frac{1}{2}}$. The Legendre series was solved for 1024 coefficients. It was then evaluated along the imaginary axis for an array of truncations, that is for $N \in \{32, 64, 128, 256, 512, 1024\}$. The distance to the actual solution was then plotted versus the location on the axis; figure 5.12(a) shows this plot for $N = 64$. A location was then visually found below which no numerical error occurred.

These location b_n empirically fit the curve:

$$b_n = \frac{32}{n} \tag{5.32}$$

Since the domains were assumed to be ellipses of foci ± 1, the b_n correspond to their minor axis, and their major axis can be found through:

$$a_n{}^2 - b_n{}^2 = 1 \tag{5.33}$$

The domains are validated by evaluating the Legendre series along the ellipse of axes (a_n, b_n) and verifying that the error remains small, compared to the exact solution. Figure 5.12(b) shows that these errors are indeed negligible, both in terms of maximum and average.

Double-root elements as far-fields

The appearance of ellipses of foci ± 1 is reminiscent of the zones define in the evaluation of the double root elements. It is therefore proposed that the expansion of the Legendre series outside of the limiting ellipse should be a double root series, in the fashion of eq.5.19.

To obtain the coefficients of the double root expansion when the coefficients of the Legendre series are known, the following method is proposed. It consists in a single matrix multiplication.

A relationship may be derived between Legendre functions and the variable ζ, using the expressions of Q_n as hypergeometric functions of z -see [2, eqs. 8.1.3, 8.1.7]- and quadratic transformations on the hypergeometric functions -see [2, eq. 15.3.19]:

$$Q_n(Z) = \frac{\Gamma(n+1)\,\Gamma\left(\frac{1}{2}\right)}{\Gamma\left(n+\frac{3}{2}\right)} \zeta^{n+1} \mathrm{F}_2^1\left(n+1, \frac{1}{2}; n+\frac{3}{2}; \zeta^2\right) \tag{5.34}$$

so that given the complex potential as a series of Legendre functions of the second kind, one can obtain an equivalent representations as a power series of the variable ζ:

$$\begin{aligned} \Omega(z) &= -\frac{1}{\pi i} \sum_{n\geq 0} \lambda_n Q_n(z) \\ &= -\frac{1}{\pi i} \sum_{n\geq 0} a_n \zeta^n \end{aligned} \tag{5.35}$$

where:

$$\mathbf{a} = [a_n]_{n\geq 0} = \overset{\mathbf{h}}{\mathbf{Q}}\lambda \tag{5.36}$$

with the matrix:

$$\overset{h}{Q} = \left[\overset{h}{Q}_{r,c}\right]_{r\geq 0, c\geq 0} \tag{5.37}$$

$$\overset{h}{Q}_{r,c} = 0, \quad c \geq r \tag{5.38}$$

$$= \frac{\Gamma\left(\frac{r+c+1}{2}\right)\Gamma\left(\frac{r-c}{2}\right)}{\Gamma\left(\frac{r+c}{2}+1\right)\Gamma\left(\frac{r-c+1}{2}\right)}\frac{1-(-1)^{r-c}}{2}, \quad r > c \tag{5.39}$$

This hypergeometric series converges slowly, and in fact not at all for $\zeta = Z = +1$. This is mostly due to the presence of log singularities in the Legendre functions of the second kind, which the hypergeometric series has difficulties emulating. This problem can be circumvented by explicitly removing the singularities using the following relationships:

$$\ln(Z \pm 1) = 2\ln(1 \pm \zeta) - \ln(2\zeta) \tag{5.40}$$

$$\ln(1 \mp \zeta) = \pm\zeta \mathrm{F}_2^1(1, 1; 2; \pm\zeta) \tag{5.41}$$

For a truncation at $N_q = 512$ of the Legendre series [3] , evaluates without numerical discrepancies within an ellipse of minor axis 0.0625 and major axis 1.001951, which is include within the ellipse defined by $0.9577 \leq |\zeta| \leq 1$. For such a threshold, the truncation in the zeta series must be operated at $N_\zeta = 607$ so that the relative error ϵ remains bound by 10^{-10}.

In this manner, the use of line dipoles of very high degrees is made possible. In turn, the availability of such elements allows the construction of a polygon surrounding any NURBS as outlined in 5.1 for the construction of a far-field complex potential based on the Direct Boundary Integral Method. Such a construction can potentially be extended to any group of analytic elements, thus bringing the possibility of constructing *superblocks*[4] of any polygonal shape. This technique, relying on the use of the Direct Boundary Integral, is an original product of the research presented here.

[3] using the standard technique, as provided by Janković -see [31]-, a small experiment may be run for N as large as 3500. Larger numbers may probably be obtained if the operator if willing to give the computer enough time, but there does not seem to be a use for such large numbers

[4] see [41]

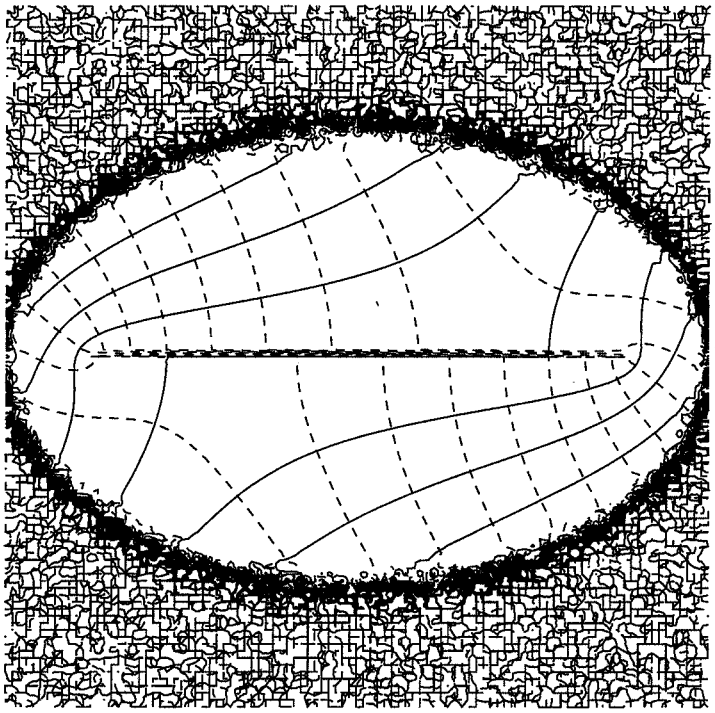

Figure 5.11: Numerical output of a clenshaw recursion for a Legendre series with $N = 64$

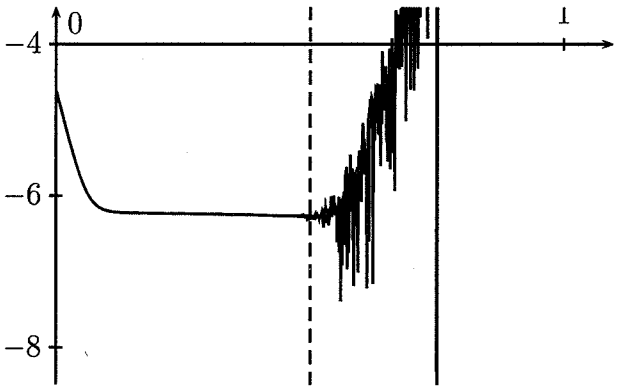

(a) logarithm of absolute error of a Legendre series with truncation at $n = 64$

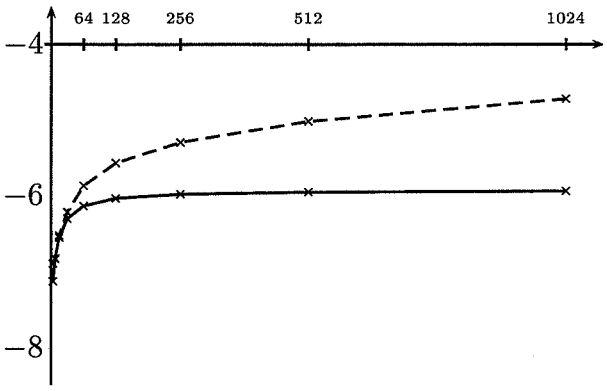

(b) maximum -dashed- and average -solid- error on the bounding ellipses

Figure 5.12: Analysis for the definition of elliptical domains of Legendre series

Chapter 6

Conclusion

6.1 Summary

In this thesis, the following points were addressed:

- Current tools for the design of groundwater flow models are inherently object centered and the use of domain discretization for the purpose of solving the mathematical model adds uncertainty.
- A method exists to solve many flow problems that does not require domain discretization, the AEM, but it currently limits the range of addressable problems because of its state of development. The lack of availability of certain shapes generated by pre-processing tools may also induce uncertainty in the model.
- Complex potential and discharge function for analytic elements along NURBS curves were provided to address the shape issue.
- Far-fields by Direct boundary integral along polygons were developed to enable the use of NURBS curve in practice by reducing their computational cost.
- Line elements of very high degree were introduced to enforce the assurance of high accuracy of the polygonal far-field expansions.

What results are three original tools that can be implemented in any analytic element code which should simplify the dialogue between GIS pre/post-processing and numerical model. The

following presents possible extensions for the research work using these three new tools.

6.2 Extensions

6.2.1 Relating model Inputs to Outputs

As pointed out in chapter 2, the modeler benefits when the outputs of his model directly relate to the inputs he provided: such direct links foster his understanding not only of the flow process, but also of the particular setting where he is attempting to simulate flow. GIS tools are object centered, and the AEM is inherently object oriented, so that producing a direct link between the two should be possible. The ideal tools for doing so seems available right now: XML, the eXtensible Markup Language, offers the facilities for defining a language for the storage and retrieval of analytic elements, which both the GIS and the computational engine can be taught. Similarly, results in the form of piezometric contours or well capture zones can be represented as objects, rather than obtained by interpolation on a grid.

6.2.2 Interface elements for the combination of resolution methods

The concept of polygonal far-field can be extended to produce elements that would allow the insertion of local domain models within an analytic element: this may be valuable to create contaminants transport models, where the differential equation's complexity need only apply close to the phenomenon. In a way, this is akin to the method of domain decomposition for the resolution of differential equations. Mathematical proofs exist that support the decomposition method, but no tool exists to implement it within the AEM; creating a far-field by direct boundary integral, an analytic extension for any domain model, that matches the heads and discharges at the boundary, might be that tool.

6.2.3 Beyond hydrogeology

The techniques provided in this thesis might be brought outside of the field of hydrogeology with limited effort.

Expanding to other physical processes

Some physical processes, such as heat transfer, share a common or similar mathematical representation as groundwater flow. In these instances, where the AEM can be directly used, the new improvements obviously may be applied as well. This may be particularly valuable in fields that study man-made products: many of these make use of NURBS curves in the design process, so that the boundary will be represented exactly instead of being approximated. This might prove a great advantage: the fewer approximations, the greater the accuracy.

Geo-referenced Information - A property model

The concept of property model is originally due to Pr. Otto Strack. In summary, the property model would allow the representation of any continuous information in the form of an analytic element model, with superposed influence functions. An Elevation Property Model would be to the AEM what Digital Elevation model is to Finite Differences, with a regular data grid, or Terrain Information Networks are to Finite Elements, with a triangulation of the domain. The advantage is that the Elevation Property model could be formally differentiated, thus providing a slope devoid of numerical noise; This could prove very useful in hydrology. In applications where information is stored directly rather than a model that attempt to simulate a physical process, the accuracy of the shape of the boundaries or location of jumps -e.g. for cliffs- is even more valuable: evaluating the size of farming fields, terrain grading for roads where the volume of soil to be moved could be obtained more accurately, etc.

It is the hope of the author that some of these suggestions for further research will be undertaken, and that the accomplishments of the present work will be fruitful for the scientific and engineering community.

Chapitre 6

Conclusion - version française

6.1 Bilan

Dans cette thèse, les points suivants ont été présentés :

- Les outils courants pour la conception de modèles d'écoulements souterrains sont intrinsèquement centrés objets et l'utilisation de discrétisation du domaine afin de résoudre le modèle mathématique ajoute de l'incertitude.
- Il existe une méthode pour la résolution de nombreux problèmes d'écoulement qui ne nécessite pas la discrétisation du domaine, l'AEM, mais qui limite pour l'heure l'étendue des problèmes gérables du fait de son état de développement. Le manque de disponibilité de certaines formes produites par certains outils de pré-production peut également induire de l'incertitude dans le modèle.
- Le potentiel complexe et la fonction de flux pour les éléments analytiques le long de courbes NURBS ont été fournis pour répondre au problème des formes.
- Des *champs lointains* par intégrales frontières directes le long de polygones ont été développés pour permettre l'utilisation des ces courbes NURBS dans la pratique, en réduisant leur coût de calcul.
- Des éléments linéaires de très haut degré ont été introduits pour assurer la production de séries asymptotiques de haute précision par les champs lointains polygonaux.

Ce qui en découle est un jeu de trois outils originaux, qui peuvent être implémentés dans n'importe quel code informatique d' éléments analytiques, et qui devrait simplifier le dialogue

entre la pré/post -analyse par SIG et le modèle numérique. La suite présente des extensions possibles au travail de recherche en utilisant ces nouveaux outils.

6.2 Extensions

6.2.1 Lier entrées et sorties de modèles

Comme avancé dans le chapitre 2, le modélisateur bénéficie d'une relation directe entre les sorties de son modèle et les entrées qu'il a fournies : un tel lien direct favorise sa compréhension non seulement du processus d'écoulement, mais aussi de l'arrangement particulier du domaine physique où il cherche à simuler l'écoulement. Les outils SIG sont centrés objet, et l'AEM est intrinsèquement orientée objet, si bien que produire un lien direct entre les deux devrait être possible. Les outils idéaux pour ce faire semblent être maintenant disponibles : XML, le langage par étiquettes extensibles, offre le cadre pour la définition d'un langage pour le stockage et la récupération d'éléments analytiques, que le SIG comme l'outil de calcul peuvent apprendre. De façon similaire, des résultats sous la forme de contours piézométriques ou de zones de captages peuvent être représentés comme objets, plutôt qu'obtenus par interpolation sur une grille.

6.2.2 Eléments interface pour l'association de méthodes de résolution

Le concept de *champs lointain* polygonal peut être étendu pour produire des éléments qui permettrait l'insertion de modèles locaux à l'intérieur d'un élément analytique : cela peut être de grande valeur pour créer des modèles de transport de contaminant, où la complexité de l'équation différentielle n'a à s'appliquer qu'à proximité du phénomène. D'un certain point de vue, cela est proche de la méthode de décomposition de domaines pour la résolution d'équations différentielles. Les preuves mathématiques sous-jacente à la méthode de décomposition existent, mais aucun outil ne l'implémente dans le contexte de l'AEM ; un nouveau type d'outil créant un champ lointain par intégrale frontière directe, une extension analytique pour n'importe quel modèle par discrétisation de domaine qui fasse correspondre charge et flux à la frontière, pourrait être intéressant.

6.2.3 Au delà de l'hydrogéologie

Les techniques fournies dans cette thèse pourraient être transférées en dehors du champs de l'hydrogéologie à moindre effort.

Etendre à d'autres processus physiques

Certains processus physiques, tel que le transfert calorifique, partagent une représentation mathématique commune ou similaire aux écoulement souterrains. Dans ces cas, où l'AEM peut être directement appliquée, les innovations peuvent évidemment être intégrées. Cela peut être particulièrement utile dans les domaines qui étudient les produits issus de production humaine : un bon nombre de ces produits fait usage des courbes NURBS dans la phase de conception, si bien que la frontière sera représentée exactement au lieu d'être approchée. Cela pourrait devenir un grand avantage : moins d'approximation signifie plus d'exactitude.

Information Geo-référencée - Un modèle de propriété

Le concept de modèle de propriété est originalement dû au Pr. Otto Strack. En bref, il permettrait la représentation de n'importe quelle information continue sous la forme d'un modèle par éléments analytiques, avec des fonctions d'influence superposées. Un modèle de propriété d'élévation serait à l'AEM ce qu'un *Digital Elevation model* est aux différences finies, avec une grille de données régulière, ou un *Terrain Information Networks* aux éléments finis, avec une tesselation du domaine. L'avantage du modèle de propriété d'élévation est qu'il peut être différencié de façon formelle, fournissant ainsi une pente sans ajout de bruit numérique. Cela serait fort utile en hydrologie. Dans les applications où l'information est stockée directement, contrairement aux modèles de simulation, la justesse et la précision de la forme de la frontière ou de la localisation de discontinuités -e.g. pour des falaises- ont d'autant plus d'importance : évaluation de la surface de champs agricoles, gradation de terrain pour les routes, etc.

L'auteur espère que ces suggestions de futures recherches seront entreprises, et que les produits du présent travail seront sources d'avancées pour les communautés scientifique et du génie.

Bibliography

[1] M. J. Ablowitz and A. S. Fokas, *Complex variables*, Cambridge University Press, 1997.

[2] M. Abramowitz and I. Stegun, *Handbook of mathematical functions*, Dover Publications Inc., New York, NY 10014, 1965.

[3] W. Anker and D. Graillot, *Aspects of coupling a multiphase/multispecies flow model to a geographic information system*, HydroInformatics '96, Balkema, 1996, pp. 151–155.

[4] M. Bakker, E.I. Anderson, T.N. Olsthoorn, and O.D.L. Strack, *Regional groundwater modelling of the yucca mountain site using analytic elements*, Journal of Hydrology **226** (1999), no. 3-4, 167–178.

[5] M. Bakker and V. Kelson, *An object-oriented design for basic analytic element classes*, unpublished report, May 2000.

[6] R. Barnes and I. Janković, *High-order line elements in modeling two-dimensional groundwater flow*, Journal of Hydrology **226** (1999), no. 3-4, 211–223, Special Issue.

[7] J. Bear, *Dynamics of fluids in porous media*, American Elsevier Publishing Company, Inc., 1972.

[8] J. Boivin, *Introduction à arc/info*, notes de cours, Université du Québec à Montréal, QC, Canada, Nov. 1997.

[9] E.J. Borowski and J.M. Borwein, *The harpercollins dictionary of mathematics*, Harper-Perennial, HarperCollinsPublishers, 10 East 53rd Street, New-York, N.Y. 10022, USA, 1991.

[10] Brebbia and Dominguez, *Boundary elements: An introductory course*, second ed., WIT Press, 1992.

[11] I.N. Bronshtein and K.A. Semendyayev, *Handbook of mathematics*, Verlag Harri Deutsch, Frankfurt, Germany, 1985.

[12] L. Collatz, *The numerical treatment of differential equations*, third ed., Springer-Verlag, 1976.

[13] H. Darcy, *Les fontaines publiques de la ville de dijon*, Corps Impériaux des Ponts et Chausées, http://gallica.bnf.fr, 1856, Public domain.

[14] W.J. de Lange, *The riza, analytic element, national groundwater model for water management in the netherlands*, MODFLOW 2001 and other modeling odeysseys.

[15] ———, *A groundwater model of the netherlands*, note 90.066, RIZA, 1991.

[16] W.J. de Lange and J.L. van der Meij, *A national groundwater model combined with a gis for water management in the netherlands*, HydroGIS '93, no. 221, IAHS, 1993, Proceedings of the Vienna conference, April 1993, pp. 333–343.

[17] ———, *Reports on nagrom*, Tech. report, TNO-GG Delft, RIZA Lelystad, 1994.

[18] G. de Marsilly, *Hydrogéologie quantitative*, Masson, Paris, France, 1981.

[19] C. Detournay, *Applications of the boundary elements to the hodograph method*, Phd thesis, University of Minnesota, Minneapolis,Minnesota 55455, 1985.

[20] H.J. Diersch, *Interactive, graphics-based finite element simulation system feflow for modeling groundwater flow, contaminant transport, and heat transport processes-* User's Manual Realease 4.7, WASY, Ltd., Berlin, 1998.

[21] D. Euvrard, *Résolution numérique des équations aux dérivées partielles de la physique, de la mécanique et des sciences de l'ingénieur: Différences finies, éléments finis, problèmes en domaines non bornés*, third ed., Dunot, 1994.

[22] G.E. Farin, *Curves and surfaces for computer aided geometric design: A practicle guide*, third ed., Academic Press, 1995.

[23] Ch. R. Fitts, *Analytic modeling of impermeable and resistant barriers*, Ground Water **35** (1997), no. 4, 312–317.

[24] Scilab Group, *Introduction to scilab*, Inst. Nat. Rech. Info. Automat., INRIA, Rocquencourt, France, www-rocq.inria.fr/scilab/doc.html.

[25] D. Guinin, F. Aubonnet, and B. Joppin, *Geometrie*, second ed., Precis de mathematiques, vol. 5, Breal, 310-320 Bd de la boissiere 93100 Montreil France, june 1989.

[26] H.M. Haitjema, *Modeling three-dimensional flow in confined aquifers using distributed singularities*, Phd thesis, University of Minnesota, Minneapolis,Minnesota 55455, 1982.

[27] ———, *Modeling three-dimensional flow in confined aquifers by superposition of both two- and three-dimensional analytic functions*, Water Resources Research **21** (1985), no. 10, 1557–1566.

[28] D.D. Hanson, J.K. Seaberg, and A.R. Streitz, *An analytic element model of two deep aquifers: a new approach to unlocking some old secrets*, MODFLOW 2001 and other modeling odeysseys.

[29] H. Y. He, *Groundwater modeling of leaky walls*, Master's thesis, Dept. of Civ. and Min. Engineering, University of Minnesota, Minneapolis, MN, USA, 1987.

[30] R.J. Hunt, M.P. Anderson, and V.A. Kelson, *Improving a complex finite-difference ground water model through the use of an analytic element screening model*, Ground Water **36** (1998), no. 6, 1011–1017.

[31] I. Janković, *High-order analytic elements in modeling groundwater flow*, Phd thesis, University of Minnesota, Minneapolis,Minnesota 55455, 1997.

[32] ———, *Split version 2.3*, Buffalo, N.Y., U.S.A, June 2001.

[33] S.R. Kraemer, H.M. Haitjema, and V.A. Kelson, *Working with whaem2000: Source water assessment for a glacial outwash wellfield, vincennes, indiana*, Office of Research and Development, US Env. Protection Agency, Research Triangle Park, NC 27711, 2000.

[34] F. Lasserre, M. Razack, and O. Banton, *A gis-linked model for the assessment of nitrate contamination in groundwater*, Journal of Hydrology **224** (1999), 81–90.

[35] Ph. Le Grand, *Analytic elements of high degree along bezier spline curves for the modelling of groundwater flow*, Ms thesis, University of Minnesota, Minneapolis, Minnesota 55455, 1999.

[36] J.A. Liggett and P.L-F.Liu, *The boundary integral equation method for porous media flow*, George Allen and Unwin, London, UK, 1983.

[37] K. Luther and H.M. Haitjema, *An analytic element solution to unconfined flow near partially penetrating wells*, Journal of Hydrology **226** (1999), no. 3-4, 197–203, Special Issue.

[38] M.G. McDonald and A. Harbaugh, *A modular three-dimensional finite-difference groundwater model*, Tech. report, U.S. Geological Survey, Reston, VA, USA, 1984.

[39] R. Miller, R.J. Barnes, and Ph. Le Grand, *Circular area-sink with polynomial infiltration*, Third Int. Conf. on the AEM, April 2000, Presentation.

[40] Muskhelishvili, *Singular integrals*, Dover Publications Inc., 1957.

[41] I. Janković O.D.L. Strack and R.J. Barnes, *The superbloack approach for the analytic element method*, Journal of Hydrology **226** (1999), no. 3-4, 179–187, Special Issue.

[42] Strack Consulting Inc. O.D.L. Strack, *Curvilinear analytic elements*, Tech. report, RIZA, the Netherlands, 1993.

[43] F. Paris and J. Canas, *Boundary element method: Fundamentals and applications*, Oxford University Press, 1997.

[44] L. Piegl and W. Tiller, *The nurbs book, 2nd edition*, second ed., Springer, Berlin, Germany, 1997.

[45] W.H. Press, S.A. Teukolsky, W.T. Vetterling, and B.P. Flannery, *Numerical recipes in c, second edition*, Cambridge University Press, Cambridge CP2 1RP, 40 West 20th Street, New York, NY 10011-4211, USA, 1992.

[46] R. B. Salamaa, Y. Lina, and J. Brouna, *Comparative study of methods of preparing hydraulic-head surfaces and the introduction of automated hydrogeological-gis techniques*, Journal of Hydrology **185** (1996), 115–136.

[47] J.K. Seaberg, *Overview of the twin cities metropolitan groundwater model, ver 1.00*, Tech. report, Minnesota Pollution Control Agency, http://www.pca.state.mn.us/water/groundwater/mm-overview.pdf, 2000.

[48] R. A. Silverman, *Complex analysis with applications*, Dover, 1990.

[49] D.R. Steward, *Vector potential functions and stream surfaces in 3d groundwater flow*, Phd thesis, University of Minnesota, Minneapolis,Minnesota 55455, 1996.

[50] ———, *Developing understanding of horizontal wells using an analytic model*, Modflow 2001 and other modeling odysseys (Golden, Co., USA) (Seo, Poeter, Zheng, and Poeter, eds.), vol. 1, Sept. 2001, p. 8.

[51] O.D.L. Strack, *Groundwater mechanics*, Prentice Hall, Englewood Cliffs, New Jersey 07632, 1989.

[52] ———, *Principles of the analytic element method*, Journal of Hydrology **226** (1999), no. 3-4, 128–138, Special Issue.

[53] ———, *Curvilinear elements*, (2003).

[54] ———, *Theory and applications of the analytic element method*, Reviews of Geophysics, in press. (2003), in press.

[55] ———, *Wirtinger calculus*, Dept. of Civil Engineering Seminar, University of Minnesota, January 2003.

[56] O.D.L. Strack and R.J. Barnes, *Object-oriented design for aem groundwater modelling*, Tech. report, RIZA, 2001.

[57] O.D.L. Strack and I. Janković, *A multi-quadric area-sink for analytic element modeling of groundwater flow*, Journal of Hydrology **226** (1999), no. 3-4, 188–196.

[58] O.E. Strack and F.D. Strack, *A tutorial to mlaem*, Strack Consulting, Inc., North Oaks, MN, USA, 1998.

[59] C.V. Theis, *The relation between the lowering of the piezometric surface and the rate and duration of discharge of a well using groundwater storage*, Trans. Amer. Geophys. Union **16** (1935), 519–524.

[60] C. D. Tomlin, *Geographic information systems and cartographic modeling*, Prentice Hall Professional Technical Reference, Feb. 1990.

[61] H.F. Weinberger, *A first course in partial differential equations with complex variables and transform methods*, John Wiley & Sons,Inc., 1965.

Summary

Using GIS for the design of groundwater models motivates the search for numerical methods that do not require the discretization of the flow domain: GIS are natively vectorized.

Numerical methods that relie on the discretization of the boundaries rather than the domain offer the advantage of retaining the native description of information in vector form as provided by the GIS, thus reducing the loss inherent to raterization and subsequent vectorization. The Analytic Element Method is especially promising. However, it lacks the capacity to handle a specific type of object, NURBS curves.

The functions necessary to allow the inclusion of these curves in the AEM are derived, and examples are provided. Their versatility is presented, also showing that existing smooth curves can be represented as NURBS, thus allowing backward compatibility, should they be replaced.

A method is offered to allow for faster model response when using these curvilinear elements, based on the Direct Boundary Integral Method. Standard line elements are also improved to allow greater precision and control in the speed-improving scheme.

Keywords: GIS, analytic elements, curvilinear elements, NURBS, Direct Boundary Integrals

Résumé

L'utilisation des SIG pour la conception de modèles d'écoulements souterrains motive la recherche de méthodes numériques qui ne requièrent pas la discrétisation du domaine de l'écoulement : les SIG sont par nature vectorisés.

Les méthodes numériques qui se fient à la discrétisation des frontières plutôt que du domaine offrent l'avantage de garder le description originale de l'information sous forme vecteur, telle que fournie par le SIG, réduisant ainsi les pertes inhérentes à la rastérisation et la vectorisation ultérieure. La méthode des éléments analytiques est particulièrement prometteuse. Cependant, il lui manque la capacité à gérer un type spécifique d'objets, les courbes NURBS.

Les fonctions nécessaires à l'inclusion de ces courbes dans le cadres de l'AEM sont dérivées, et des exemples sont fournis. Leur souplesse est présentée, et on montre que les formes courbes existantes dans l'AEM peuvent être représentées par des NURBS, permettant ainsi la compatibilité, si elles devaient être supplantées.

Une méthode est proposée pour améliorer le temps de réponse des modèles lorsque les éléments curvilinéaires sont utilisés, basée sur la méthode des intégrales frontières directes. Les éléments linéaires classiques sont également améliorés pour permettre meilleurs précision et contrôle dans la technique d'accélération.

Mots clef : SIG, éléments analytiques, éléments curvilinéaires, NURBS, Intégrales Frontières Directes